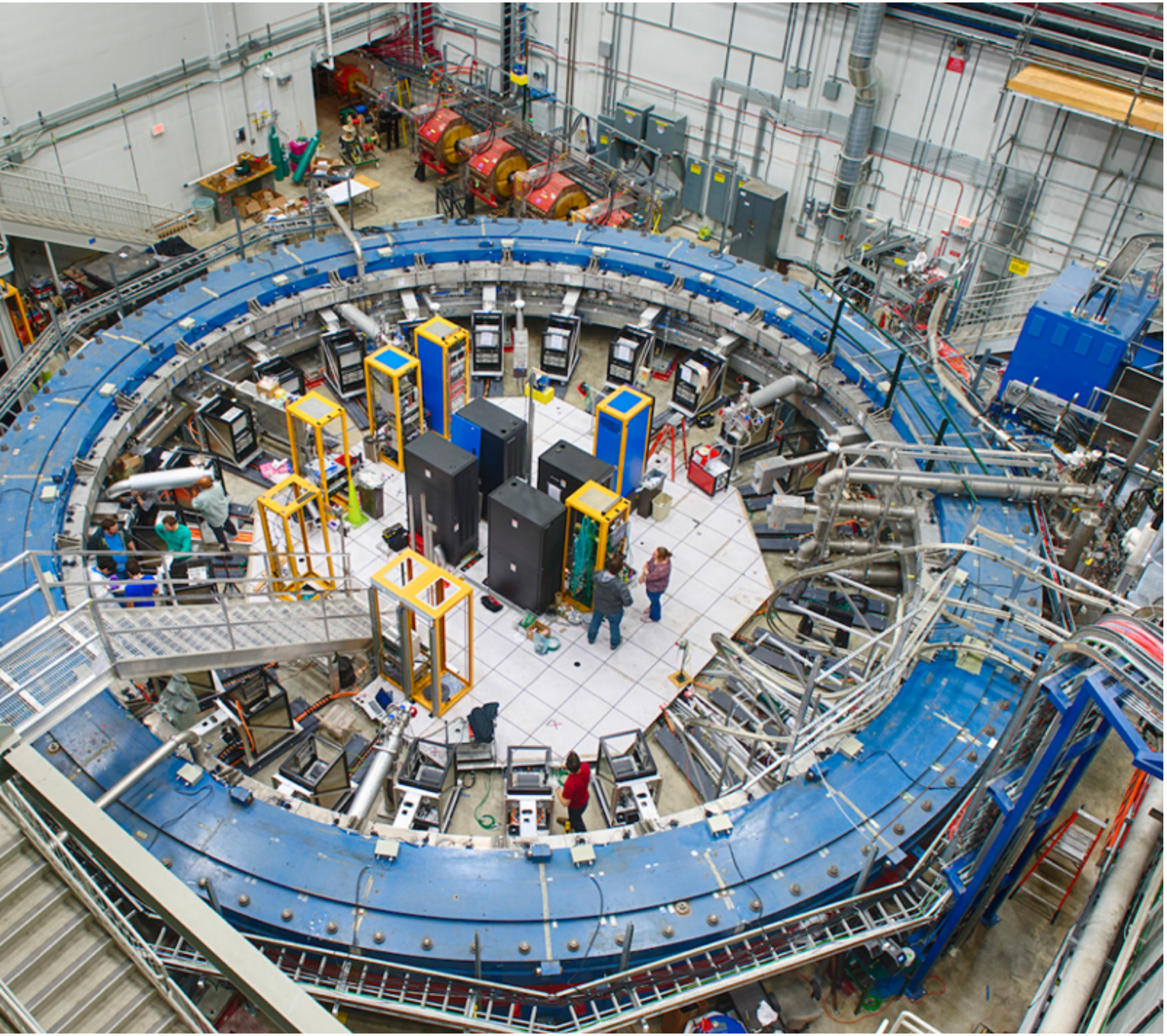

The first results of the Muon g-2 experiment at Fermilab

Prof. Dr. Martin Fertl

Muon g-2 Symposium

University of Stavanger

April 22nd, 2021

JOHANNES GUTENBERG UNIVERSITÄT MAINZ

Outline

Status of theory vs. experiment before April 7th, 2021

The Muon g-2 experiment at FNAL

- The measurement principle
- The muon source
- The muon storage ring and its instrumentation

The data analysis chain

- The anomalous spin precession frequency and its corrections
- The precision magnetic field and its corrections

The result

The magnetic moment of a charged lepton

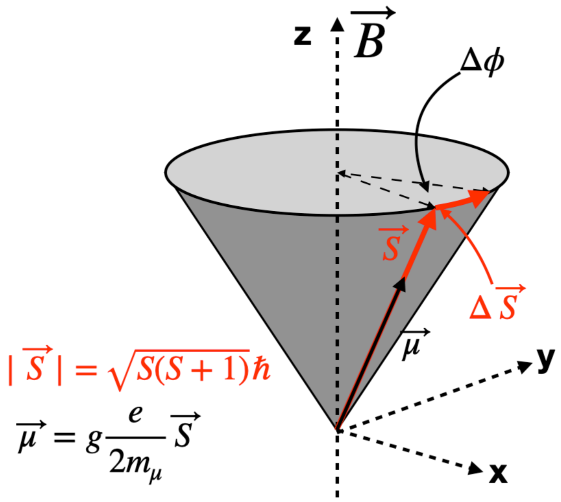

Charged particle with magnetic dipole moment and spin

$$\vec{\mu} = g\frac{q}{2m}\vec{s}$$

The magnetic moment of a charged lepton

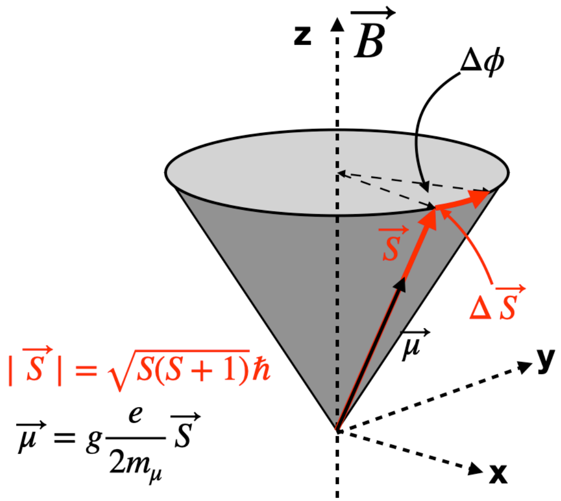

Charged particle with magnetic dipole moment and spin

$$\vec{\mu} = g\frac{q}{2m}\vec{s}$$

For a point-like charged lepton with spin 1/2 Dirac predicts $g = 2$

(P. Dirac, The Quantum Theory of the Electron, Proc. R. Soc. Lond. A 1928 **117**)

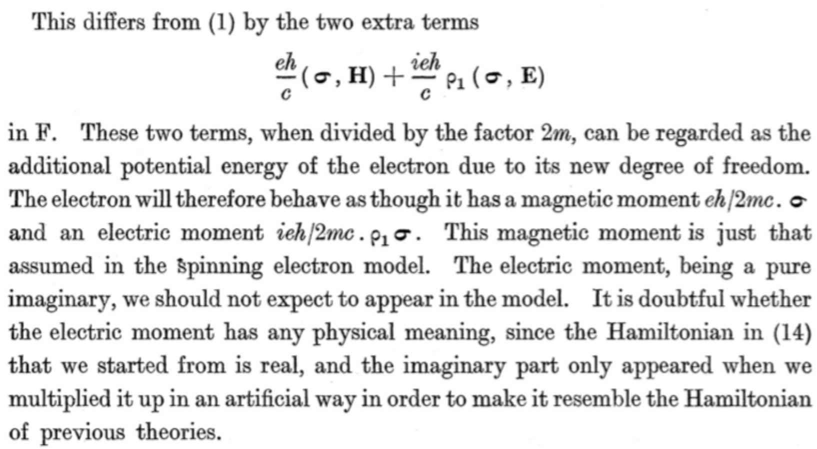

This differs from (1) by the two extra terms

$$\frac{eh}{c}(\boldsymbol{\sigma}, \mathbf{H}) + \frac{ieh}{c}\rho_1(\boldsymbol{\sigma}, \mathbf{E})$$

in F. These two terms, when divided by the factor $2m$, can be regarded as the additional potential energy of the electron due to its new degree of freedom. The electron will therefore behave as though it has a magnetic moment $eh/2mc \,.\, \boldsymbol{\sigma}$ and an electric moment $ieh/2mc \,.\, \rho_1 \boldsymbol{\sigma}$. This magnetic moment is just that assumed in the spinning electron model. The electric moment, being a pure imaginary, we should not expect to appear in the model. It is doubtful whether the electric moment has any physical meaning, since the Hamiltonian in (14) that we started from is real, and the imaginary part only appeared when we multiplied it up in an artificial way in order to make it resemble the Hamiltonian of previous theories.

The magnetic moment of a charged lepton

Charged particle with magnetic dipole moment and spin

$$\vec{\mu} = g\frac{q}{2m}\vec{s}$$

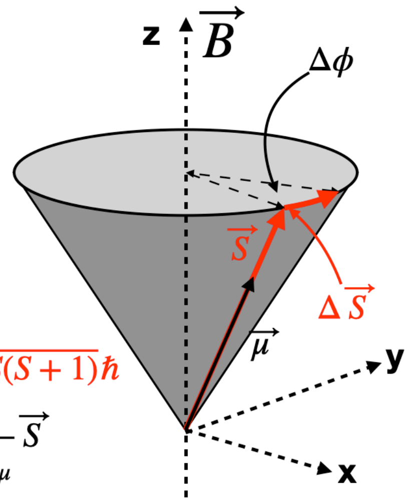

$|\vec{S}| = \sqrt{S(S+1)}\hbar$

$\vec{\mu} = g\frac{e}{2m_{\mu}}\vec{S}$

For a point-like charged lepton with spin 1/2 Dirac predicts $g = 2$

(P. Dirac, The Quantum Theory of the Electron, Proc. R. Soc. Lond. A 1928 **117**)

This differs from (1) by the two extra terms

$$\frac{eh}{c}(\boldsymbol{\sigma}, \mathbf{H}) + \frac{ieh}{c}\rho_1(\boldsymbol{\sigma}, \mathbf{E})$$

in F. These two terms, when divided by the factor $2m$, can be regarded as the additional potential energy of the electron due to its new degree of freedom. The electron will therefore behave as though it has a magnetic moment $eh/2mc \,.\, \boldsymbol{\sigma}$ and an electric moment $ieh/2mc \,.\, \rho_1 \boldsymbol{\sigma}$. This magnetic moment is just that assumed in the spinning electron model. The electric moment, being a pure imaginary, we should not expect to appear in the model. It is doubtful whether the electric moment has any physical meaning, since the Hamiltonian in (14) that we started from is real, and the imaginary part only appeared when we multiplied it up in an artificial way in order to make it resemble the Hamiltonian of previous theories.

The magnetic moment of a charged lepton

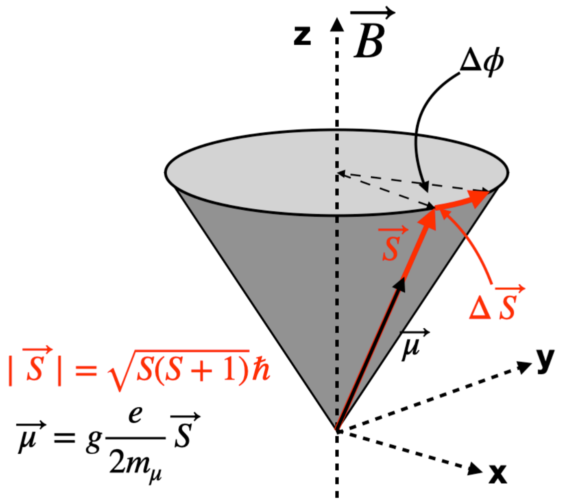

Charged particle with magnetic dipole moment and spin

$$\vec{\mu} = g\frac{q}{2m}\vec{s}$$

For a point-like charged lepton with spin 1/2 Dirac predicts $g = 2$

(P. Dirac, The Quantum Theory of the Electron, Proc. R. Soc. Lond. A 1928 **117**)

This differs from (1) by the two extra terms

$$\frac{eh}{c}(\boldsymbol{\sigma}, \mathbf{H}) + \frac{ieh}{c}\rho_1(\boldsymbol{\sigma}, \mathbf{E})$$

in F. These two terms, when divided by the factor $2m$, can be regarded as the additional potential energy of the electron due to its new degree of freedom. The electron will therefore behave as though it has a magnetic moment $eh/2mc \cdot \boldsymbol{\sigma}$ and an electric moment $ieh/2mc \cdot \rho_1\boldsymbol{\sigma}$. This magnetic moment is just that assumed in the spinning electron model. The electric moment, being a pure imaginary, we should not expect to appear in the model. It is doubtful whether the electric moment has any physical meaning, since the Hamiltonian in (14) that we started from is real, and the imaginary part only appeared when we multiplied it up in an artificial way in order to make it resemble the Hamiltonian of previous theories. EDM searches are another powerful SM test!

SM prediction meets the experiment

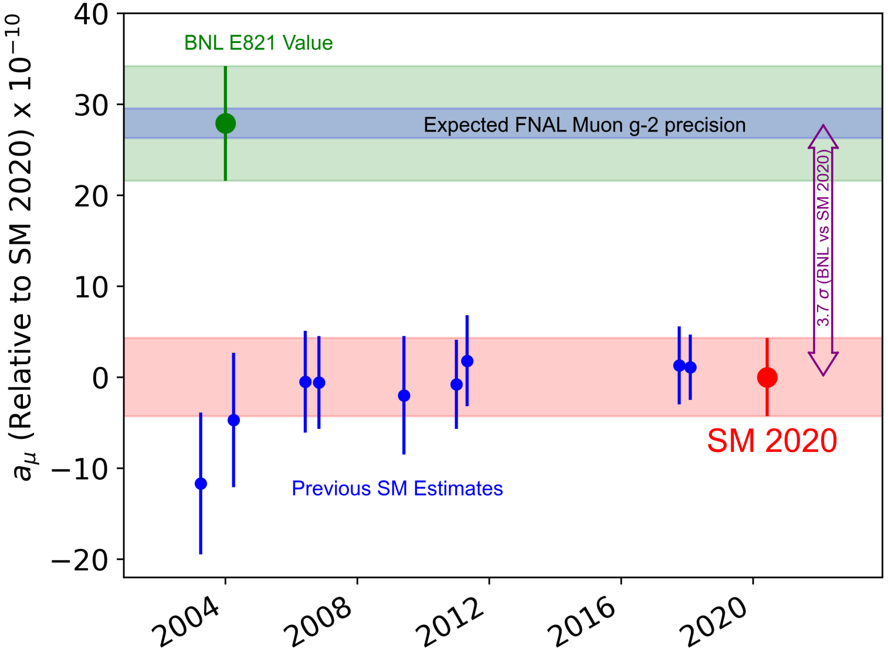

SM prediction meets the experiment

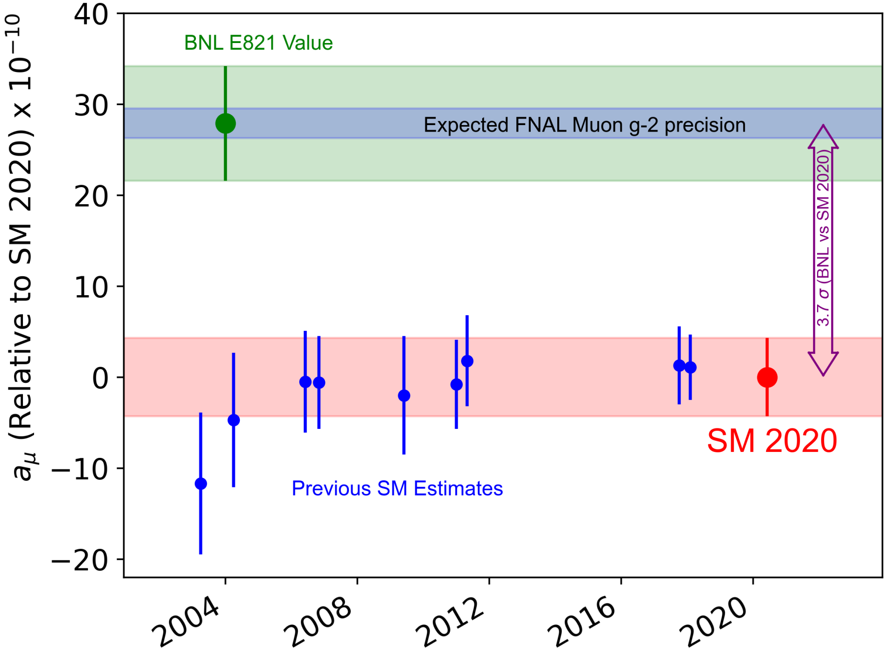

Experiment (BNL E821): $a_\mu^{\mathrm{BNL}} = 116592089 \pm 63$ (540 ppb)

Total SM prediction: $a_\mu^{\mathrm{SM}} = 116591810 \pm 43$ (368 ppb)

SM prediction meets the experiment

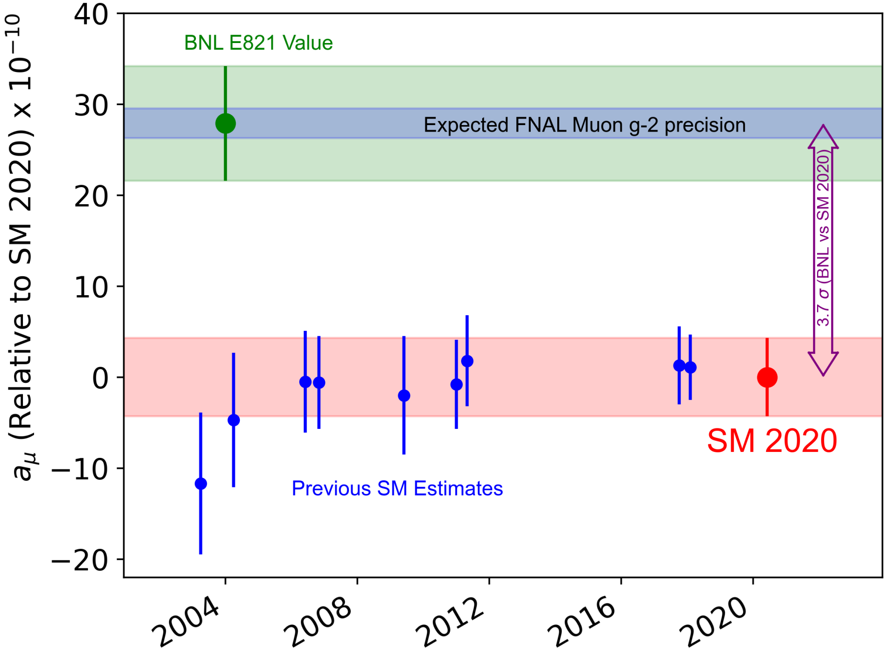

Experiment (BNL E821): $a_\mu^{\mathrm{BNL}} = 116592089 \pm 63$ (540 ppb)

Total SM prediction: $a_\mu^{\mathrm{SM}} = 116591810 \pm 43$ (368 ppb)

Discrepancy: $\Delta a_\mu = a_\mu^{\mathrm{exp}} - a_\mu^{\mathrm{SM}} = \left(279 \pm 76\right) \times 10^{-11}$

SM prediction meets the experiment

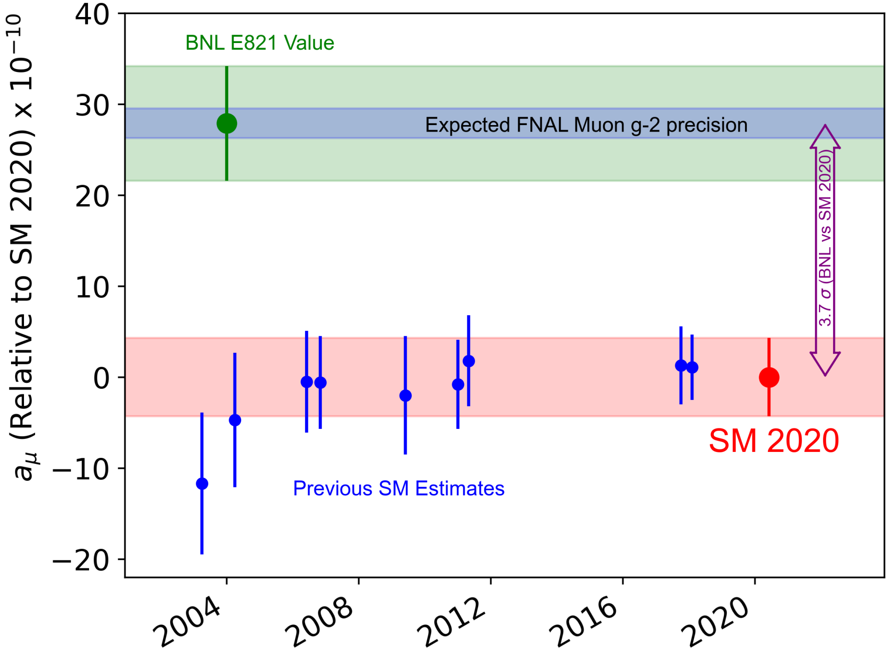

Experiment (BNL E821): $a_\mu^{\mathrm{BNL}} = 116592089 \pm 63$ (540 ppb)

Total SM prediction: $a_\mu^{\mathrm{SM}} = 116591810 \pm 43$ (368 ppb)

Discrepancy: $\Delta a_\mu = a_\mu^{\exp} - a_\mu^{\mathrm{SM}} = (279 \pm 76) \times 10^{-11}$

Evolved to 3.7 σ deviation between SM and BNL experiment!

SM prediction meets the experiment

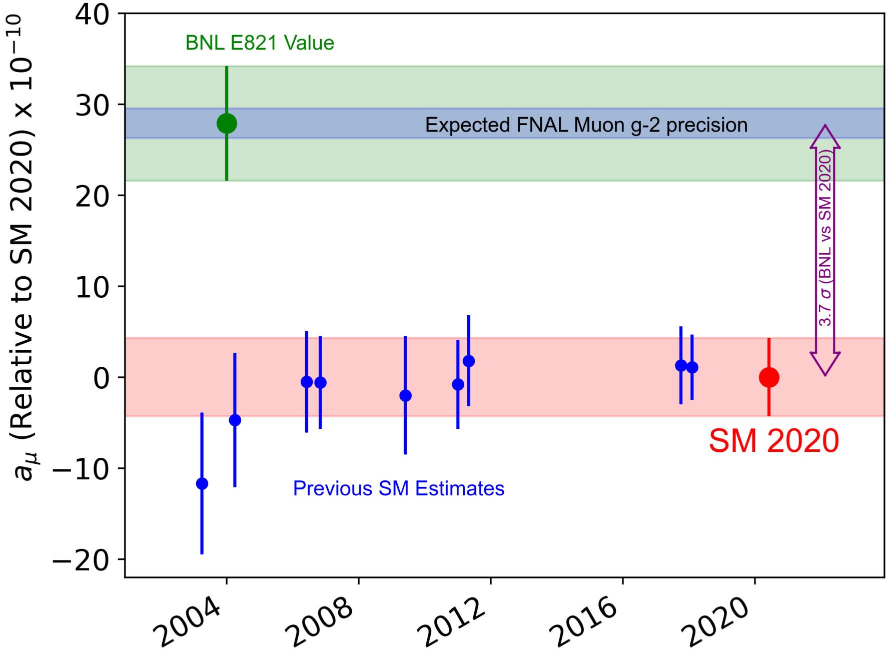

Experiment (BNL E821): $a_\mu^{\mathrm{BNL}} = 116592089 \pm 63$ (540 ppb)

Total SM prediction: $a_\mu^{\mathrm{SM}} = 116591810 \pm 43$ (368 ppb)

Discrepancy: $\Delta a_\mu = a_\mu^{\exp} - a_\mu^{\mathrm{SM}} = (279 \pm 76) \times 10^{-11}$

Evolved to 3.7 σ deviation between SM and BNL experiment!

Goal of the Muon g-2 experiment at Fermi National Laboratory

Reduction of experimental uncertainty by a factor 4!

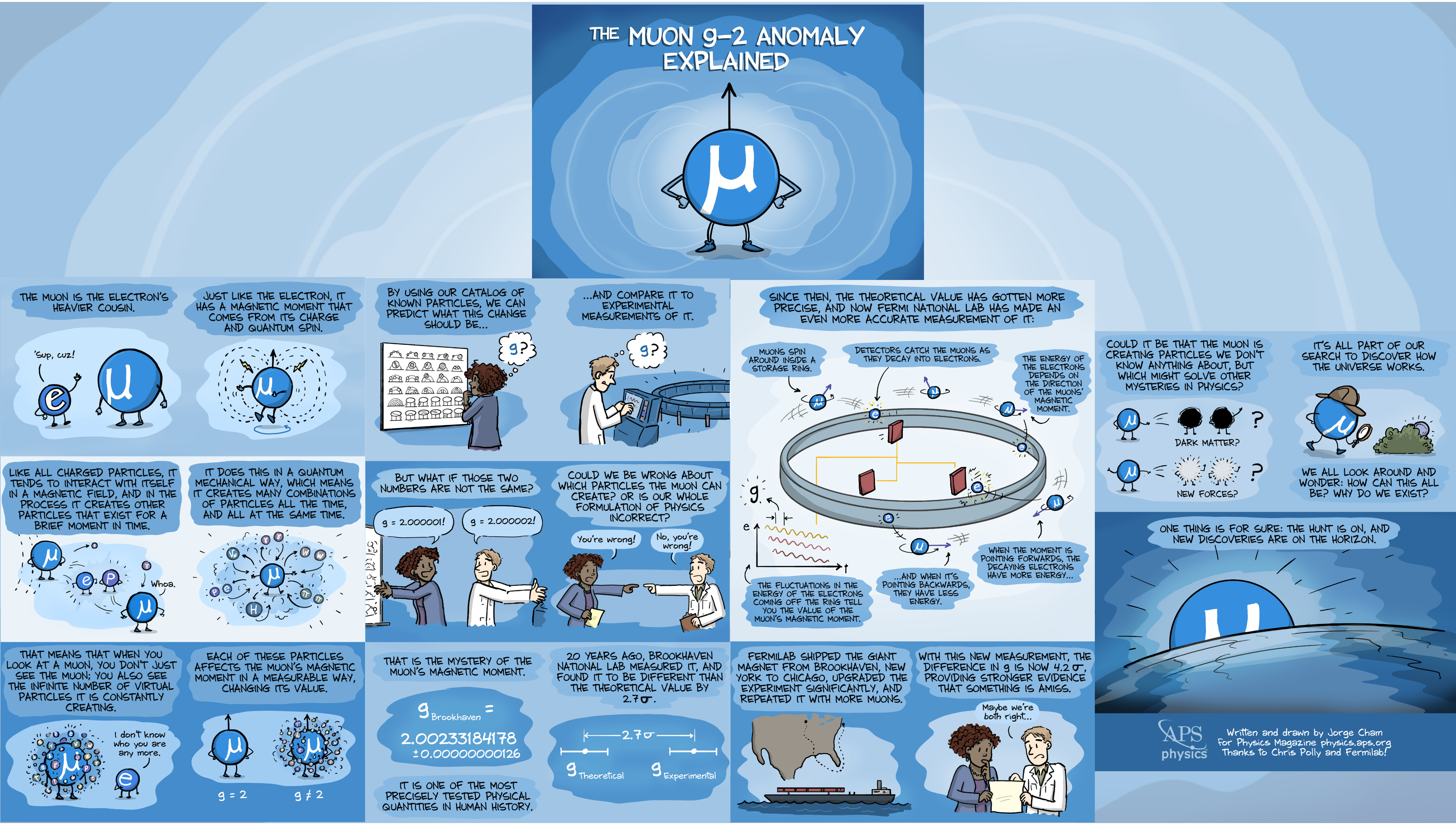
THE MUON g–2 ANOMALY EXPLAINED
THE MUON IS THE ELECTRON'S HEAVIER COUSIN.
'Sup, cuz!
JUST LIKE THE ELECTRON, IT HAS A MAGNETIC MOMENT THAT COMES FROM ITS CHARGE AND QUANTUM SPIN.
LIKE ALL CHARGED PARTICLES, IT TENDS TO INTERACT WITH ITSELF IN A MAGNETIC FIELD, AND IN THE PROCESS IT CREATES OTHER PARTICLES THAT EXIST FOR A BRIEF MOMENT IN TIME.
Whoa.
IT DOES THIS IN A QUANTUM MECHANICAL WAY, WHICH MEANS IT CREATES MANY COMBINATIONS OF PARTICLES ALL THE TIME, AND ALL AT THE SAME TIME.
THAT MEANS THAT WHEN YOU LOOK AT A MUON, YOU DON'T JUST SEE THE MUON; YOU ALSO SEE THE INFINITE NUMBER OF VIRTUAL PARTICLES IT IS CONSTANTLY CREATING.
I don't know who you are any more.
EACH OF THESE PARTICLES AFFECTS THE MUON'S MAGNETIC MOMENT IN A MEASURABLE WAY, CHANGING ITS VALUE.
g = 2
g ≠ 2
BY USING OUR CATALOG OF KNOWN PARTICLES, WE CAN PREDICT WHAT THIS CHANGE SHOULD BE...
g?
...AND COMPARE IT TO EXPERIMENTAL MEASUREMENTS OF IT.
g?
BUT WHAT IF THOSE TWO NUMBERS ARE NOT THE SAME?
g = 2.000001!
g = 2.000002!
COULD WE BE WRONG ABOUT WHICH PARTICLES THE MUON CAN CREATE? OR IS OUR WHOLE FORMULATION OF PHYSICS INCORRECT?
You're wrong!
No, you're wrong!
THAT IS THE MYSTERY OF THE MUON'S MAGNETIC MOMENT.
$g_{\text{Brookhaven}}$ =
2.00233184178
±0.00000000126
IT IS ONE OF THE MOST PRECISELY TESTED PHYSICAL QUANTITIES IN HUMAN HISTORY.
20 YEARS AGO, BROOKHAVEN NATIONAL LAB MEASURED IT, AND FOUND IT TO BE DIFFERENT THAN THE THEORETICAL VALUE BY 2.7σ.
2.7σ
$g_{\text{Theoretical}}$
$g_{\text{Experimental}}$
SINCE THEN, THE THEORETICAL VALUE HAS GOTTEN MORE PRECISE, AND NOW FERMI NATIONAL LAB HAS MADE AN EVEN MORE ACCURATE MEASUREMENT OF IT:
MUONS SPIN AROUND INSIDE A STORAGE RING.
DETECTORS CATCH THE MUONS AS THEY DECAY INTO ELECTRONS.
THE ENERGY OF THE ELECTRONS DEPENDS ON THE DIRECTION OF THE MUONS' MAGNETIC MOMENT.
g
e
t
THE FLUCTUATIONS IN THE ENERGY OF THE ELECTRONS COMING OFF THE RING TELL YOU THE VALUE OF THE MUON'S MAGNETIC MOMENT.
...AND WHEN IT'S POINTING BACKWARDS, THEY HAVE LESS ENERGY.
WHEN THE MOMENT IS POINTING FORWARDS, THE DECAYING ELECTRONS HAVE MORE ENERGY...
FERMILAB SHIPPED THE GIANT MAGNET FROM BROOKHAVEN, NEW YORK TO CHICAGO, UPGRADED THE EXPERIMENT SIGNIFICANTLY, AND REPEATED IT WITH MORE MUONS.
WITH THIS NEW MEASUREMENT, THE DIFFERENCE IN g IS NOW 4.2σ, PROVIDING STRONGER EVIDENCE THAT SOMETHING IS AMISS.
Maybe we're both right...
COULD IT BE THAT THE MUON IS CREATING PARTICLES WE DON'T KNOW ANYTHING ABOUT, BUT WHICH MIGHT SOLVE OTHER MYSTERIES IN PHYSICS?
DARK MATTER?
NEW FORCES?
IT'S ALL PART OF OUR SEARCH TO DISCOVER HOW THE UNIVERSE WORKS.
WE ALL LOOK AROUND AND WONDER: HOW CAN THIS ALL BE? WHY DO WE EXIST?
ONE THING IS FOR SURE: THE HUNT IS ON, AND NEW DISCOVERIES ARE ON THE HORIZON.
APS physics
Written and drawn by Jorge Cham
For Physics Magazine physics.aps.org
Thanks to Chris Polly and Fermilab!

The two clocks of a charged lepton

A *relativistic* charged lepton circulating a homogenous magnetic field experiences two effects:

The two clocks of a charged lepton

A *relativistic* charged lepton circulating a homogenous magnetic field experiences two effects:

Cyclotron motion

Equilibrium between centrifugal and Lorentz force

Cyclotron frequency

$$\vec{\omega}_{\mathrm{c}} = -\frac{Qe}{m\gamma}\vec{B}$$

The two clocks of a charged lepton

A *relativistic* charged lepton circulating a homogenous magnetic field experiences two effects:

Cyclotron motion

Equilibrium between centrifugal and Lorentz force

Cyclotron frequency

$$\vec{\omega}_{\mathrm{c}} = -\frac{Qe}{m\gamma}\vec{B}$$

Spin precession

Coupling of magnetic moment and field

Larmor frequency

$$\vec{\omega}_{\mathrm{s}} = -g\frac{Qe}{2m}\vec{B} - \left(1-\gamma\right)\frac{Qe}{\gamma m}\vec{B}$$

The two clocks of a charged lepton

A *relativistic* charged lepton circulating a homogenous magnetic field experiences two effects:

Cyclotron motion

Equilibrium between centrifugal and Lorentz force

Cyclotron frequency

$$\vec{\omega}_{\mathrm{c}} = -\frac{Qe}{m\gamma}\vec{B}$$

Spin precession

Coupling of magnetic moment and field

Larmor frequency

$$\vec{\omega}_{\mathrm{s}} = -g\frac{Qe}{2m}\vec{B} - (1-\gamma)\frac{Qe}{\gamma m}\vec{B}$$

Anomalous spin precession frequency

$$\vec{\omega}_{\mathrm{a}} = \vec{\omega}_{\mathrm{s}} - \vec{\omega}_{\mathrm{c}} = -\left(\frac{g-2}{2}\right)\vec{B} = -a\frac{Qe}{m}\vec{B}$$

The two clocks of a charged lepton

A *relativistic* charged lepton circulating a homogenous magnetic field experiences two effects:

<u>Cyclotron motion</u>

Equilibrium between centrifugal and Lorentz force

<u>Cyclotron frequency</u>

$$\vec{\omega}_{\mathrm{c}} = -\frac{Qe}{m\gamma}\vec{B}$$

<u>Spin precession</u>

Coupling of magnetic moment and field

<u>Larmor frequency</u>

$$\vec{\omega}_{\mathrm{s}} = -g\frac{Qe}{2m}\vec{B} - (1-\gamma)\frac{Qe}{\gamma m}\vec{B}$$

<u>Anomalous spin precession frequency</u>

$$\vec{\omega}_{\mathrm{a}} = \vec{\omega}_{\mathrm{s}} - \vec{\omega}_{\mathrm{c}} = -\left(\frac{g-2}{2}\right)\vec{B} = -a\frac{Qe}{m}\vec{B}$$

Independent of particle momentum!

The two clocks of a charged lepton

A *relativistic* charged lepton circulating a homogenous magnetic field experiences two effects:

<u>Cyclotron motion</u>

Equilibrium between centrifugal and Lorentz force

<u>Cyclotron frequency</u>

$$\vec{\omega}_c = -\frac{Qe}{m\gamma}\vec{B}$$

<u>Spin precession</u>

Coupling of magnetic moment and field

<u>Larmor frequency</u>

$$\vec{\omega}_s = -g\frac{Qe}{2m}\vec{B} - (1-\gamma)\frac{Qe}{\gamma m}\vec{B}$$

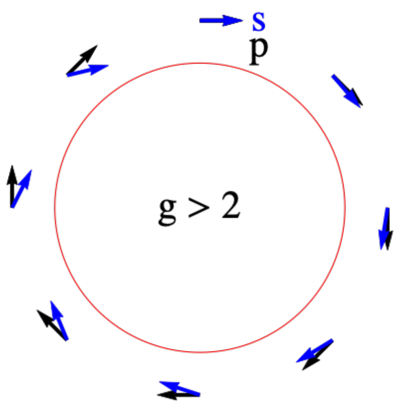

<u>Anomalous spin precession frequency</u>

$$\vec{\omega}_a = \vec{\omega}_s - \vec{\omega}_c = -\left(\frac{g-2}{2}\right)\vec{B} = -a\frac{Qe}{m}\vec{B}$$

Independent of particle momentum!

Clock frequency shifts for muons in motion

For muons moving relativistically in a superposition of general electric and magnetic fields

$$\vec{\omega}_{\mathrm{a}} = \vec{\omega}_{\mathrm{s}} - \vec{\omega}_{\mathrm{c}} = -\frac{e}{m}\left[a_{\mu}\vec{B} - a_{\mu}\left(\frac{\gamma}{\gamma+1}\right)\left(\vec{\beta}\cdot\vec{B}\right)\vec{\beta} - \left(a_{\mu} - \frac{1}{\gamma^{2}-1}\right)\frac{\vec{\beta}\times\vec{E}}{c}\right]$$

Clock frequency shifts for muons in motion

For muons moving relativistically in a superposition of general electric and magnetic fields

$$\vec{\omega}_{\mathrm{a}} = \vec{\omega}_{\mathrm{s}} - \vec{\omega}_{\mathrm{c}} = -\frac{e}{m}\left[a_\mu \vec{B} - a_\mu \left(\frac{\gamma}{\gamma+1}\right)\left(\vec{\beta}\cdot\vec{B}\right)\vec{\beta} - \left(a_\mu - \frac{1}{\gamma^2-1}\right)\frac{\vec{\beta}\times\vec{E}}{c}\right]$$

Non-relativistic and
circular motion limit

Clock frequency shifts for muons in motion

For muons moving relativistically in a superposition of general electric and magnetic fields

$$\vec{\omega}_{\mathrm{a}} = \vec{\omega}_{\mathrm{s}} - \vec{\omega}_{\mathrm{c}} = -\frac{e}{m}\left[a_\mu \vec{B} - a_\mu \left(\frac{\gamma}{\gamma+1}\right)\left(\vec{\beta}\cdot\vec{B}\right)\vec{\beta} - \left(a_\mu - \frac{1}{\gamma^2-1}\right)\frac{\vec{\beta}\times\vec{E}}{c}\right]$$

Non-relativistic and
circular motion limit

Vertical muon motion along
the magnetic field lines
“pitch correction”

Clock frequency shifts for muons in motion

For muons moving relativistically in a superposition of general electric and magnetic fields

$$\vec{\omega}_{\mathrm{a}} = \vec{\omega}_{\mathrm{s}} - \vec{\omega}_{\mathrm{c}} = -\frac{e}{m}\left[a_\mu \vec{B} - a_\mu \left(\frac{\gamma}{\gamma+1}\right)\left(\vec{\beta}\cdot\vec{B}\right)\vec{\beta} - \left(a_\mu - \frac{1}{\gamma^2-1}\right)\frac{\vec{\beta}\times\vec{E}}{c}\right]$$

Non-relativistic and circular motion limit

Vertical muon motion along the magnetic field lines "pitch correction"

Relativistically generated magnetic field "electric field correction"

Clock frequency shifts for muons in motion

For muons moving relativistically in a superposition of general electric and magnetic fields

$$\vec{\omega}_{\mathrm{a}} = \vec{\omega}_{\mathrm{s}} - \vec{\omega}_{\mathrm{c}} = -\frac{e}{m}\left[a_\mu \vec{B} - a_\mu \left(\frac{\gamma}{\gamma+1}\right)\left(\vec{\beta}\cdot\vec{B}\right)\vec{\beta} - \left(a_\mu - \frac{1}{\gamma^2-1}\right)\frac{\vec{\beta}\times\vec{E}}{c}\right]$$

Non-relativistic and circular motion limit

Vertical muon motion along the magnetic field lines "pitch correction"

Relativistically generated magnetic field "electric field correction"

Magnetic field maps and temporal interpolation

Clock frequency shifts for muons in motion

For muons moving relativistically in a superposition of general electric and magnetic fields

$$\vec{\omega}_{\mathrm{a}} = \vec{\omega}_{\mathrm{s}} - \vec{\omega}_{\mathrm{c}} = -\frac{e}{m}\left[a_\mu \vec{B} - a_\mu \left(\frac{\gamma}{\gamma+1}\right)\left(\vec{\beta}\cdot\vec{B}\right)\vec{\beta} - \left(a_\mu - \frac{1}{\gamma^2-1}\right)\frac{\vec{\beta}\times\vec{E}}{c}\right]$$

Non-relativistic and circular motion limit

Vertical muon motion along the magnetic field lines "pitch correction"

Relativistically generated magnetic field "electric field correction"

Magnetic field maps and temporal interpolation

Reconstruction of complex beam dynamics

Clock frequency shifts for muons in motion

For muons moving relativistically in a superposition of general electric and magnetic fields

$$\vec{\omega}_{\mathrm{a}} = \vec{\omega}_{\mathrm{s}} - \vec{\omega}_{\mathrm{c}} = -\frac{e}{m}\left[a_\mu \vec{B} - a_\mu \left(\frac{\gamma}{\gamma+1}\right)\left(\vec{\beta}\cdot\vec{B}\right)\vec{\beta} - \left(a_\mu - \frac{1}{\gamma^2-1}\right)\frac{\vec{\beta}\times\vec{E}}{c}\right]$$

Non-relativistic and circular motion limit

Vertical muon motion along the magnetic field lines "pitch correction"

Relativistically generated magnetic field "electric field correction"

Magnetic field maps and temporal interpolation

Reconstruction of complex beam dynamics

FNAL E989: $E \neq 0$ suppressed at $\gamma = 29.3$ "magic momentum"

The muon g-2 experiment at Fermilab

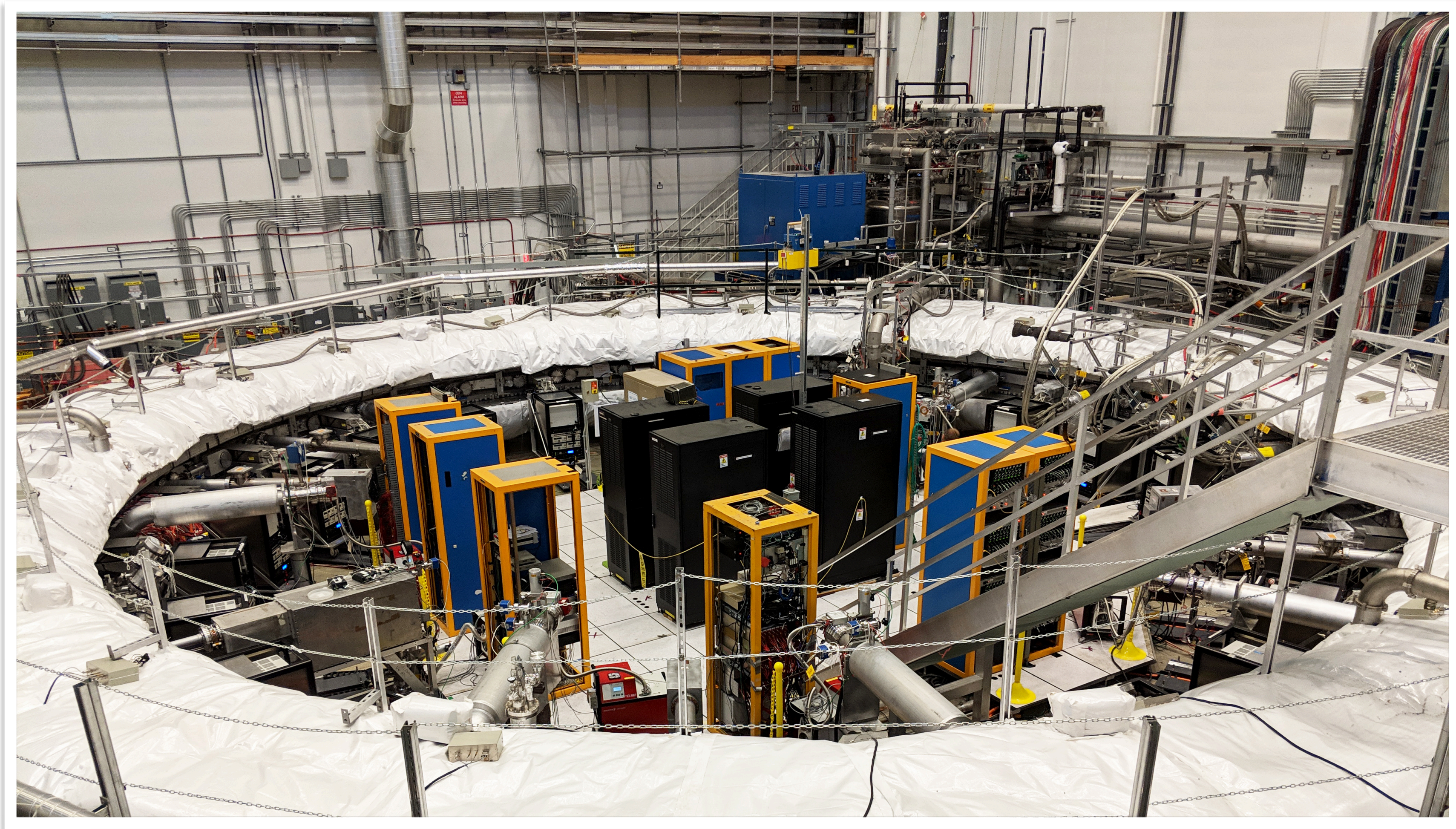

JG|U

The Muon g-2 collaboration

Domestic Universities
- Boston
- Cornell
- Illinois
- James Madison
- Kentucky
- Massachusetts
- Michigan
- Michigan State
- Mississippi
- Northern Illinois
- Regis
- UT Austin
- Virginia
- Washington

National Labs
- Argonne
- Brookhaven
- Fermilab

China
- Shanghai Jao Tong University

United Kingdom
- Lancaster
- Liverpool
- University College London

Italy
- Frascati
- Molise
- Naples
- Pisa
- Roma 2
- Trieste
- Udine

Germany
- JGU Mainz
- TU Dresden

Russia
- JINR/Dubna
- Novosibirsk

South Korea
- CAPP/IBS
- KAIST

The Fermilab muon campus

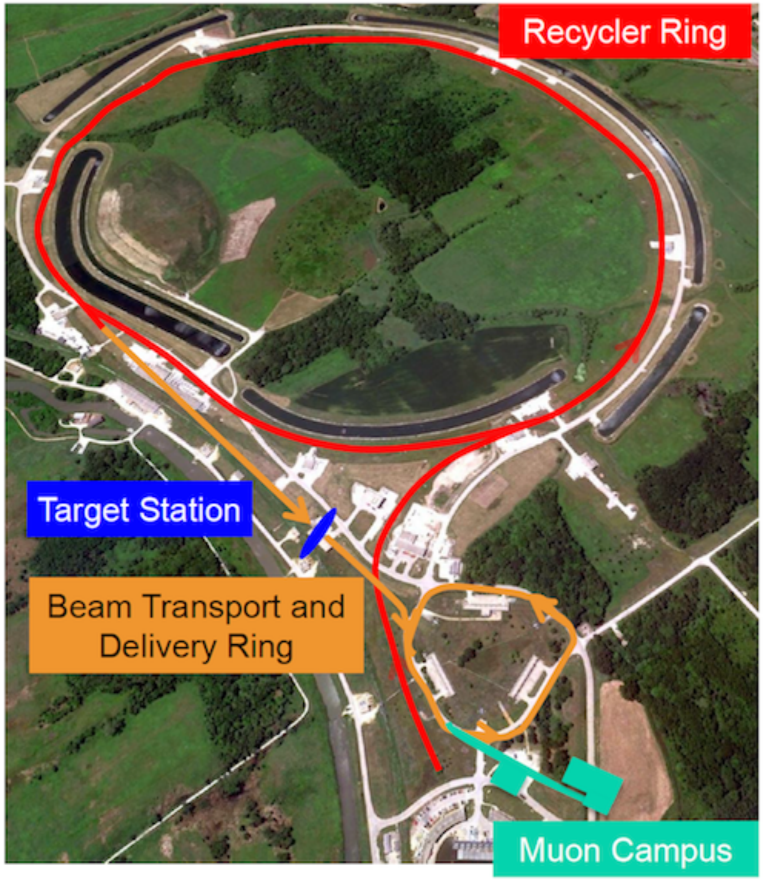

Figure courtesy: M. Convery

The Fermilab muon campus

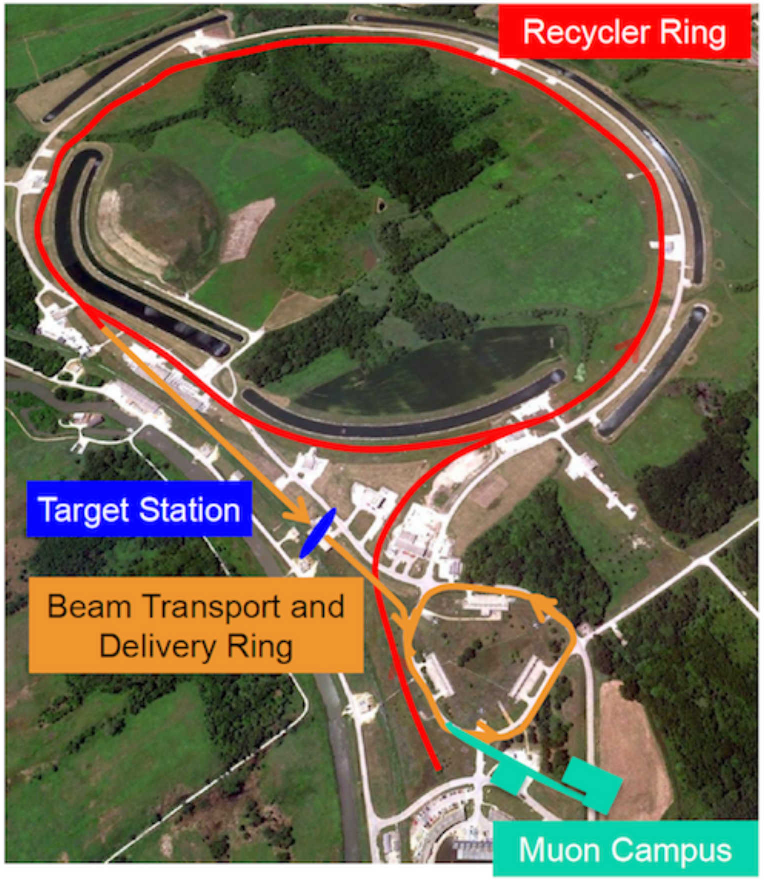

Figure courtesy: M. Convery

A bright source of pulsed polarized muons is needed!

The Fermilab muon campus

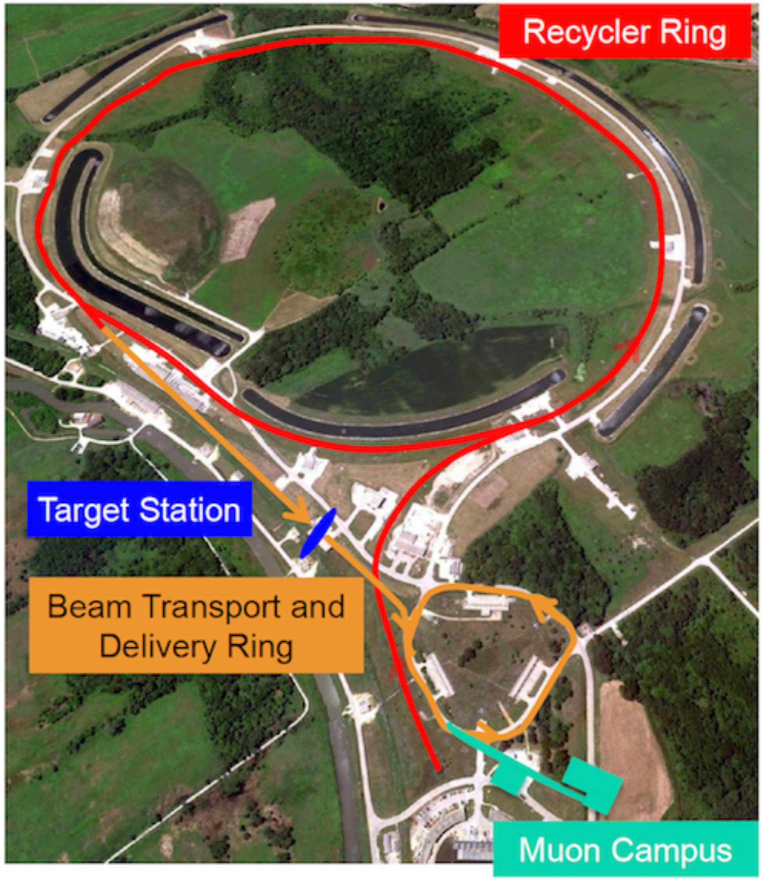

Figure courtesy: M. Convery

A bright source of pulsed polarized muons is needed!

8 GeV p^+ strike target, 120 ns bunch length

The Fermilab muon campus

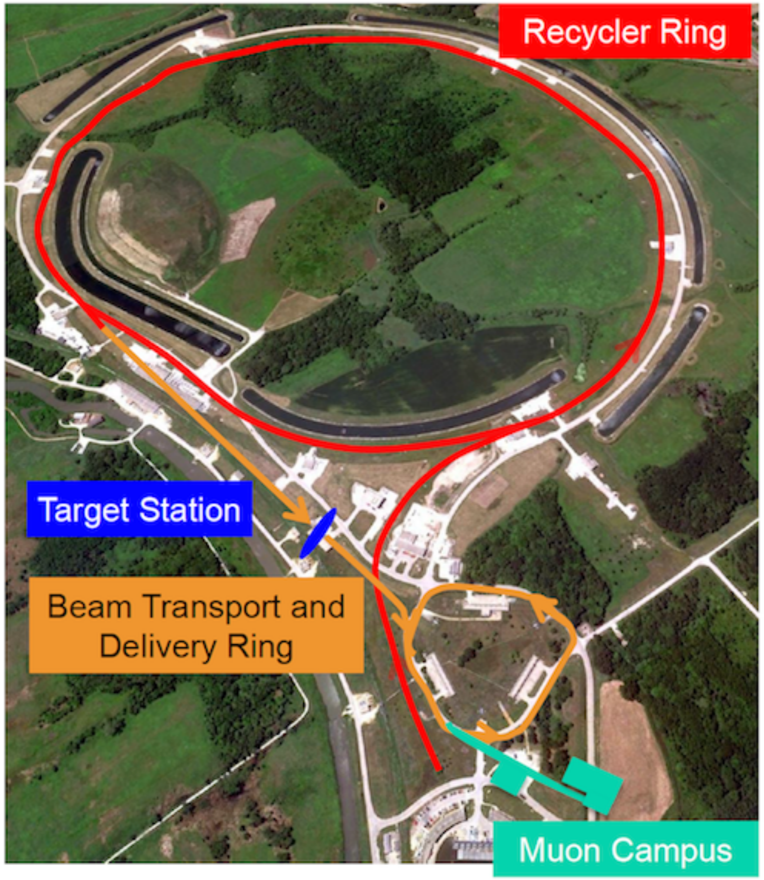

Figure courtesy: M. Convery

A bright source of pulsed polarized muons is needed!

8 GeV p^+ strike target, 120 ns bunch length

8 bunches spaced by 10 ms, second bunch train 200 ms later

The Fermilab muon campus

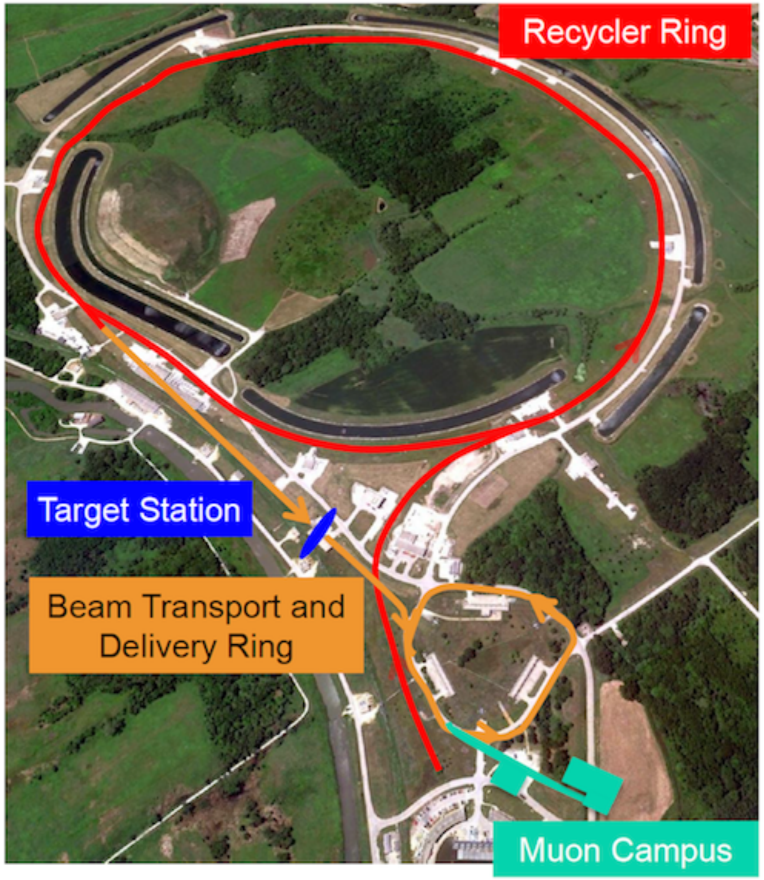

Figure courtesy: M. Convery

A bright source of pulsed polarized muons is needed!

8 GeV p^+ strike target, 120 ns bunch length

8 bunches spaced by 10 ms, second bunch train 200 ms later

Pion production in the target:

$$p^+ + p^+ \rightarrow p^+ + n + \pi^+$$

The Fermilab muon campus

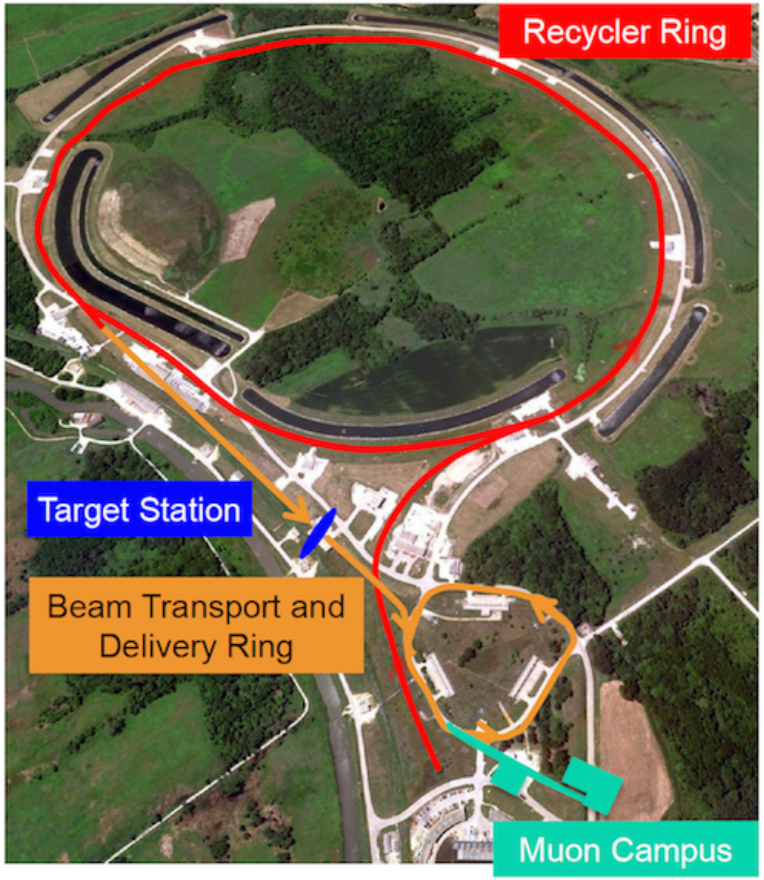

Figure courtesy: M. Convery

A bright source of pulsed polarized muons is needed!

8 GeV p^+ strike target, 120 ns bunch length

8 bunches spaced by 10 ms, second bunch train 200 ms later

Pion production in the target:

$$p^+ + p^+ \rightarrow p^+ + n + \pi^+$$

Focus the “debris” into a momentum selective beam line

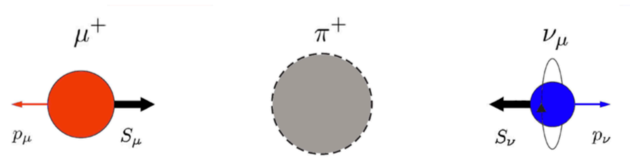

ν_μ must be left-handed → μ^+ also left-handed!

Figures: K.S. Khaw, PhD thesis, ETH Zürich, 2015

The weak interaction is not left-right-symmetric!

Figure: R. Hahn, Fermilab in the context of “Charge-parity violation“
https://www.symmetrymagazine.org/article/charge-parity-violation

The Fermilab muon campus

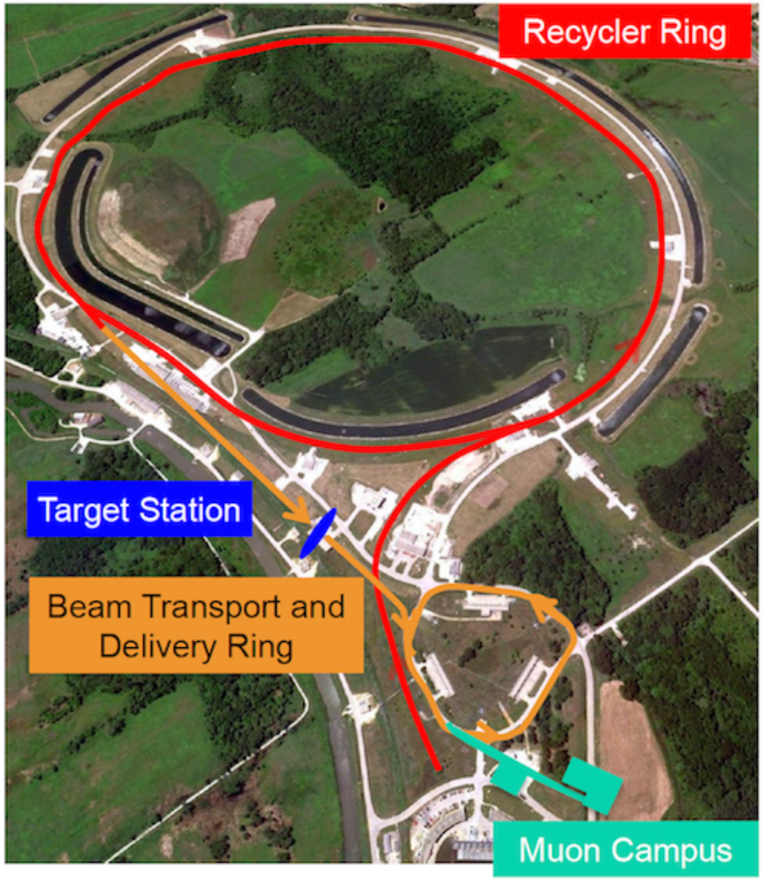

Figure courtesy: M. Convery

The Fermilab muon campus

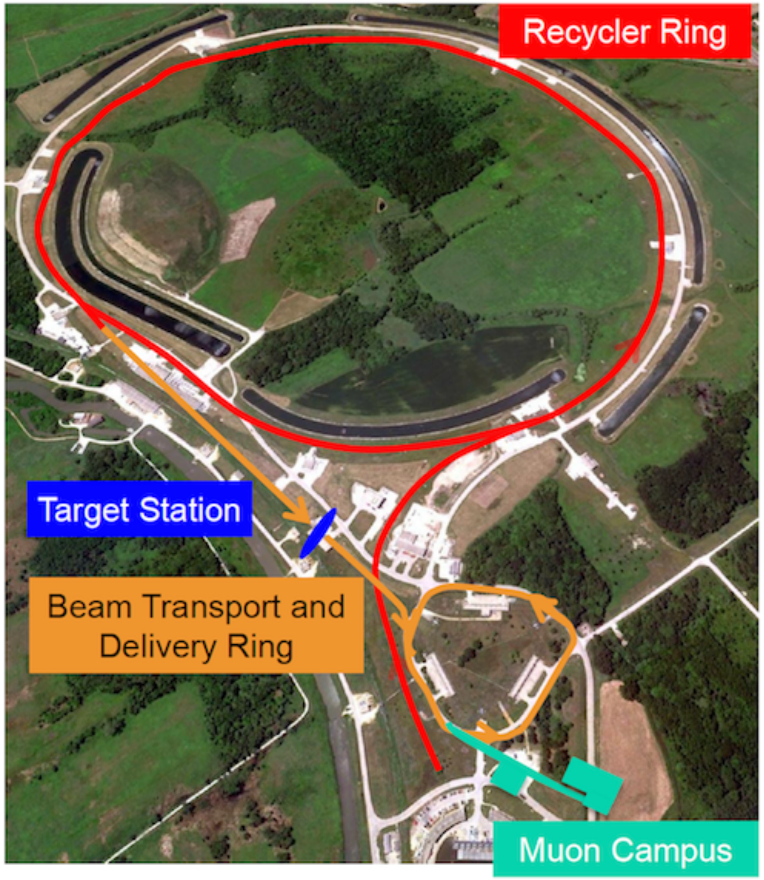

Figure courtesy: M. Convery

M2/M3 optimized to transport positive particles with

$$p = 3.094\,\mathrm{GeV/c} \pm 2\,\%$$

The Fermilab muon campus

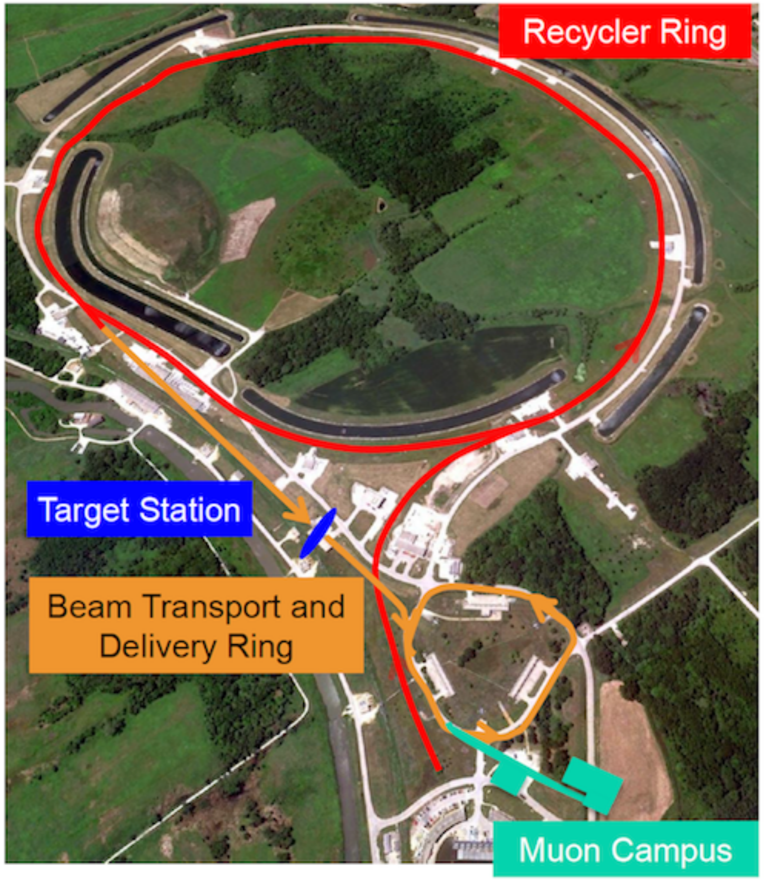

Figure courtesy: M. Convery

M2/M3 optimized to transport positive particles with

$$p = 3.094\,\mathrm{GeV/c} \pm 2\,\%$$

At the end of M2 and M3 beam line:

- 80% of pions have decayed to muons (polarization ~95%)
- 20% beam contamination: decay e^+, surviving π^+, p^+ from the primary beam

The Fermilab muon campus

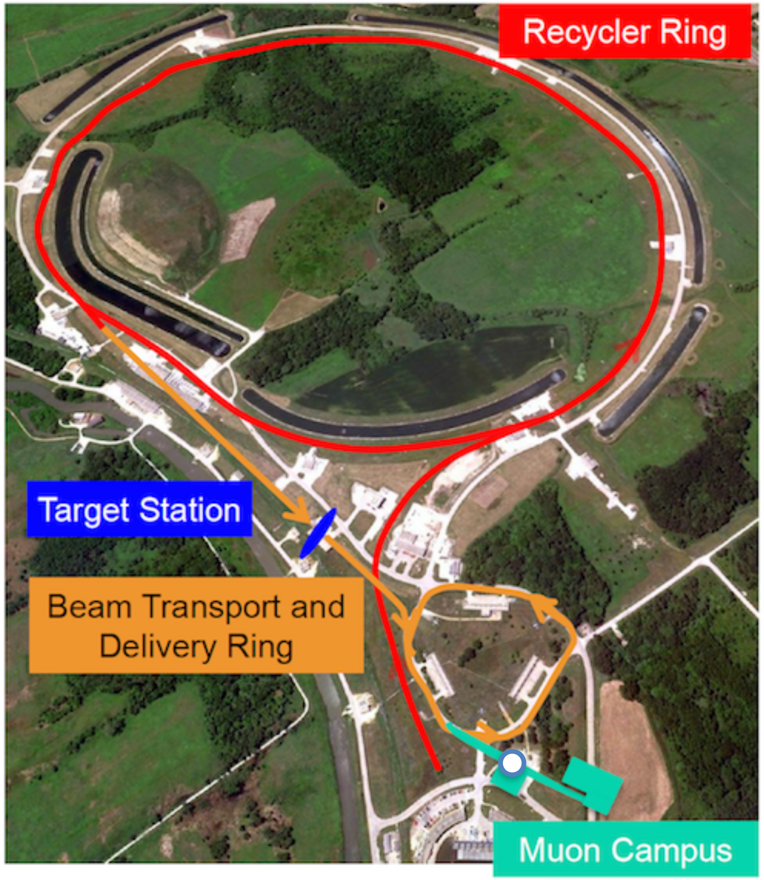

Figure courtesy: M. Convery

M2/M3 optimized to transport positive particles with

$$p = 3.094\,\mathrm{GeV/c} \pm 2\,\%$$

At the end of M2 and M3 beam line:

- 80% of pions have decayed to muons (polarization ~95%)
- 20% beam contamination:
  decay e^+, surviving π^+, p^+ from the primary beam

Beam purification in energy-dispersive delivery ring:
μ^+ outrun p^+, π^+ decay away

The Fermilab muon campus

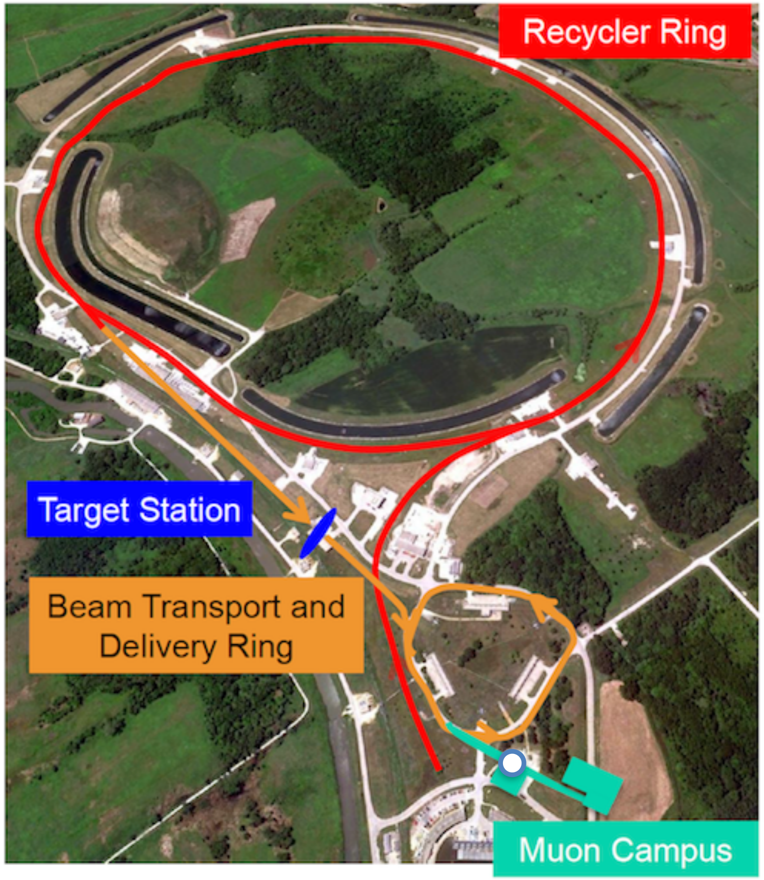

Figure courtesy: M. Convery

M2/M3 optimized to transport positive particles with

$$p = 3.094\,\mathrm{GeV/c} \pm 2\,\%$$

At the end of M2 and M3 beam line:

- 80% of pions have decayed to muons (polarization ~95%)
- 20% beam contamination:
  decay e^+, surviving π^+, p^+ from the primary beam

Beam purification in energy-dispersive delivery ring:
μ^+ outrun p^+, π^+ decay away

Pure lepton beam: 60 - 70% μ^+, 30 - 40% e^+

From Upton, NY to Batavia, IL

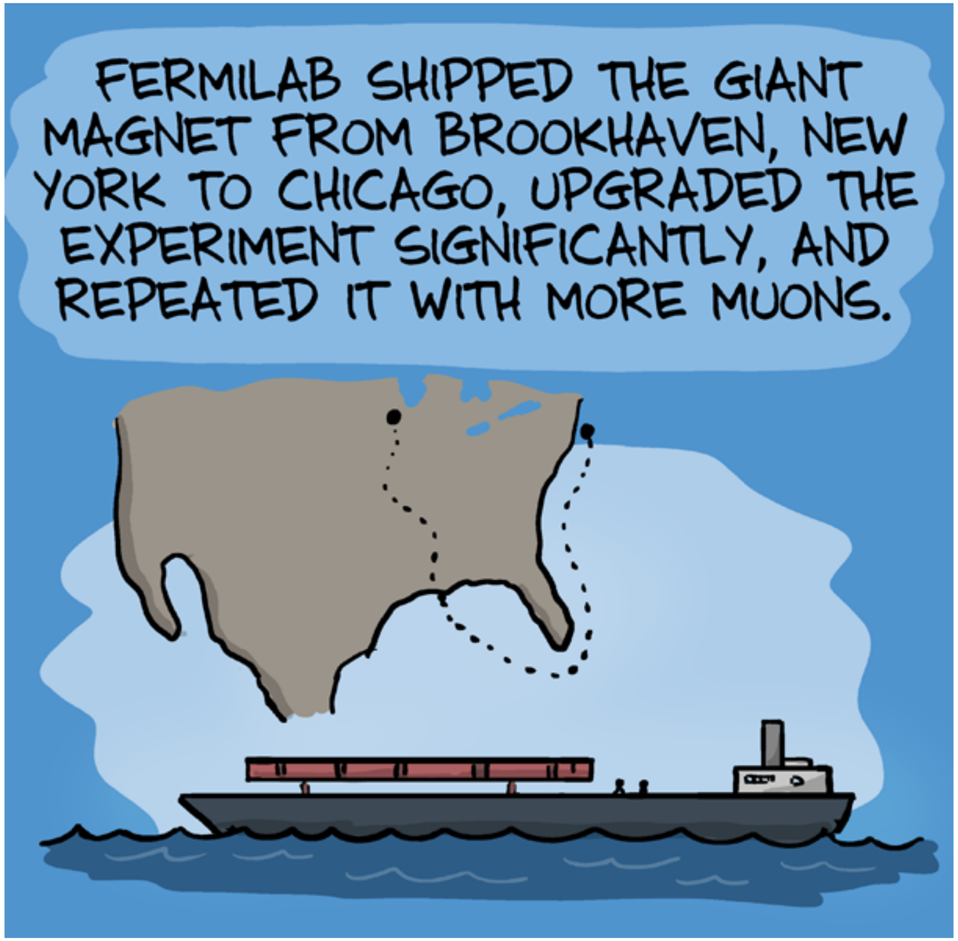

From Upton, NY to Batavia, IL

The superconducting magnet in MC1

Particles from delivery ring

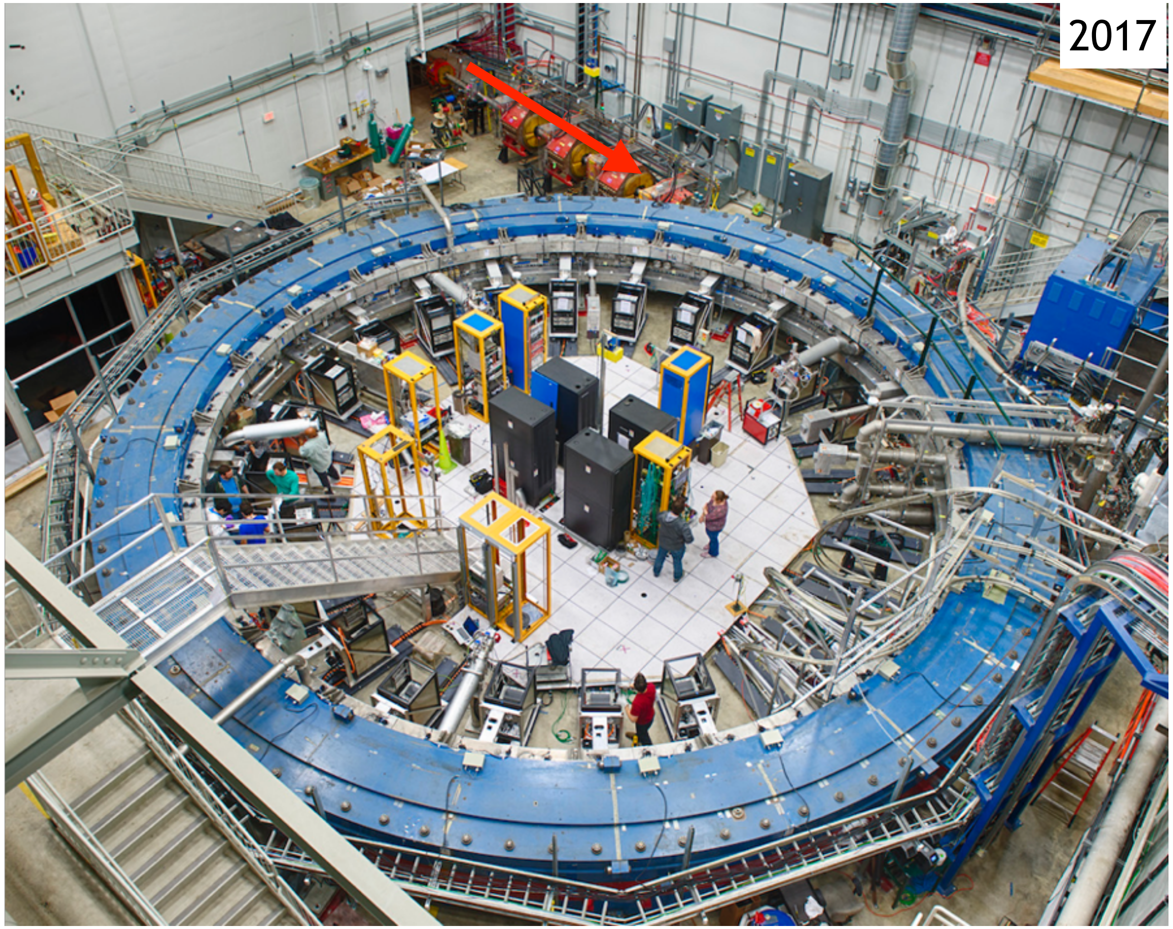

Magic momentum: $p_\mu^{\text{magic}} = 3.094\,\mathrm{GeV/c} \pm 0.5\,\%$

The superconducting magnet in MC1

Particles from delivery ring

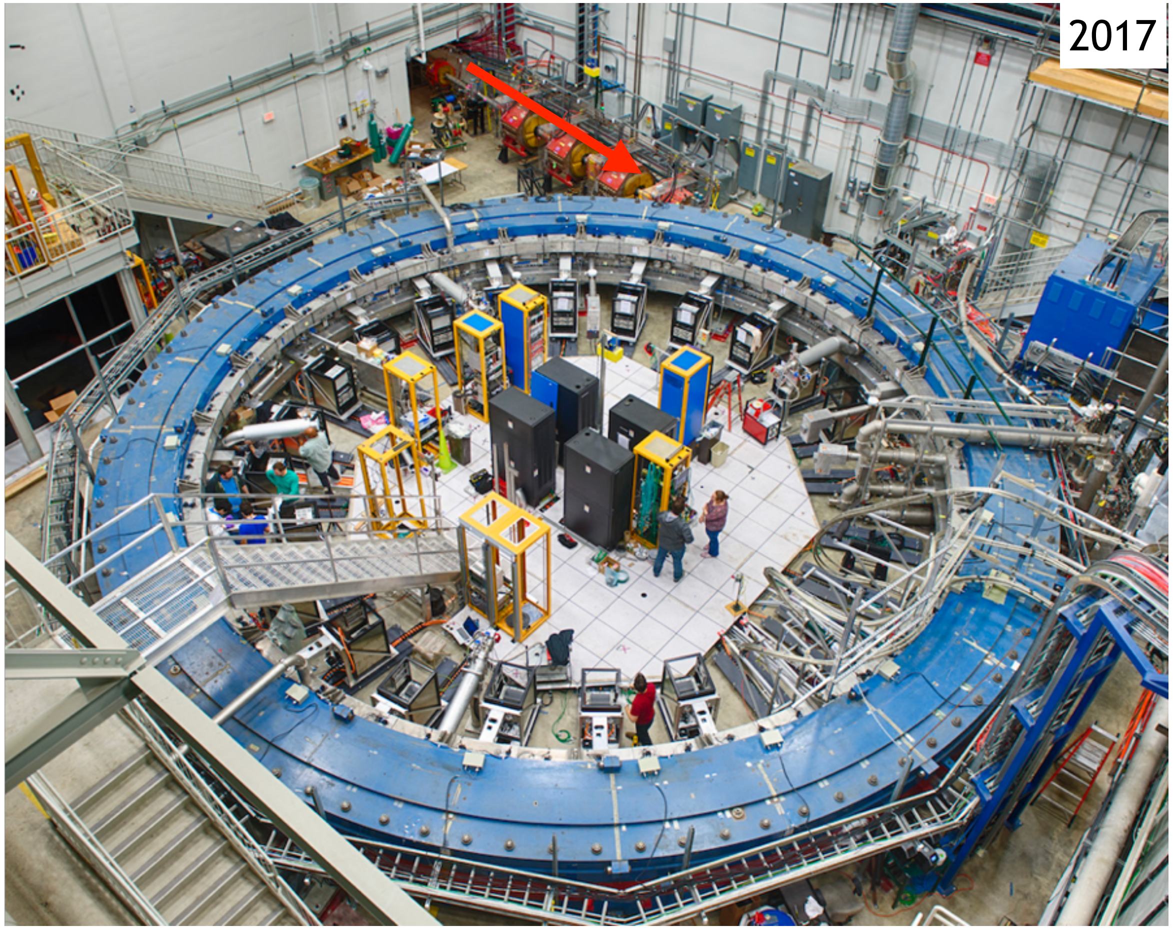

Magic momentum: $p_\mu^{\text{magic}} = 3.094\,\text{GeV/c} \pm 0.5\,\%$

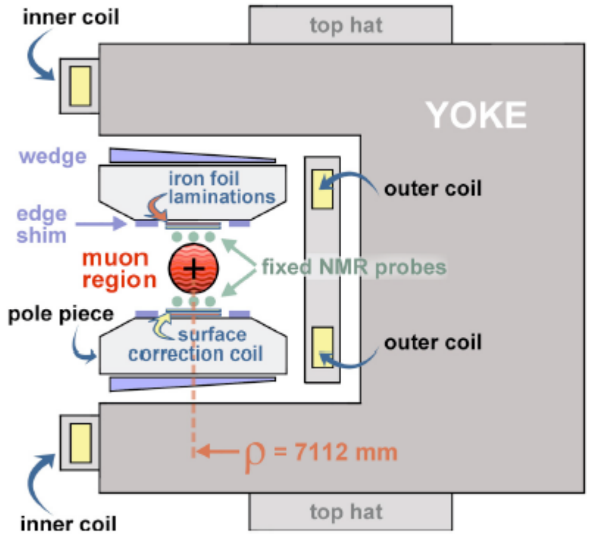

3 cryostats with 4 superconducting coils (5300 A)
1.45 T vertical magnetic field
90 mm muon storage region
180 mm gap for vacuum chambers

The muon inflector magnet

Particles from delivery ring

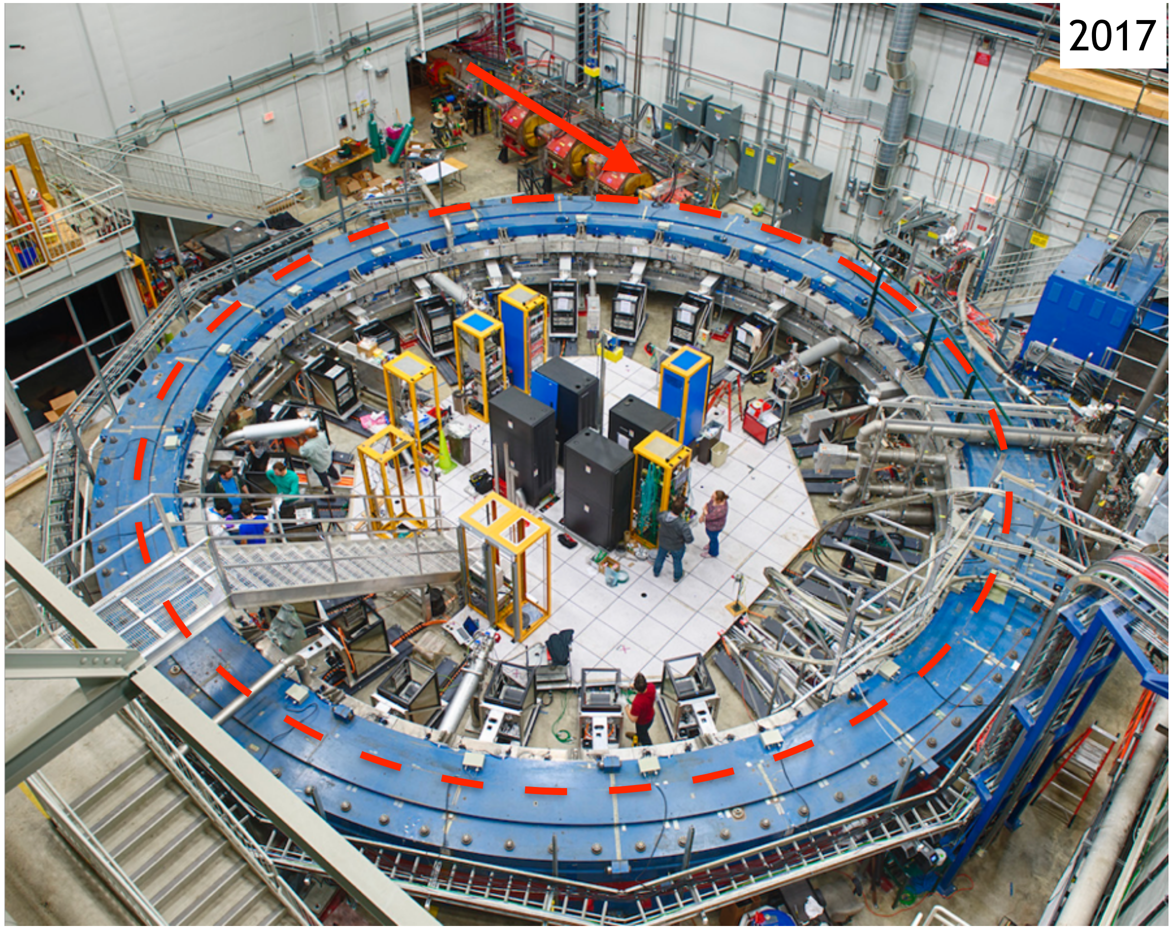

2017

Superconducting inflector magnet cancels return B field in iron yoke to make muon travel straight!

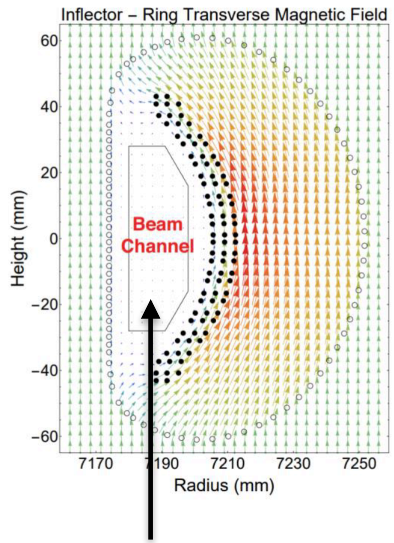

Field free region

The fast kicker

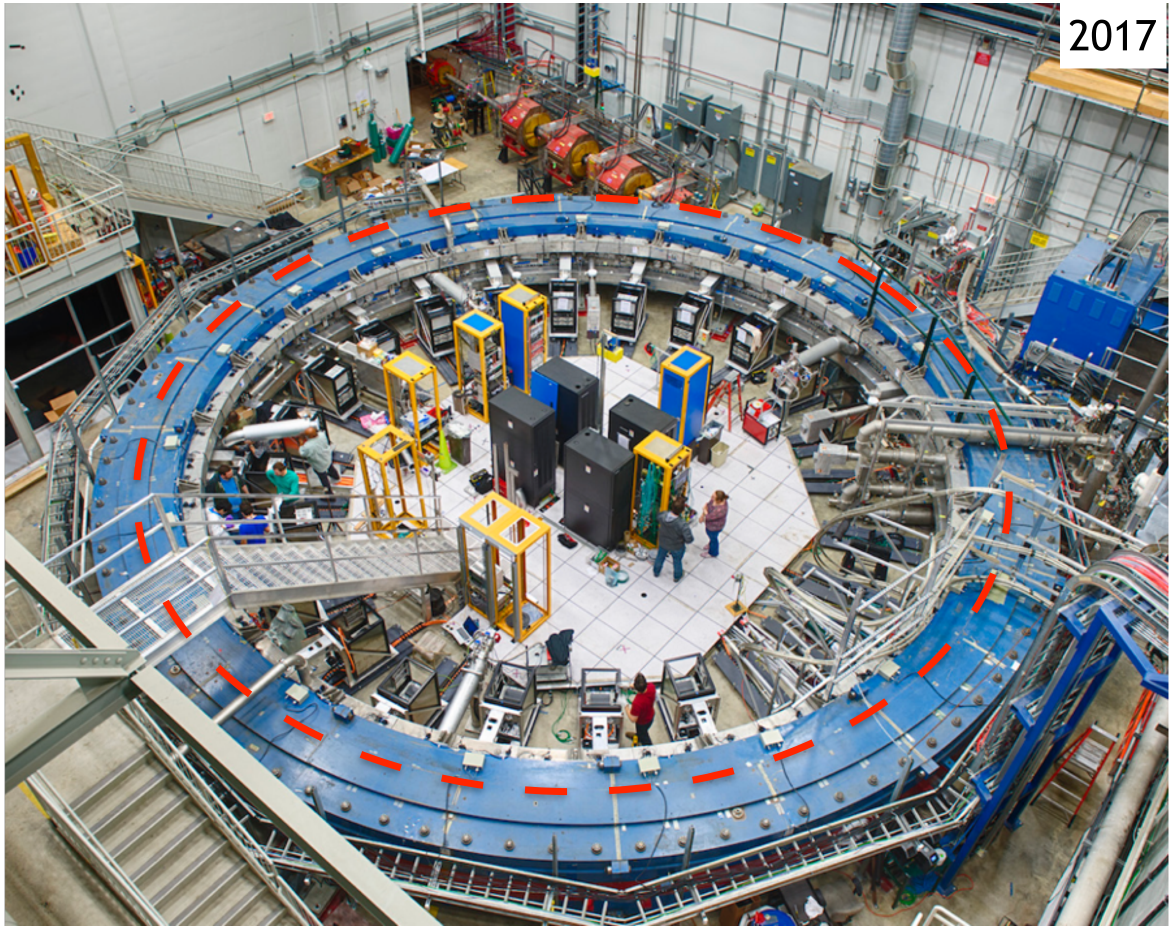

Kick the muons on their storage orbit within one revolution (≈ 150 ns)

The fast kicker

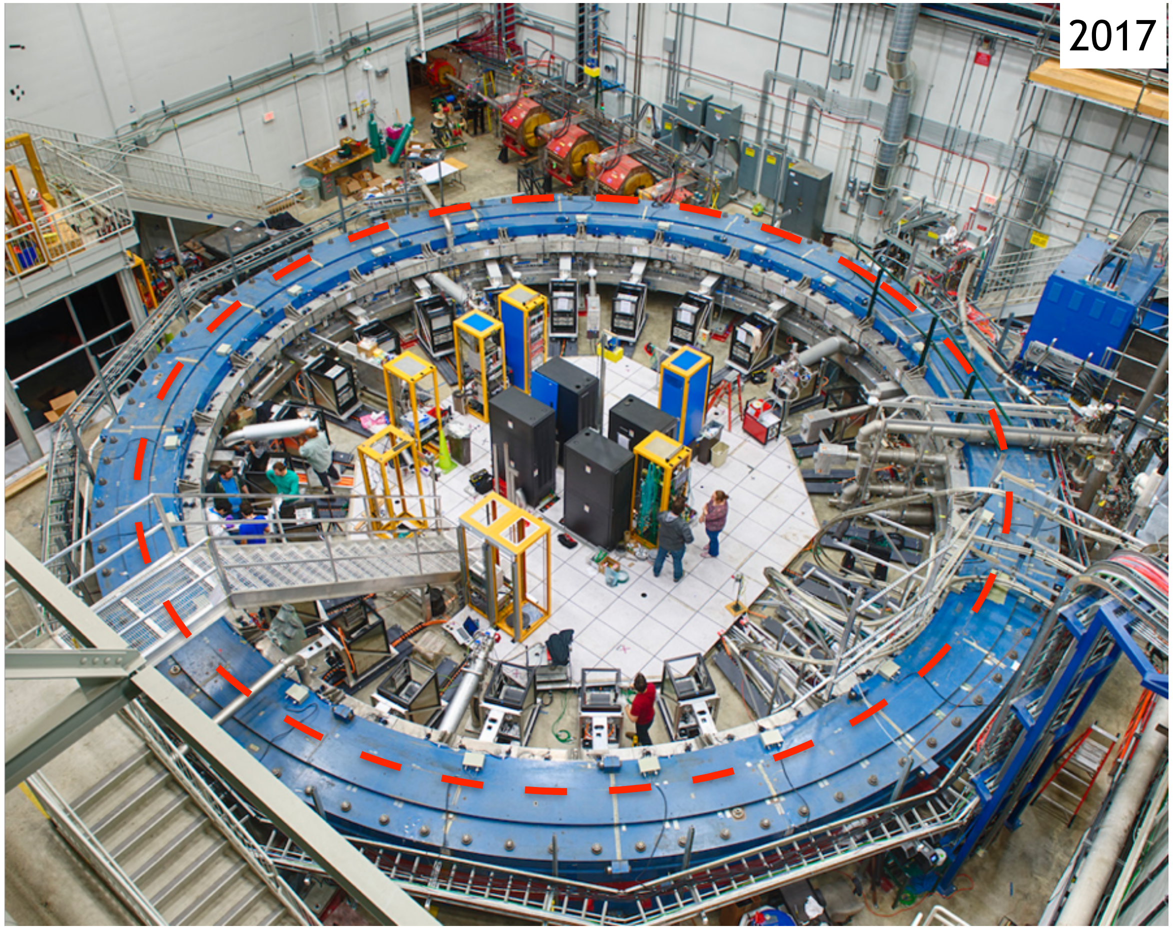

Kick the muons on their storage orbit within one revolution (≈ 150 ns)

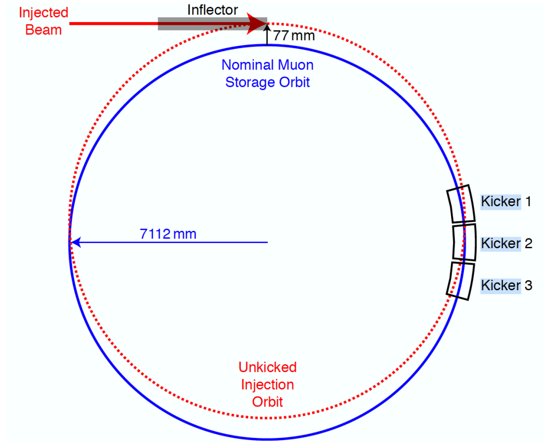

The fast kicker

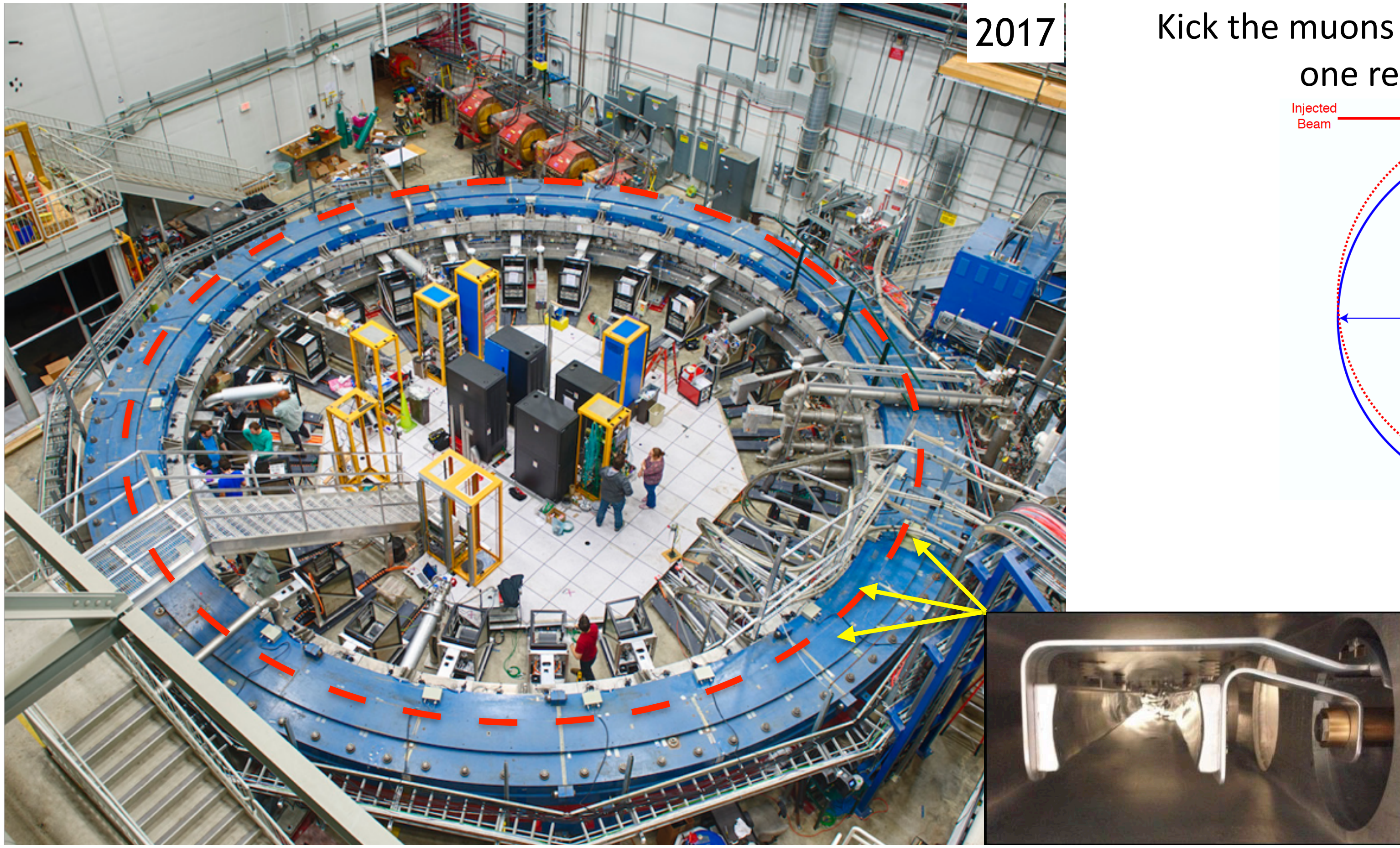

Kick the muons on their storage orbit within one revolution (≈ 150 ns)

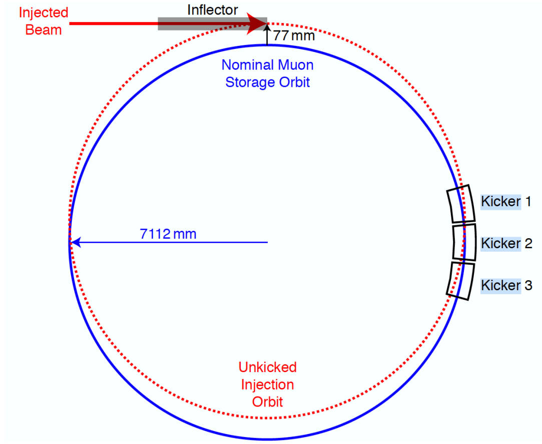

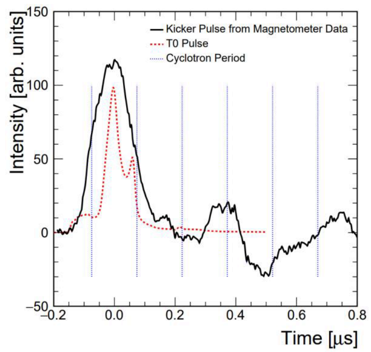

The fast kicker

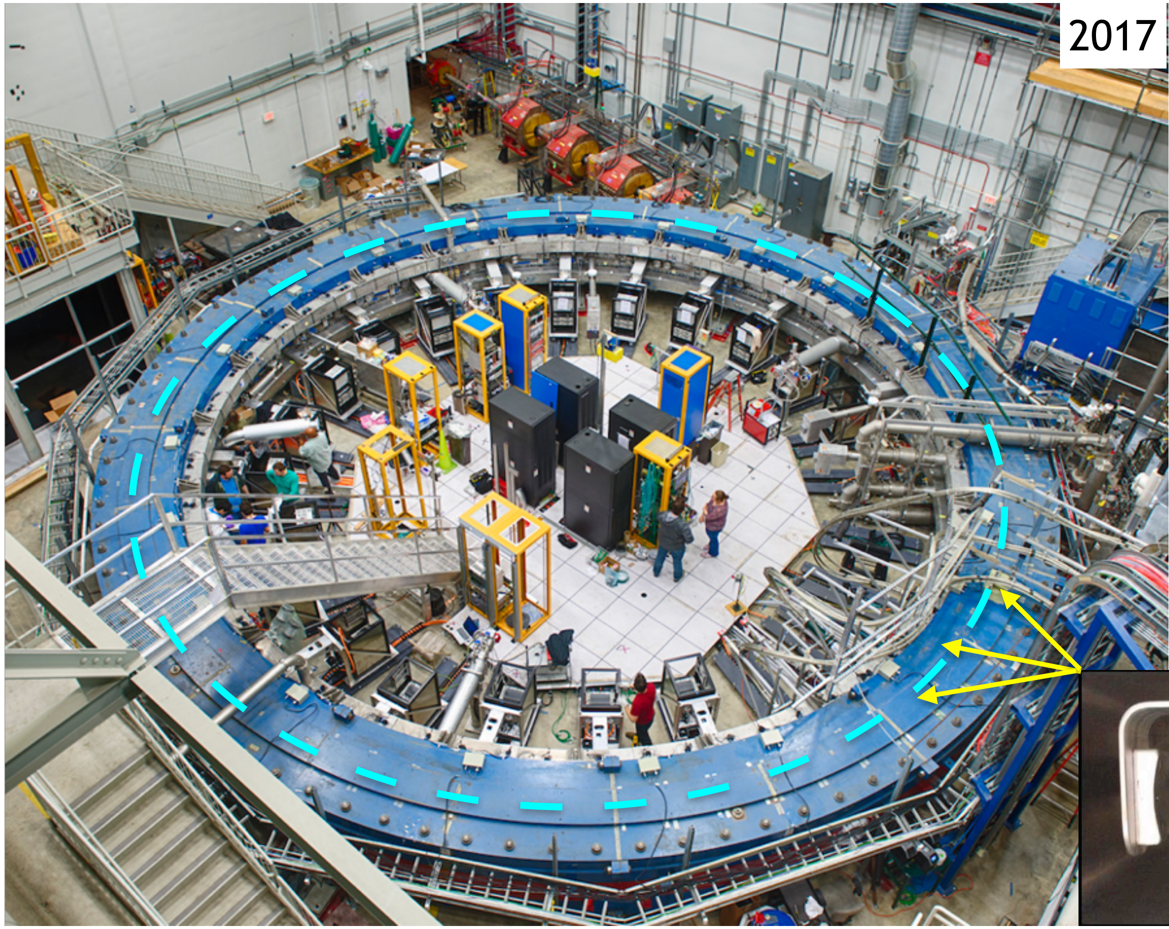

Kick the muons on their storage orbit within one revolution (≈ 150 ns)

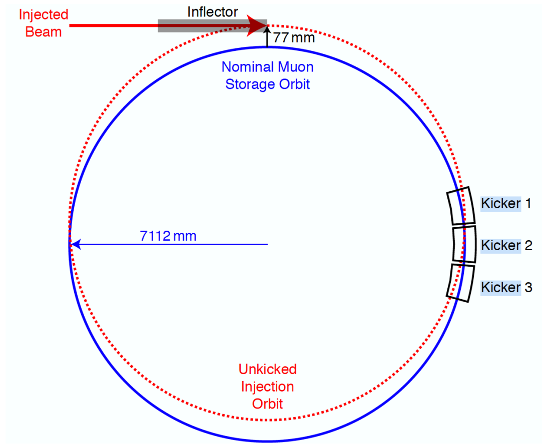

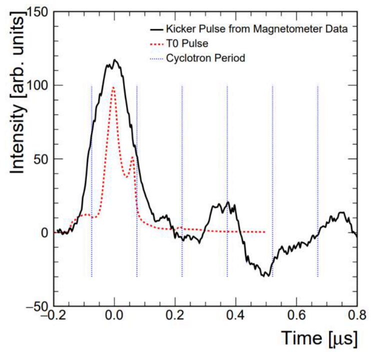

The electrostatic quadrupoles

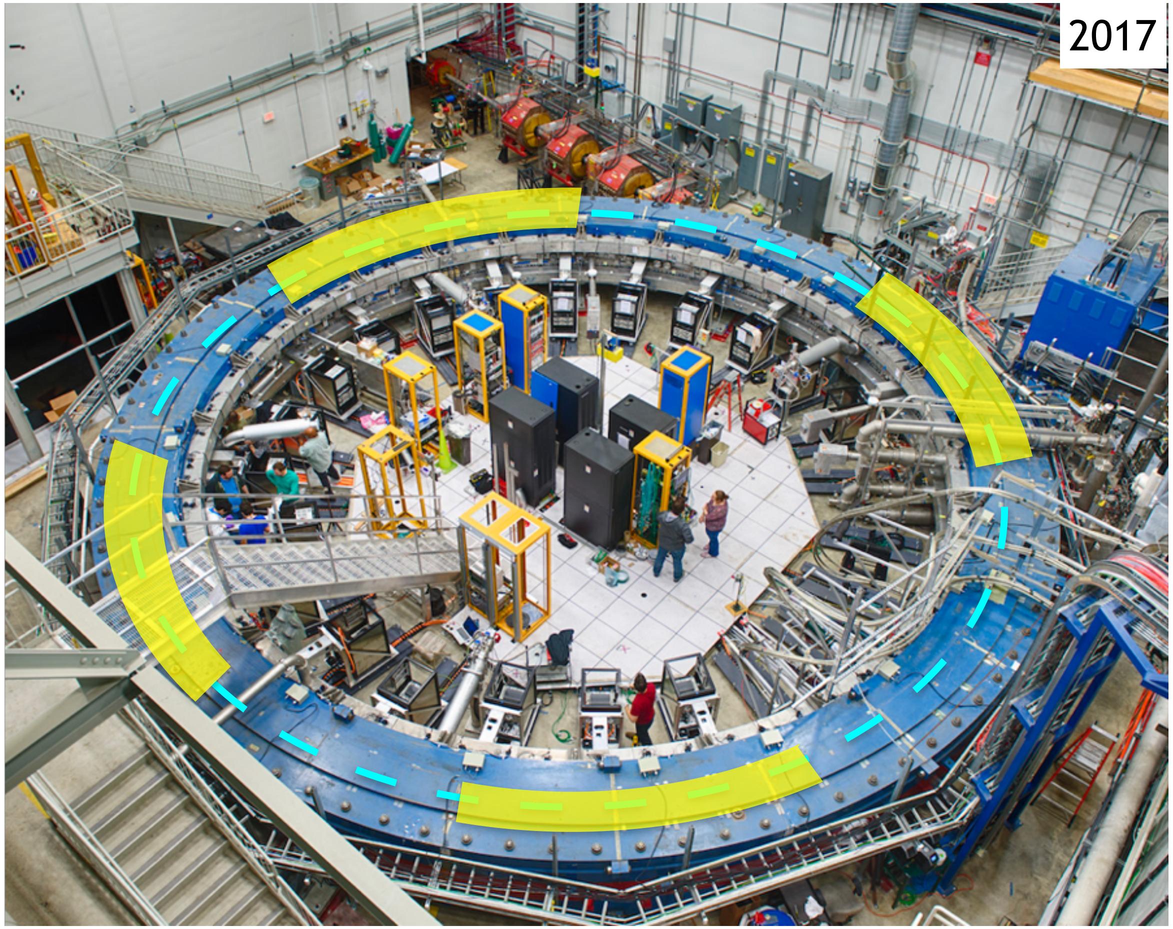

Pulsed “electrostatic” quadrupoles

Vertical focusing and confinement of muon beam

Quasi-penning trap cover 43% of the ring

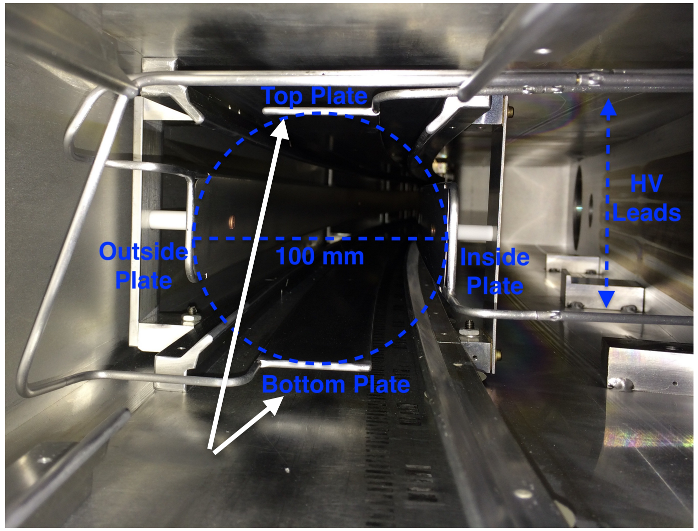

The electrostatic quadrupoles

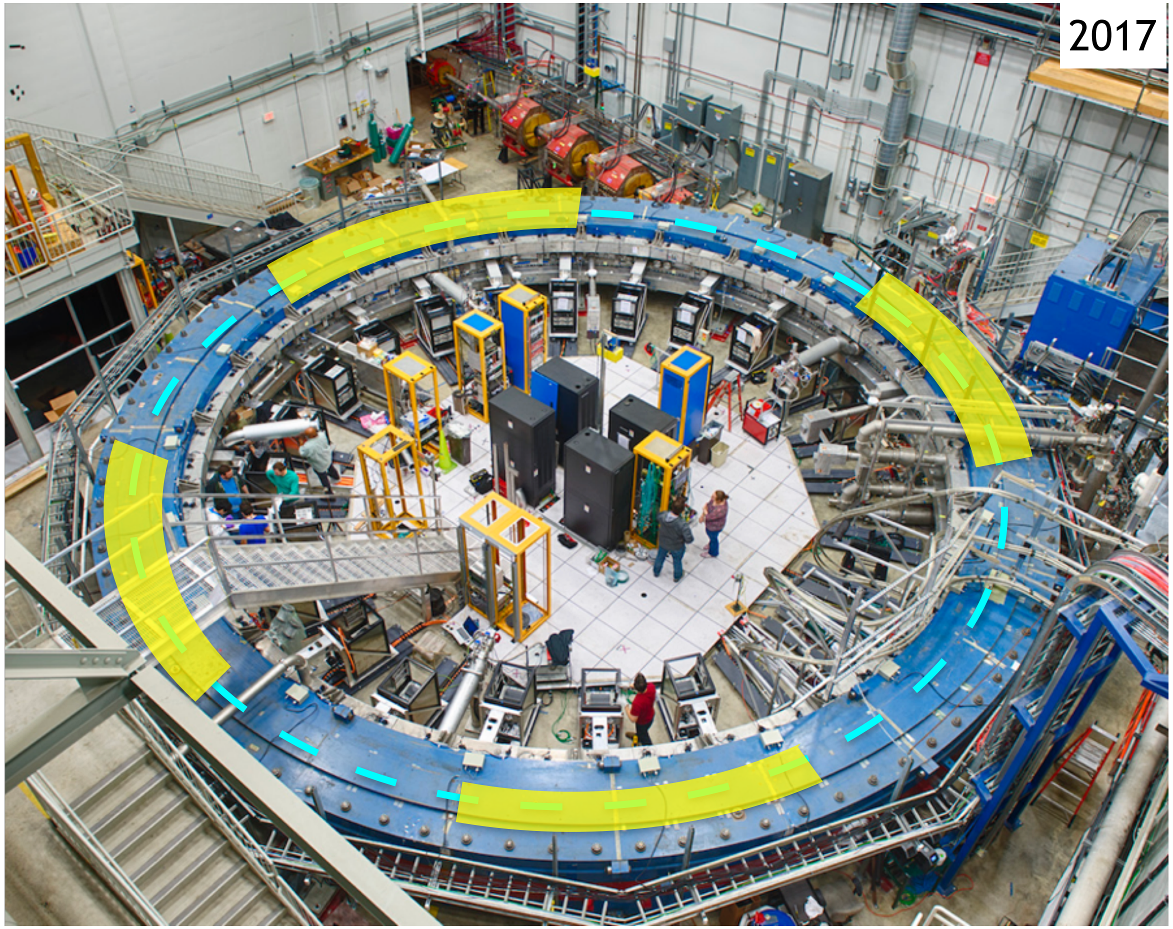

Pulsed “electrostatic” quadrupoles

Vertical focusing and confinement of muon beam

Quasi-penning trap cover 43% of the ring

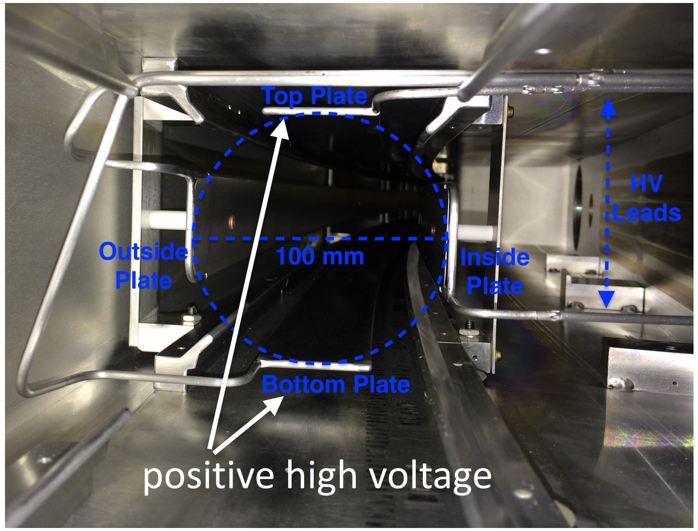

The positron calorimeter system

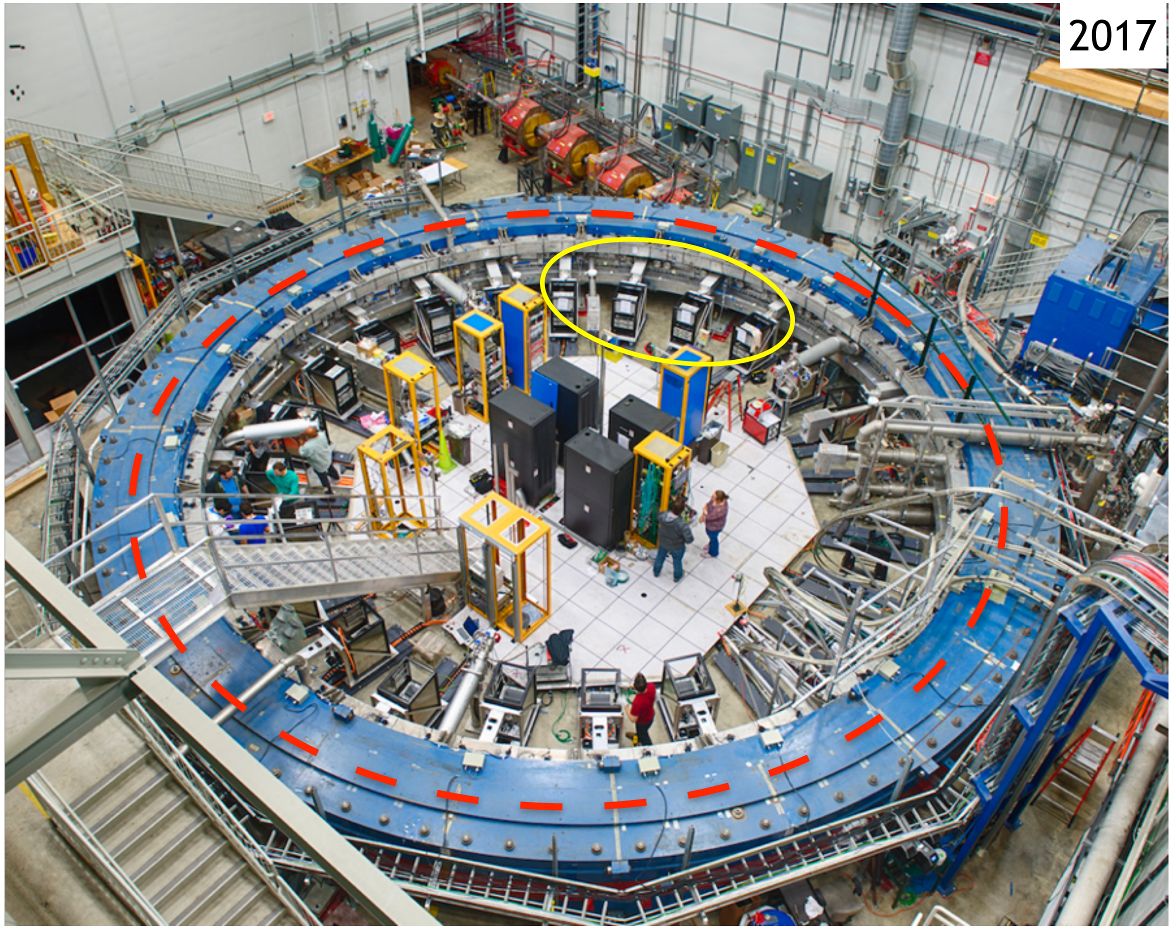

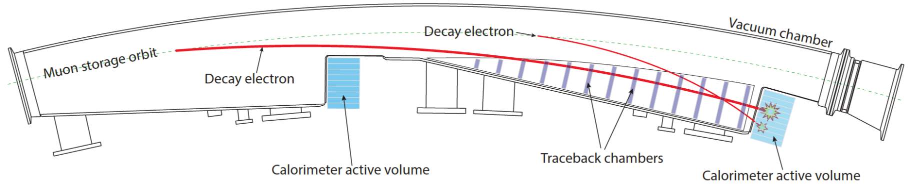

24 calorimeter stations to detect the decay positrons
9 x 6 arrays of PbF_2 crystals (Cherenkov detectors!)

The positron calorimeter system

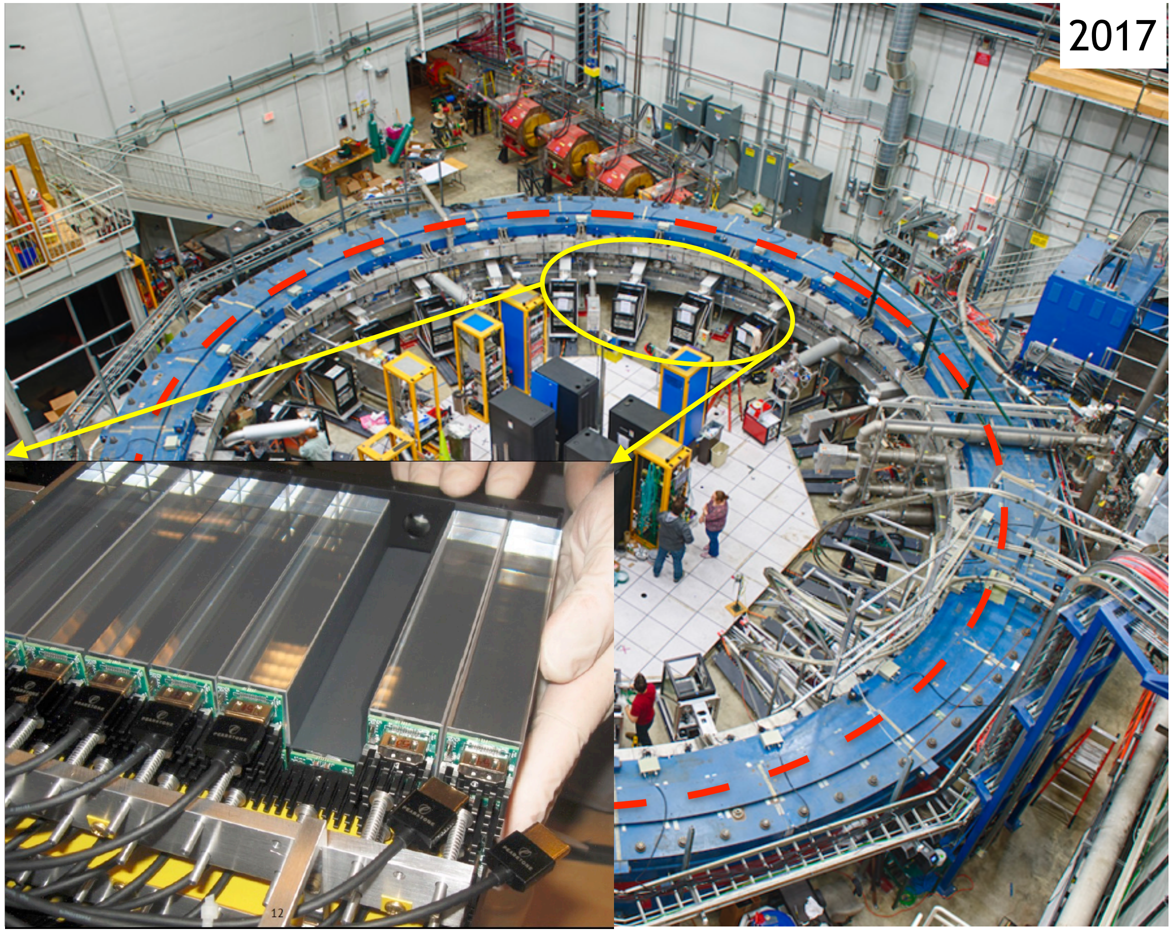

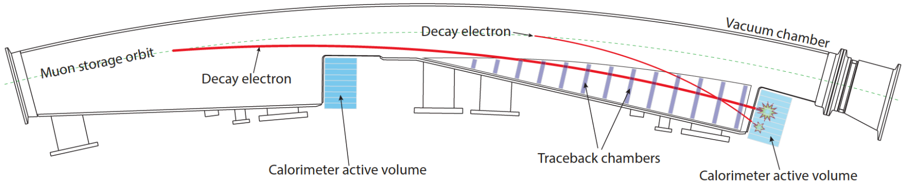

24 calorimeter stations to detect the decay positrons
9 x 6 arrays of PbF_2 crystals (Cherenkov detectors!)

The positron calorimeter system

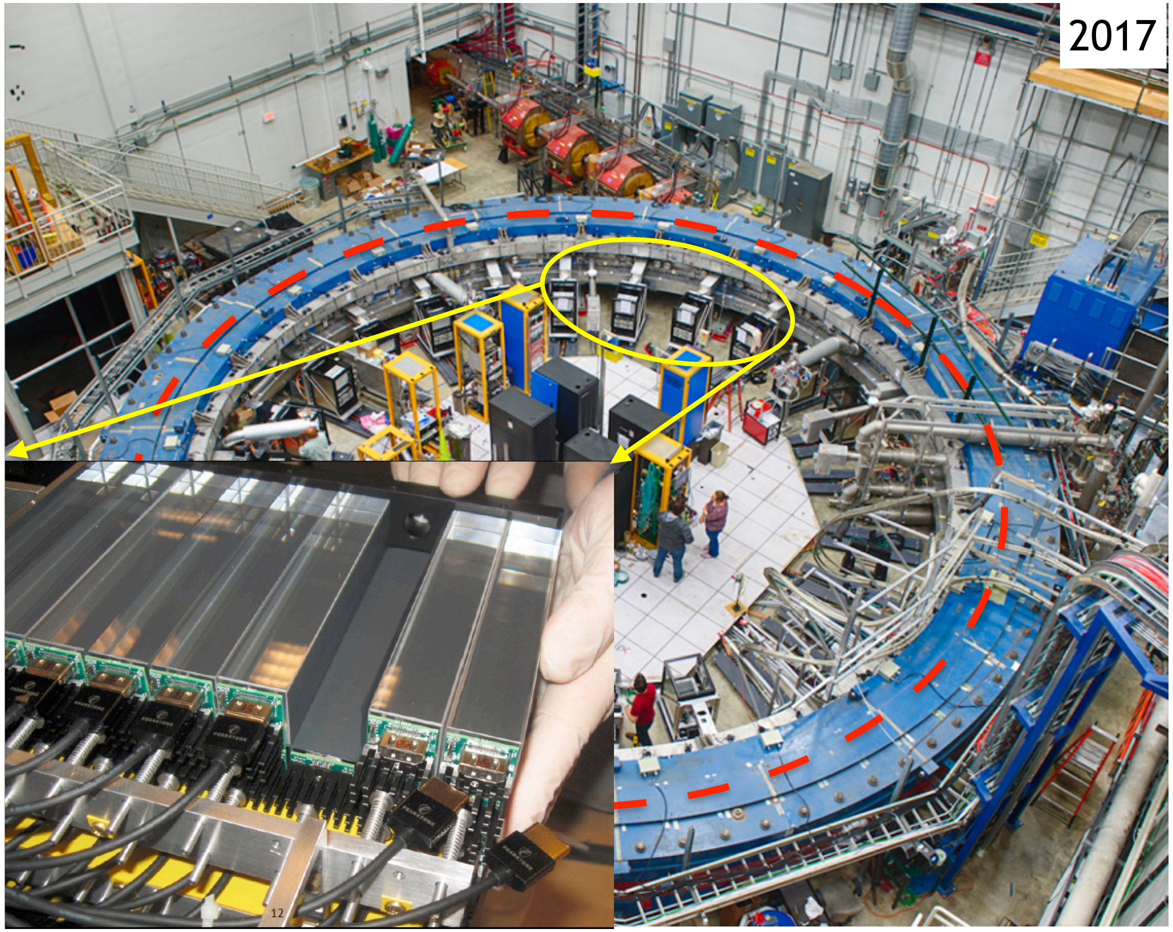

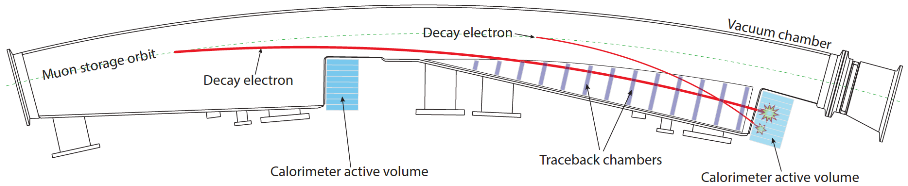

24 calorimeter stations to detect the decay positrons
9 x 6 arrays of PbF_2 crystals (Cherenkov detectors!)

In the muon rest frame

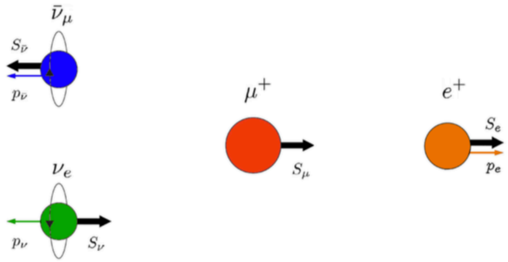

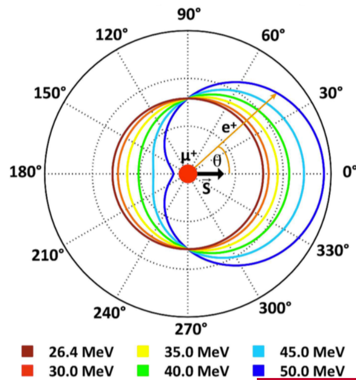

Wiggle plot basics and laser calibration system

Spin precession in muon rest frame

transforms to

above-energy-threshold count rate
modulation in laboratory frame

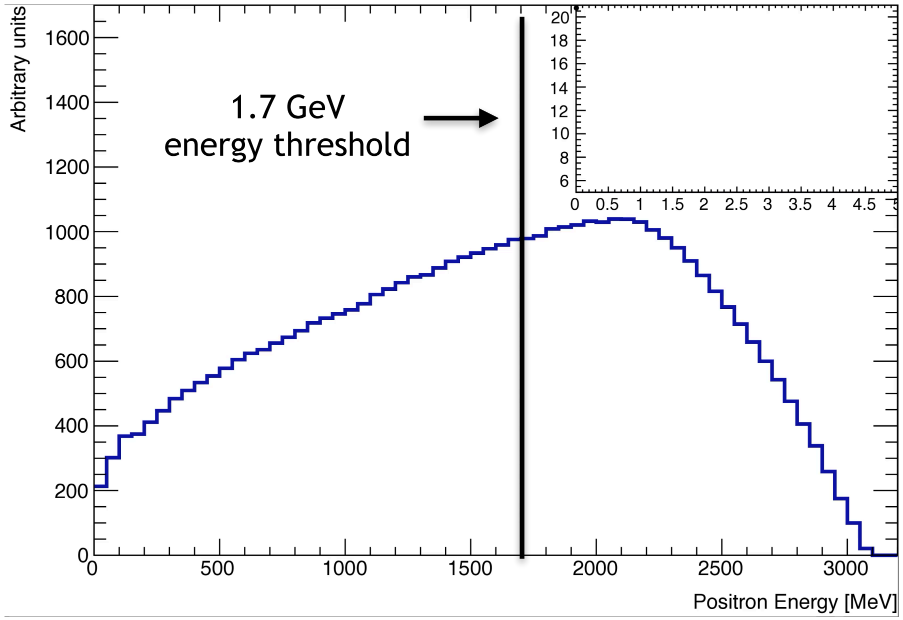

Wiggle plot basics and laser calibration system

Spin precession in muon rest frame

transforms to

above-energy-threshold count rate modulation in laboratory frame

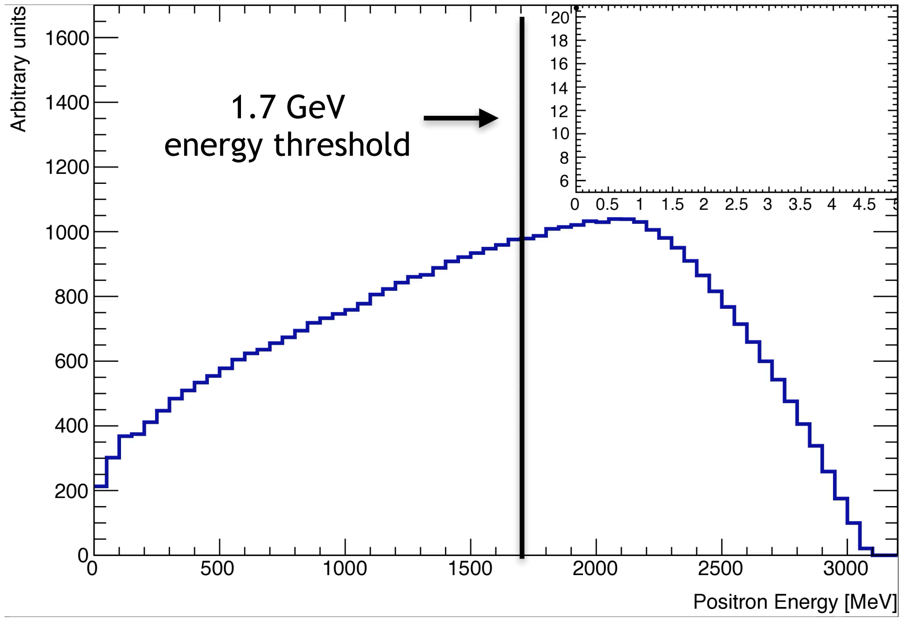

Wiggle plot basics and laser calibration system

Spin precession in muon rest frame

transforms to

above-energy-threshold count rate modulation in laboratory frame

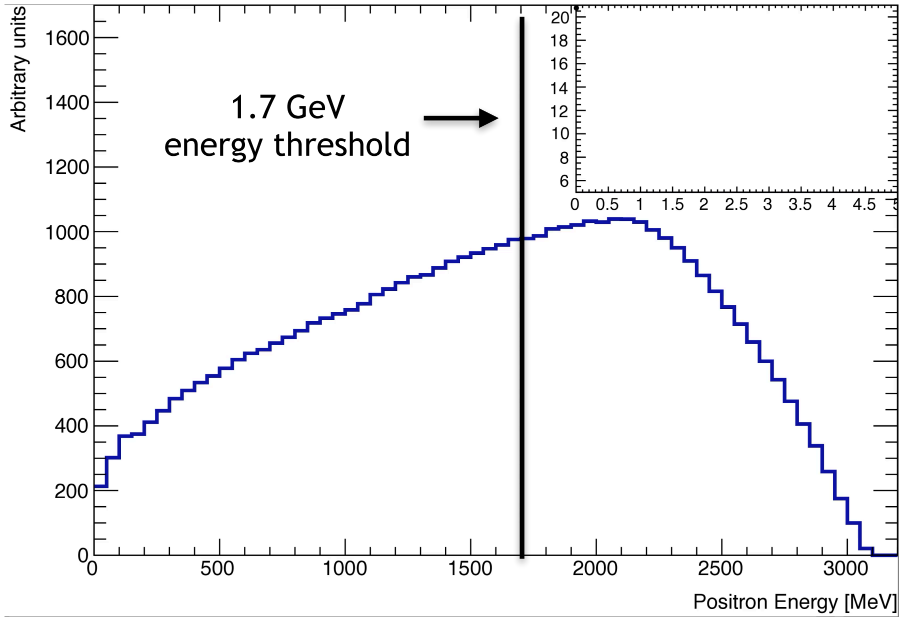

Dedicated laser calibration system to ensure energy calibration of calorimeter system

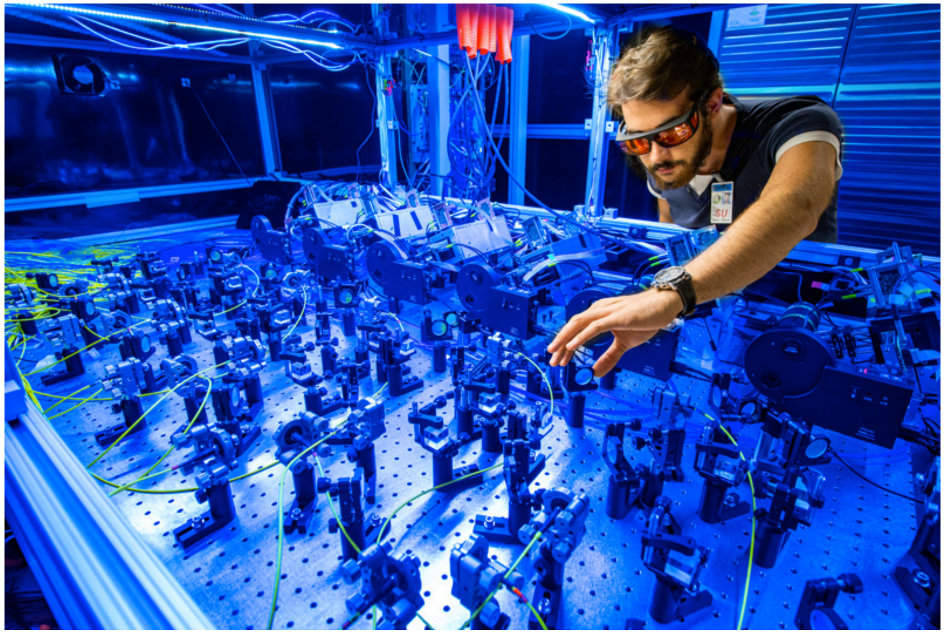

The straw tracker stations

Determine e^+ trajectory to decay position and extrapolate to find muon beam distribution!

Input for beam dynamics simulations

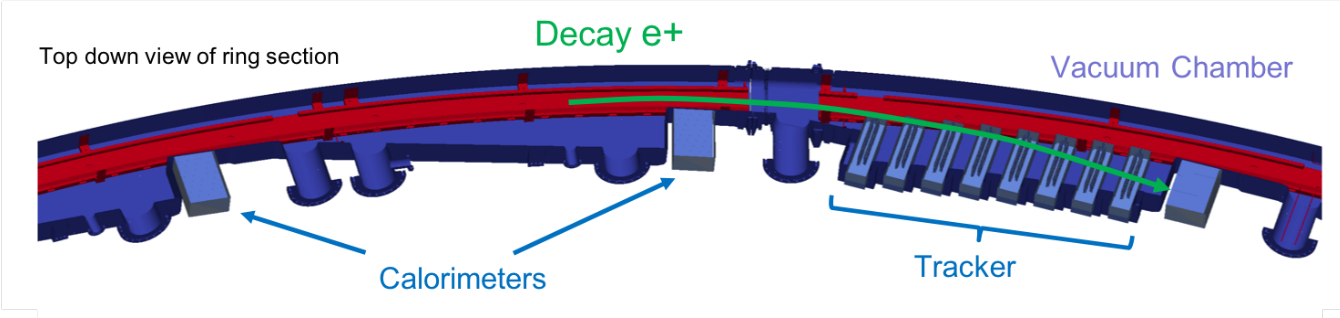

The straw tracker stations

Determine e+ trajectory to decay position and extrapolate to find muon beam distribution!

Input for beam dynamics simulations

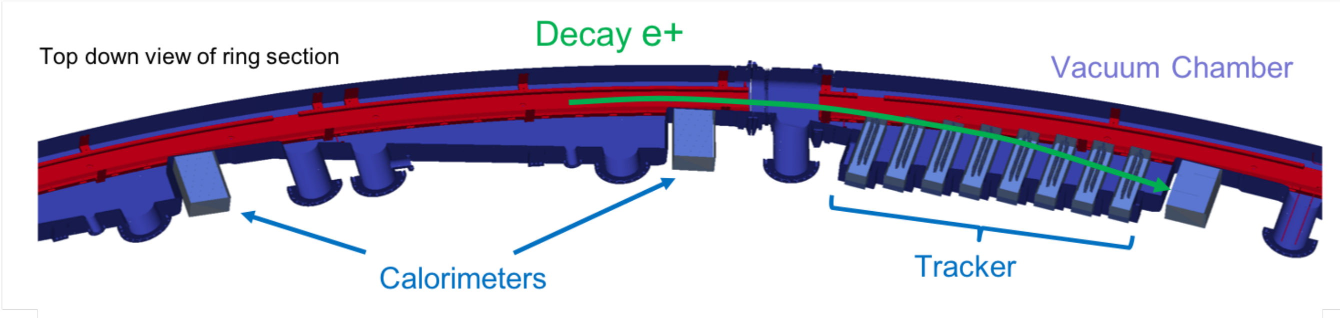

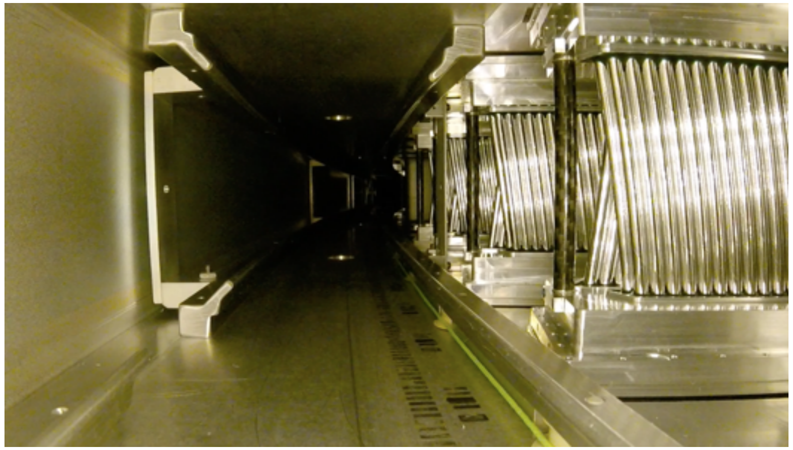

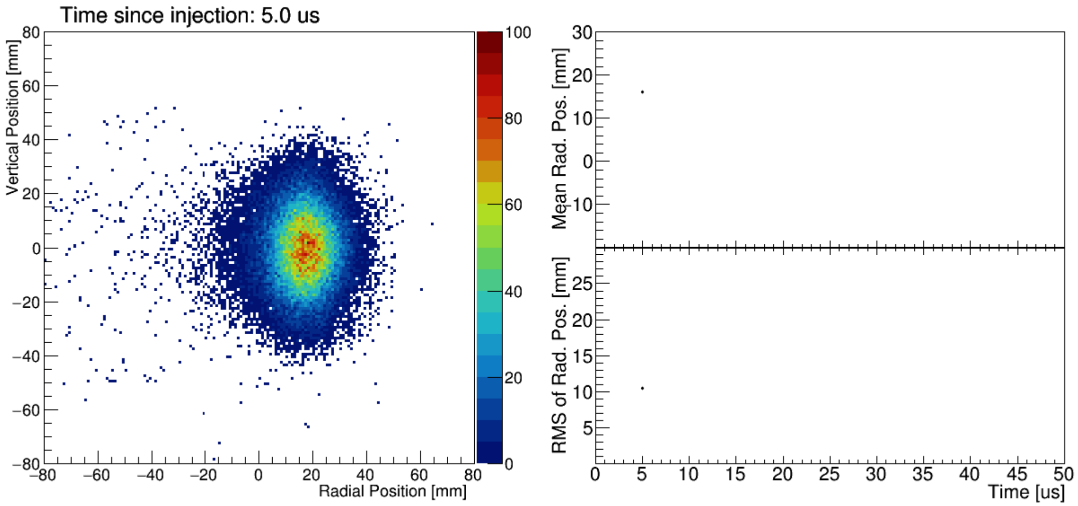

All the analysis is available for you to look at in detail

arXiv:2104.03240v1; Accepted by Phys. Rev. Accel. Beams

Beam dynamics corrections to the Run-1 measurement of the muon anomalous magnetic moment at Fermilab

T. Albahri,[38] A. Anasta...
T. Barrett,[6] F. Bedeschi,[11]
T. Bowcock,[38] G.
S. P. Chang,[18,5] A. Cha
L. Cotrozzi,[11,31] J.
G. Di Sciascio,[12] I
M. Farooq,[41] R. Fate

PHYSICAL REVIEW D **103,** 072002 (2021)

Editors' Suggestion | Featured in Physics

Measurement of the anomalous precession frequency of the muon in the Fermilab Muon $g-2$ Experiment

T. Albahri,[38] A. Anastasi,[11,a]
T. Barrett,[6] A. Basti,[11]
E. Bottalico,[11,31] T. Bow
S. P. Chang,[18,5] A. Chapelai
J. D. Crnkovic,[3,36,42] S. Da

PHYSICAL REVIEW A **103**, 042208 (2021)

Featured in Physics

Magnetic-field measurement and analysis for the Muon $g-2$ Experiment at Fermilab

T. Albahri,[39] A. Anastasi,[1
F. Bedeschi,[11] M. Berz,[20]
G. Cantatore,[13,34] R. M. Carey
R. Chislett,[36] J. Choi,[5] Z
S. Dabagov,[9,‖] P. T. Det
V. N. Duginov,[17] M. Ead
A. Fioretti,[11,14] D. Flay,[41] N. S
L. K. Gibbons,[6] A. Gioios
F. Gray,[24] S. Haciomeroglu,[5] T
G. Hesketh,[36] A. Hibbert,[3
P. Kammel,[48] M. Kargianto

PHYSICAL REVIEW LETTERS **126,** 141801 (2021)

Editors' Suggestion | Featured in Physics

Measurement of the Positive Muon Anomalous Magnetic Moment to 0.46 ppm

B. Abi,[44] T. Albahri,[39] S. Al-Kilani,[36] D. Allspach,[7] L. P. Alonzi,[48] A. Anastasi,[11,a] A. Anisenkov,[4,b] F. Azfar,[44] K. Badgley,[7] S. Baeßler,[47,c] I. Bailey,[19,d] V. A. Baranov,[17] E. Barlas-Yucel,[37] T. Barrett,[6] E. Barzi,[7] A. Basti,[11,32] F. Bedeschi,[11] A. Behnke,[22] M. Berz,[20] M. Bhattacharya,[43] H. P. Binney,[48] R. Bjorkquist,[6] P. Bloom,[21] J. Bono,[7] E. Bottalico,[11,32] T. Bowcock,[39] D. Boyden,[22] G. Cantatore,[13,34] R. M. Carey,[2] J. Carroll,[39] B. C. K. Casey,[7] D. Cauz,[35,8] S. Ceravolo,[9] R. Chakraborty,[38] S. P. Chang,[18,5] A. Chapelain,[6] S. Chappa,[7] S. Charity,[7] R. Chislett,[36] J. Choi,[5] Z. Chu,[26,e] T. E. Chupp,[42]

JG|U

The data set collected so far

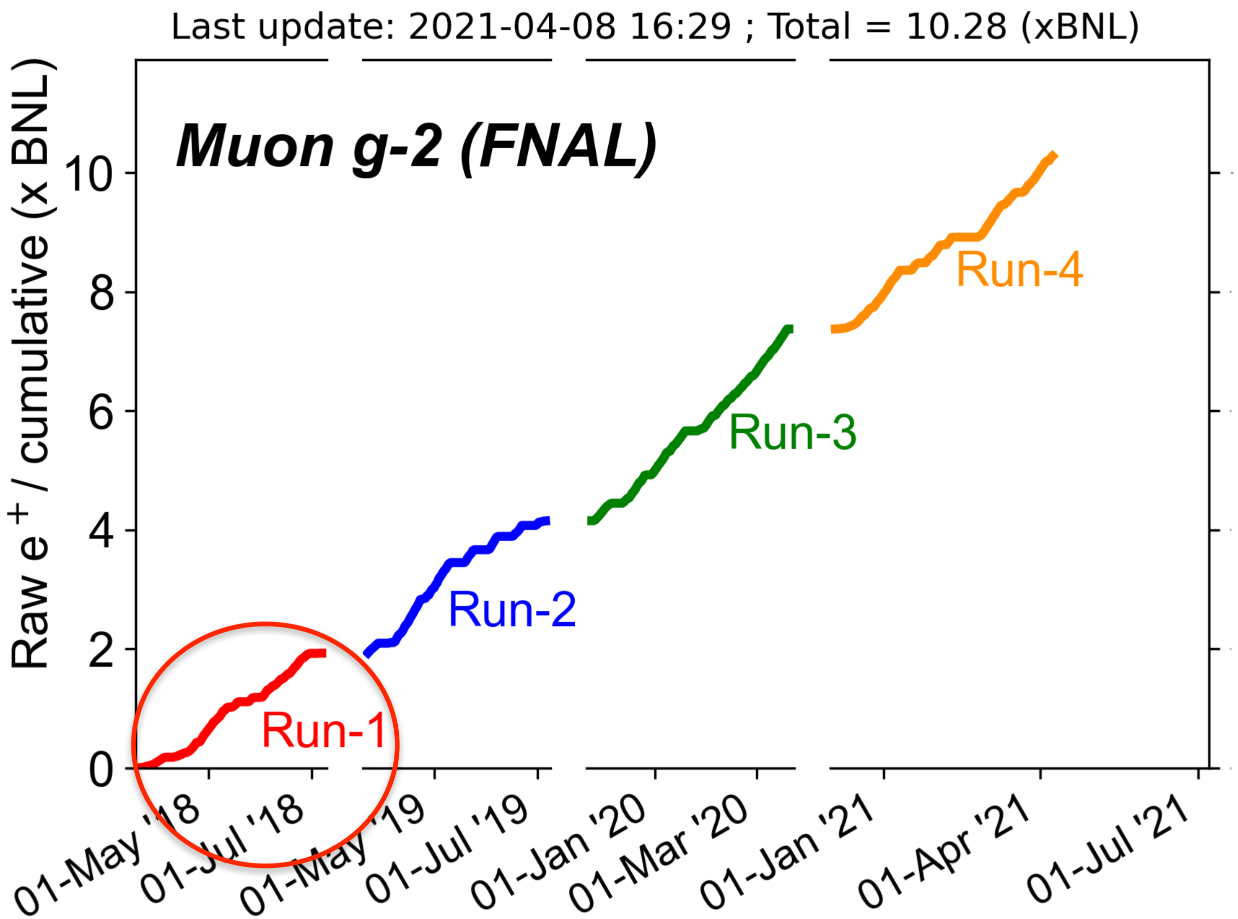

The four Run 1 datasets

Dataset	Date	Field index n ESQ HV [kV]	Kicker HV [kV]	Number of positrons
1a	Apr 22, 2018 - Apr 25, 2018	0.108 18.3	130	0.9×10^9
1b	Apr 26, 2018 - May 02, 2018	0.120 20.4	137	1.3×10^9
1c	May 04, 2018 - May 12, 2018	0.120 20.4	132	2.0×10^9
1d	Jun 06, 2018- Jun 29, 2018	0.108 18.3	125	4.0×10^9

Extracting a_μ - the basic idea

External measurements to anchor B and e to other high-precision measurements and calculations

$$a_\mu = \frac{\omega_\mathrm{a}}{\tilde{B}} \frac{m_\mu}{e}$$

Extracting a_μ - the basic idea

External measurements to anchor B and e to other high-precision measurements and calculations

$$e = \frac{4 m_e \mu_e}{\hbar g_e}$$

$$a_\mu = \frac{\omega_a}{\tilde{B}} \frac{m_\mu}{e} = \frac{\omega_a}{\tilde{\omega}'_p (T_r)} \frac{\mu'_p (T_r)}{\mu_e (H)} \frac{\mu_e (H)}{\mu_e} \frac{m_\mu}{m_e} \frac{g_e}{2}$$

$$\tilde{B} = \frac{\hbar \tilde{\omega}'_p}{2 \mu'_p}$$

Extracting a_μ - the external ingredients

External measurements to anchor B and e to other high-precision measurements and calculations

$$a_\mu = \frac{\omega_a}{\tilde{B}} \frac{m_\mu}{e} = \frac{\omega_a}{\tilde{\omega}'_p(T_r)} \frac{\mu'_p(T_r)}{\mu_e(H)} \frac{\mu_e(H)}{\mu_e} \frac{m_\mu}{m_e} \frac{g_e}{2}$$

Extracting a_μ - the external ingredients

External measurements to anchor B and e to other high-precision measurements and calculations

$$\frac{\mu'_p(T_r)}{\mu_e(H)}$$

10.5 ppb uncertainty
at T_r = 34.7°C

Metrologia 13, 179 (1977)

$$a_\mu = \frac{\omega_a}{\tilde{B}}\frac{m_\mu}{e} = \frac{\omega_a}{\tilde{\omega}'_p(T_r)}\boxed{\frac{\mu'_p(T_r)}{\mu_e(H)}}\frac{\mu_e(H)}{\mu_e}\frac{m_\mu}{m_e}\frac{g_e}{2}$$

Extracting a_μ - the external ingredients

External measurements to anchor B and e to other high-precision measurements and calculations

$$\frac{\mu'_p(T_r)}{\mu_e(H)}$$

10.5 ppb uncertainty
at T_r = 34.7°C

Metrologia 13, 179 (1977)

$$\frac{\mu_e(H)}{\mu_e}$$

Bound state QED calculation
exact

Rev. Mod. Phys. 88, 035009 (2016)

$$a_\mu = \frac{\omega_a}{\tilde{B}}\frac{m_\mu}{e} = \frac{\omega_a}{\tilde{\omega}'_p(T_r)}\boxed{\frac{\mu'_p(T_r)}{\mu_e(H)}}\boxed{\frac{\mu_e(H)}{\mu_e}}\frac{m_\mu}{m_e}\frac{g_e}{2}$$

JG|U

Extracting a_μ - the external ingredients

External measurements to anchor B and e to other high-precision measurements and calculations

$$\frac{\mu'_p(T_r)}{\mu_e(H)}$$

10.5 ppb uncertainty
at T_r = 34.7°C

Metrologia 13, 179 (1977)

$$\frac{\mu_e(H)}{\mu_e}$$

Bound state QED calculation
exact

Rev. Mod. Phys. 88, 035009 (2016)

$$a_\mu = \frac{\omega_a}{\tilde{B}}\frac{m_\mu}{e} = \frac{\omega_a}{\tilde{\omega}'_p(T_r)} \boxed{\frac{\mu'_p(T_r)}{\mu_e(H)}} \boxed{\frac{\mu_e(H)}{\mu_e}} \boxed{\frac{m_\mu}{m_e}} \frac{g_e}{2}$$

$$\frac{m_\mu}{m_e}$$

Muonium hyperfine splitting
22 ppb uncertainty

Phys. Rev. Lett. 82, 11 (1999)

JG|U

Extracting a_μ - the external ingredients

External measurements to anchor B and e to other high-precision measurements and calculations

$$\frac{\mu_p'(T_r)}{\mu_e(H)}$$

10.5 ppb uncertainty
at T_r = 34.7°C

Metrologia 13, 179 (1977)

$$\frac{\mu_e(H)}{\mu_e}$$

Bound state QED calculation
exact

Rev. Mod. Phys. 88, 035009 (2016)

$$a_\mu = \frac{\omega_a}{\tilde{B}}\frac{m_\mu}{e} = \frac{\omega_a}{\tilde{\omega}_p'(T_r)}\boxed{\frac{\mu_p'(T_r)}{\mu_e(H)}}\boxed{\frac{\mu_e(H)}{\mu_e}}\boxed{\frac{m_\mu}{m_e}}\boxed{\frac{g_e}{2}}$$

$$\frac{m_\mu}{m_e}$$

Muonium hyperfine splitting
22 ppb uncertainty

Phys. Rev. Lett. 82, 11 (1999)

$$\frac{g_e}{2}$$

Measurement with
0.28 ppt uncertainty

Phys. Rev. A 83, 052122 (2011)

Extracting a_μ - the external ingredients

External measurements to anchor B and e to other high-precision measurements and calculations

$$\frac{\mu'_\mathrm{p}(T_\mathrm{r})}{\mu_\mathrm{e}(H)}$$

10.5 ppb uncertainty
at T_r = 34.7°C

Metrologia 13, 179 (1977)

$$\frac{\mu_\mathrm{e}(H)}{\mu_\mathrm{e}}$$

Bound state QED calculation
exact

Rev. Mod. Phys. 88, 035009 (2016)

$$a_\mu = \frac{\omega_\mathrm{a}}{\tilde{B}}\frac{m_\mu}{e} = \frac{\omega_\mathrm{a}}{\tilde{\omega}'_\mathrm{p}(T_\mathrm{r})}\boxed{\frac{\mu'_\mathrm{p}(T_\mathrm{r})}{\mu_\mathrm{e}(H)}}\boxed{\frac{\mu_\mathrm{e}(H)}{\mu_\mathrm{e}}}\boxed{\frac{m_\mu}{m_\mathrm{e}}}\boxed{\frac{g_\mathrm{e}}{2}}$$

Total uncertainty
from external quantities:
24 ppb

$$\frac{m_\mu}{m_\mathrm{e}}$$

Muonium hyperfine splitting
22 ppb uncertainty

Phys. Rev. Lett. 82, 11 (1999)

$$\frac{g_\mathrm{e}}{2}$$

Measurement with
0.28 ppt uncertainty

Phys. Rev. A 83, 052122 (2011)

Extracting a_μ - our challenge

$$a_\mu = \frac{\omega_a}{\tilde{B}'}\frac{m_\mu}{e} = \frac{\omega_a}{\tilde{\omega}'_p\left(T_r\right)}\frac{\mu'_p\left(T_r\right)}{\mu_e(H)}\frac{\mu_e(H)}{\mu_e}\frac{m_\mu}{m_e}\frac{g_e}{2}$$

Extracting a_μ - our challenge

$$a_\mu = \frac{\omega_a}{\tilde{B}'}\frac{m_\mu}{e} = \boxed{\frac{\omega_a}{\tilde{\omega}'_p(T_r)}}\frac{\mu'_p(T_r)}{\mu_e(H)}\frac{\mu_e(H)}{\mu_e}\frac{m_\mu}{m_e}\frac{g_e}{2}$$

$$R' = \boxed{\frac{\omega_a}{\tilde{\omega}'_p}} = \frac{f_{\mathrm{clock}}\,\omega_a^{\mathrm{meas}}\left(1 + C_e + C_p + C_{ml} + C_{pa}\right)}{f_{\mathrm{calib}}\left\langle M(x, y, \phi)\,\omega_p(x, y, \phi)\right\rangle\left(1 + B_k + B_q\right)}$$

JG|U

Extracting a_μ - our tools

$$R' = \frac{\omega_a}{\tilde{\omega}'_p} = \frac{f_{\mathrm{clock}}\, \omega_a^{\mathrm{meas}} \left(1 + C_e + C_p + C_{ml} + C_{pa}\right)}{f_{\mathrm{calib}} \left\langle M(x, y, \phi)\, \omega'_p(x, y, \phi) \right\rangle \left(1 + B_k + B_q\right)}$$

Extracting a_μ - our tools

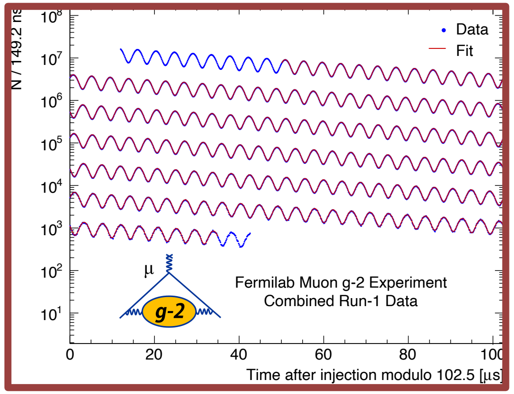

Anomalous spin precession frequency

$$R' = \frac{\omega_a}{\tilde{\omega}'_p} = \frac{f_{\text{clock}} \boxed{\omega_a^{\text{meas}}} \left(1 + C_e + C_p + C_{ml} + C_{pa}\right)}{f_{\text{calib}} \left\langle M(x, y, \phi)\, \omega'_p(x, y, \phi) \right\rangle \left(1 + B_k + B_q\right)}$$

Extracting a_μ - our tools

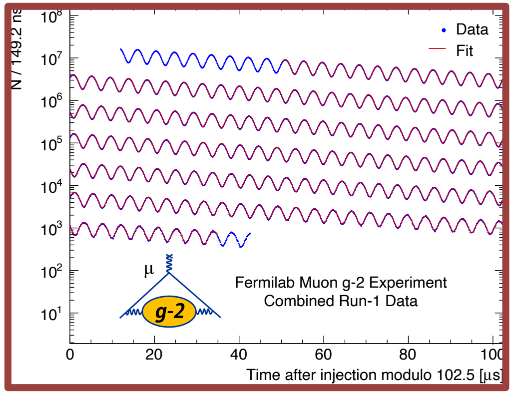

Anomalous spin precession frequency

Muon beam dynamics corrections

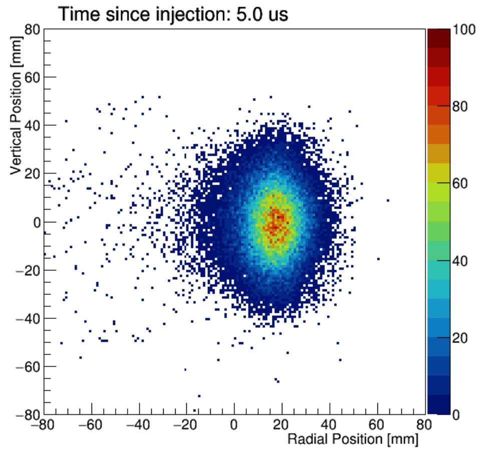

$$R' = \frac{\omega_a}{\tilde{\omega}'_p} = \frac{f_{\mathrm{clock}}\, \boxed{\omega_a^{\mathrm{meas}}} \boxed{\left(1 + C_e + C_p + C_{ml} + C_{pa}\right)}}{f_{\mathrm{calib}} \left\langle M(x,y,\phi)\, \omega'_p(x,y,\phi) \right\rangle \left(1 + B_k + B_q\right)}$$

Extracting a_μ - our tools

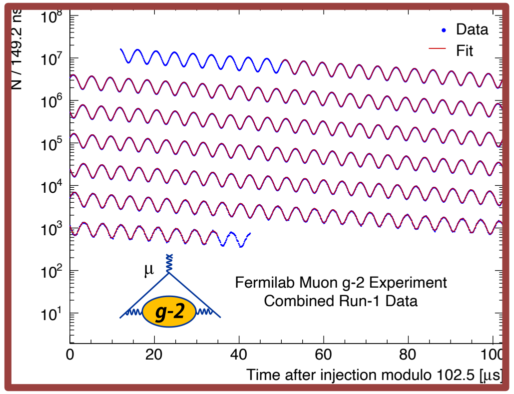

Anomalous spin precession frequency

Muon beam dynamics corrections

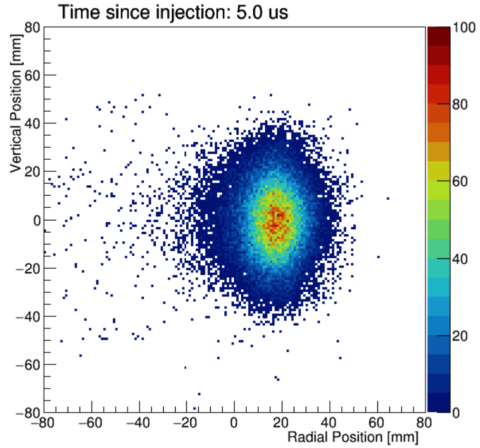

$$R' = \frac{\omega_a}{\tilde{\omega}'_p} = \frac{f_{\mathrm{clock}}\,\boxed{\omega_a^{\mathrm{meas}}}\,\boxed{\left(1 + C_e + C_p + C_{ml} + C_{pa}\right)}}{f_{\mathrm{calib}}\left\langle \boxed{M\left(x, y, \phi\right)}\,\omega'_p\left(x, y, \phi\right)\right\rangle\left(1 + B_k + B_q\right)}$$

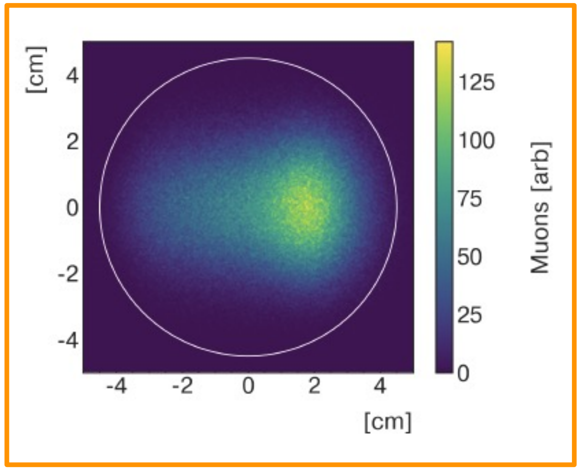

Spatial muon distribution

Extracting a_μ - our tools

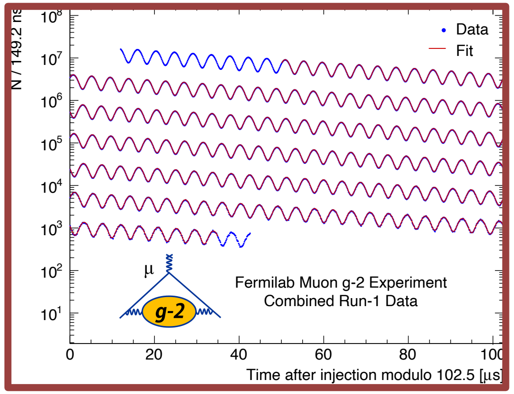

Anomalous spin precession frequency

Muon beam dynamics corrections

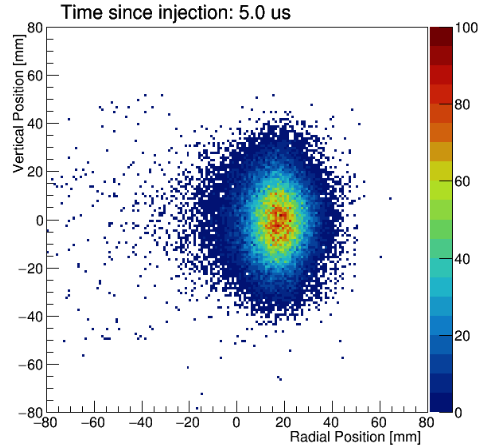

$$R' = \frac{\omega_a}{\tilde{\omega}'_p} = \frac{f_{\mathrm{clock}}\, \boxed{\omega_a^{\mathrm{meas}}}\, \boxed{\left(1 + C_e + C_p + C_{ml} + C_{pa}\right)}}{f_{\mathrm{calib}} \left\langle \boxed{M(x,y,\phi)}\, \boxed{\omega'_p(x,y,\phi)} \right\rangle \left(1 + B_k + B_q\right)}$$

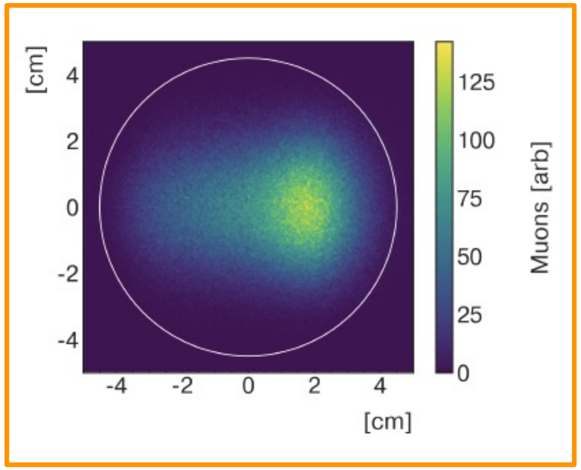

Spatial muon distribution

Spatial distribution of magnetic field

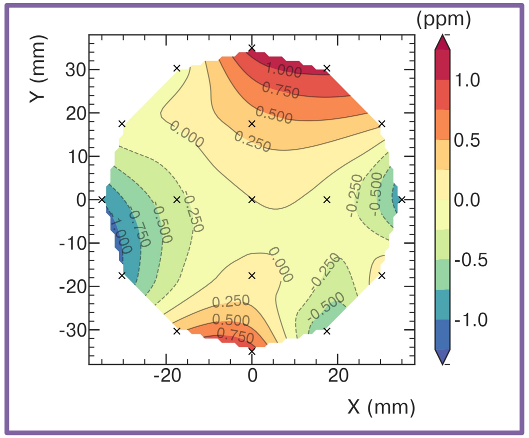

Extracting a_μ - our tools

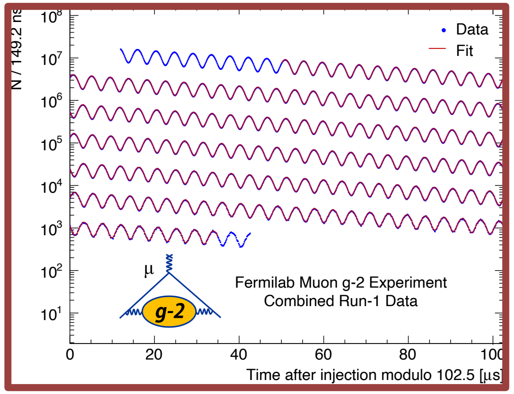

Anomalous spin precession frequency

Muon beam dynamics corrections

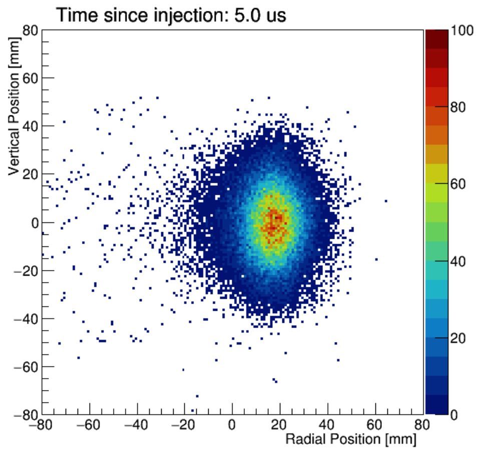

$$R' = \frac{\omega_a}{\tilde{\omega}'_p} = \frac{f_{\mathrm{clock}} \boxed{\omega_a^{\mathrm{meas}}} \boxed{\left(1 + C_e + C_p + C_{ml} + C_{pa}\right)}}{f_{\mathrm{calib}} \left\langle \boxed{M\left(x, y, \phi\right)} \boxed{\omega'_p\left(x, y, \phi\right)} \right\rangle \left(\boxed{1 + B_k + B_q}\right)}$$

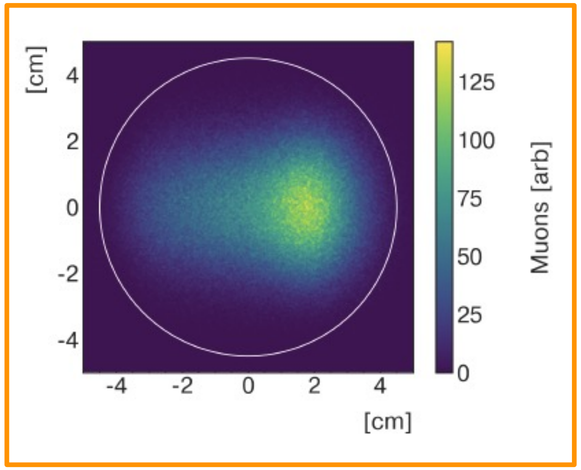

Spatial muon distribution

Spatial distribution of magnetic field

Transient magnetic fields

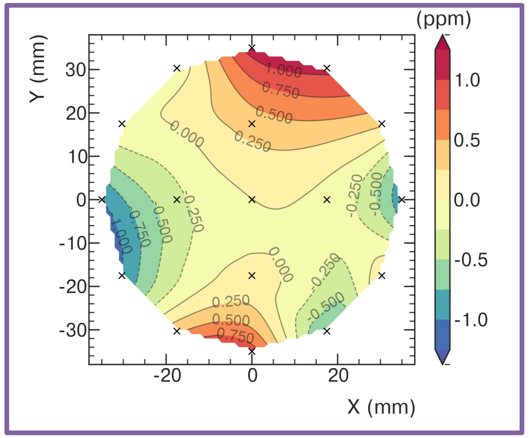

M. Fertl - Stavanger, April 22nd 2021

Extracting a_μ - our tools

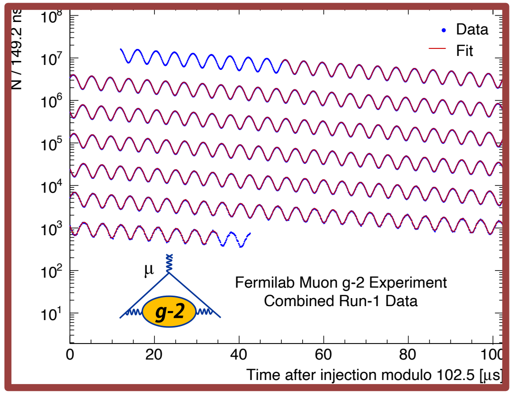

Anomalous spin precession frequency

Muon beam dynamics corrections

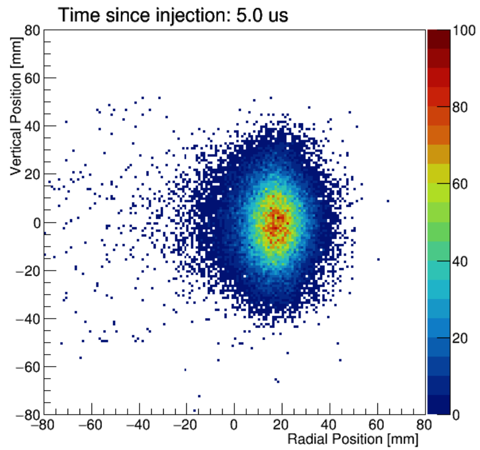

$$R' = \frac{\omega_a}{\tilde{\omega}'_p} = \frac{f_{\mathrm{clock}}\,\boxed{\omega_a^{\mathrm{meas}}}\boxed{\left(1 + C_e + C_p + C_{ml} + C_{pa}\right)}}{\boxed{f_{\mathrm{calib}}}\left\langle \boxed{M(x,y,\phi)}\,\boxed{\omega'_p(x,y,\phi)} \right\rangle \left(\boxed{1 + B_k + B_q}\right)}$$

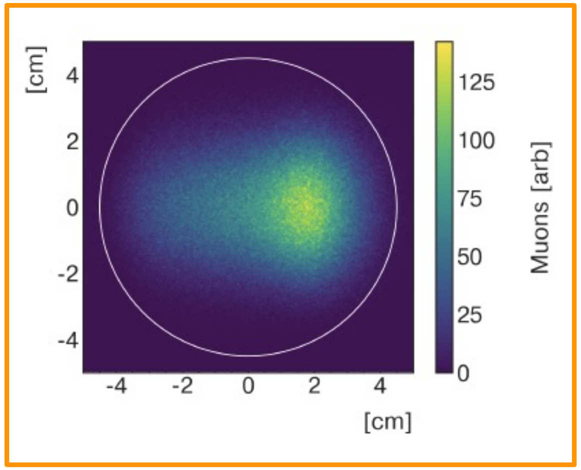

Spatial muon distribution

Spatial distribution of magnetic field

Transient magnetic fields

Calibration

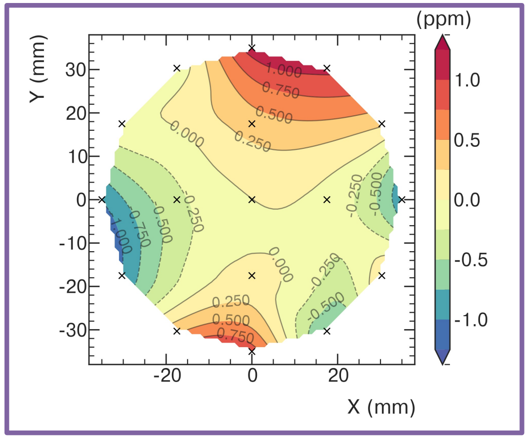

Extracting a_μ - our tools

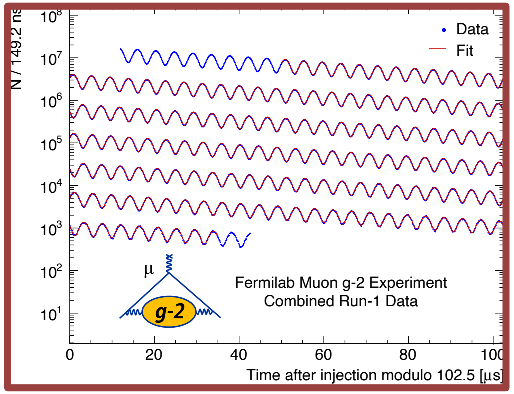

Anomalous spin precession frequency

Muon beam dynamics corrections

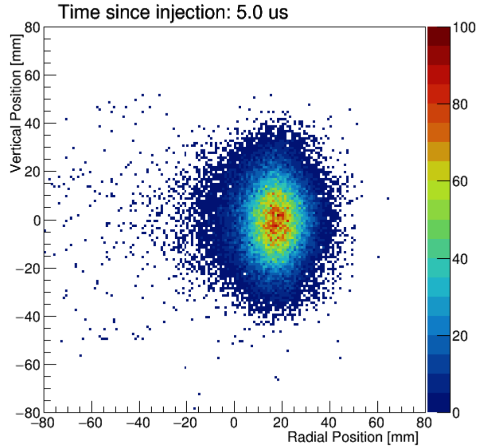

Clock blinding

$$R' = \frac{\omega_a}{\tilde{\omega}'_p} = \frac{f_{\text{clock}}\,\omega_a^{\text{meas}}\left(1 + C_e + C_p + C_{ml} + C_{pa}\right)}{f_{\text{calib}}\left\langle M(x,y,\phi)\,\omega'_p(x,y,\phi)\right\rangle\left(1 + B_k + B_q\right)}$$

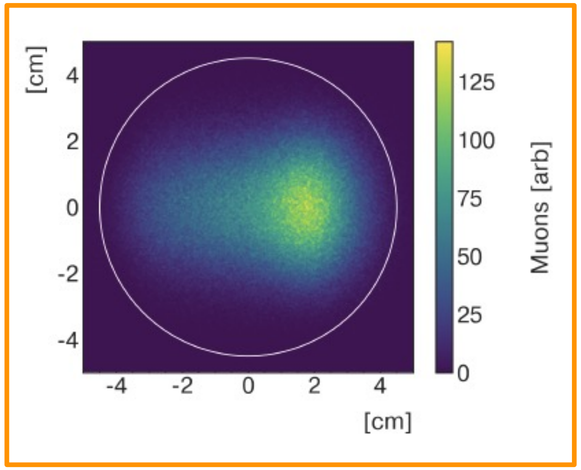

Spatial muon distribution

Spatial distribution of magnetic field

Transient magnetic fields

Calibration

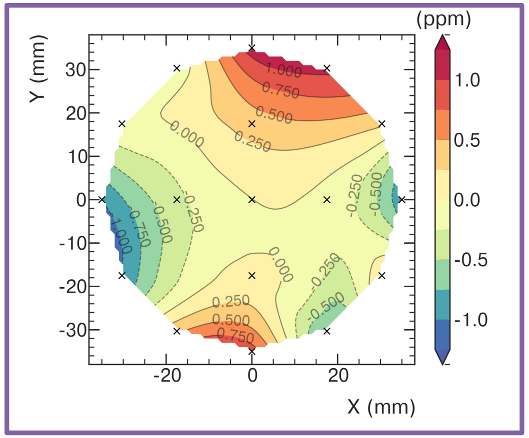

The master formula and the uncertainty table

$$R' = \frac{\omega_{\mathrm{a}}}{\omega'_{\mathrm{p}}} = \frac{f_{\mathrm{clock}}\, \omega_{\mathrm{a}}^{\mathrm{meas}} \left(1 + C_{\mathrm{e}} + C_{\mathrm{p}} + C_{\mathrm{ml}} + C_{\mathrm{pa}}\right)}{f_{\mathrm{calib}} \left\langle M\left(x, y, \phi\right) \omega'_{\mathrm{p}}\left(x, y, \phi\right)\right\rangle \left(1 + B_{\mathrm{k}} + B_{\mathrm{q}}\right)}$$

Quantity	Correction Terms (ppb)	Uncertainty (ppb)
ω_a^m (statistical)	–	434
ω_a^m (systematic)	–	56
C_e	489	53
C_p	180	13
C_{ml}	-11	5
C_{pa}	-158	75
$f_{\mathrm{calib}}\langle\omega_p(x,y,\phi) \times M(x,y,\phi)\rangle$	–	56
B_k	-27	37
B_q	-17	92
$\mu'_p(34.7°)/\mu_e$	–	10
m_μ/m_e	–	22
$g_e/2$	–	0
Total systematic	–	157
Total fundamental factors	–	25
Totals	544	462

Uncertainty dominated by statistics!

Already surpassed the anticipated goal!

Work in progress for runs 2-5!

Total uncertainty dominated by statistics!

Extract $\omega_{\mathrm{a}}^{\mathrm{meas}}$ from the wiggle plot

Extract ω_a^{meas} from the wiggle plot

Histogram of decay e⁺ arrival times (wiggle plot)

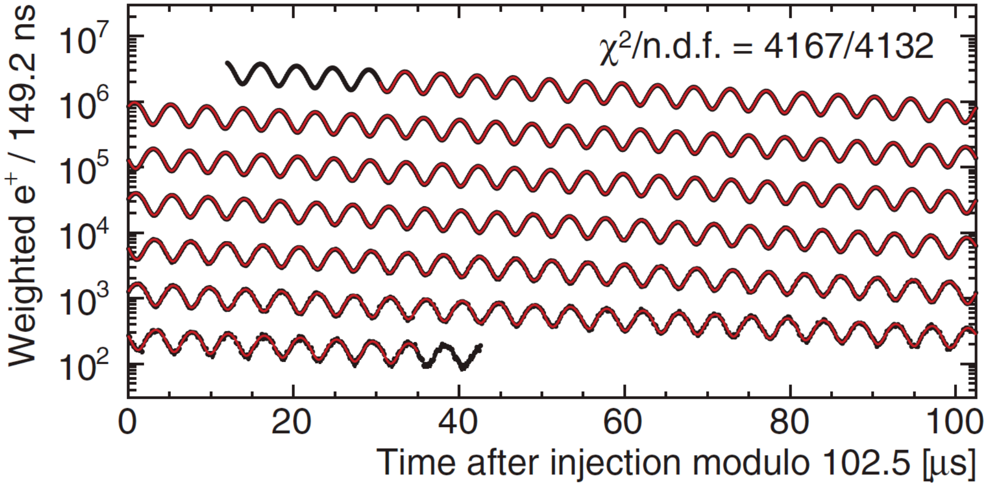

3 independent event reconstruction schemes
11 different and independent analyses
6 independent groups

Extract ω_a^{meas} from the wiggle plot

Histogram of decay e⁺ arrival times (wiggle plot)

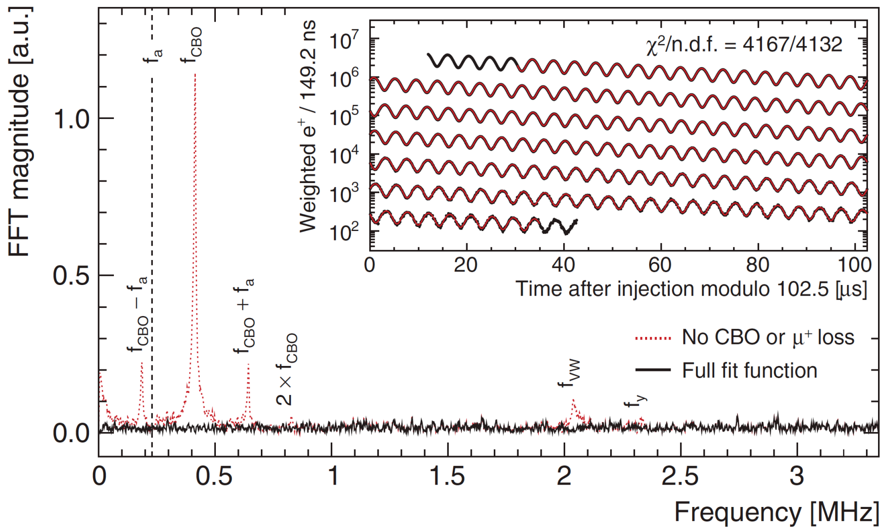

3 independent event reconstruction schemes
11 different and independent analyses
6 independent groups

Complex beam dynamics encoded in wiggle plot

Extract ω_a^{meas} from the wiggle plot

Histogram of decay e⁺ arrival times (wiggle plot)

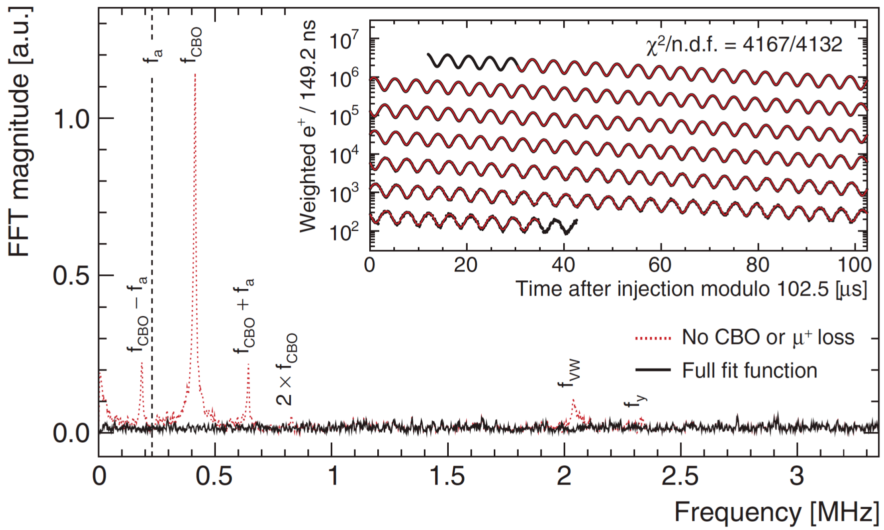

3 independent event reconstruction schemes
11 different and independent analyses
6 independent groups

Complex beam dynamics encoded in wiggle plot

Separate analyses for Runs 1a-1d

Extensive systematic checks passed:
→ "Software" unblinding to check consistency, hardware blinding still in place

Extract ω_a^{meas} from the wiggle plot

Histogram of decay e⁺ arrival times (wiggle plot)

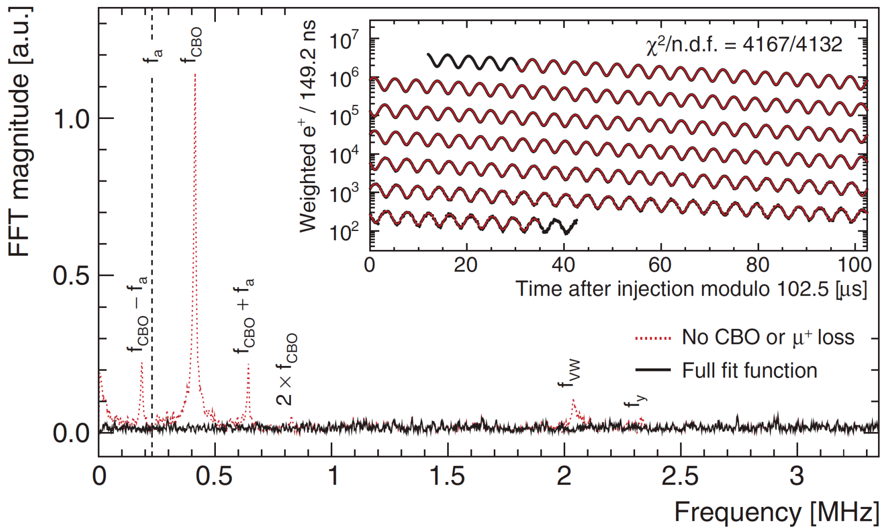

3 independent event reconstruction schemes
11 different and independent analyses
6 independent groups

Complex beam dynamics encoded in wiggle plot

Separate analyses for Runs 1a-1d

Extensive systematic checks passed:
→ "Software" unblinding to check consistency, hardware blinding still in place

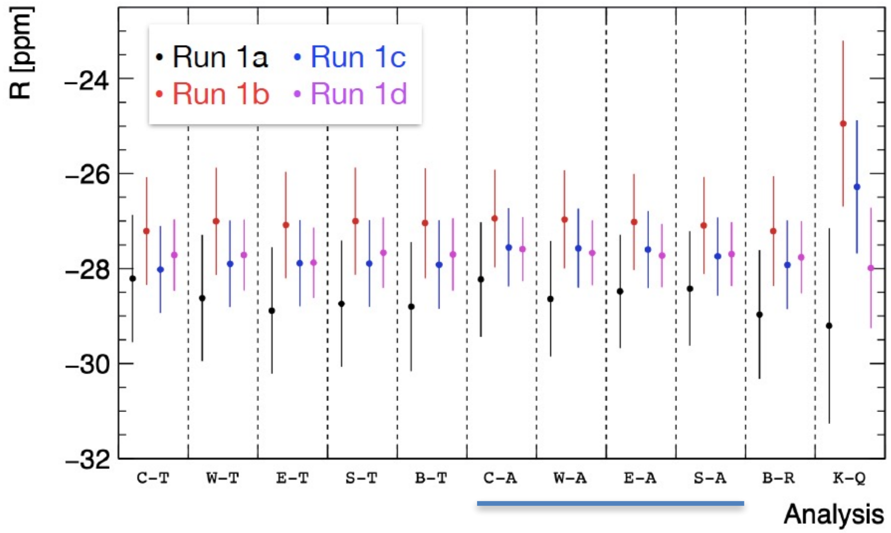

Extract ω_a^{meas} from the wiggle plot

Histogram of decay e⁺ arrival times (wiggle plot)

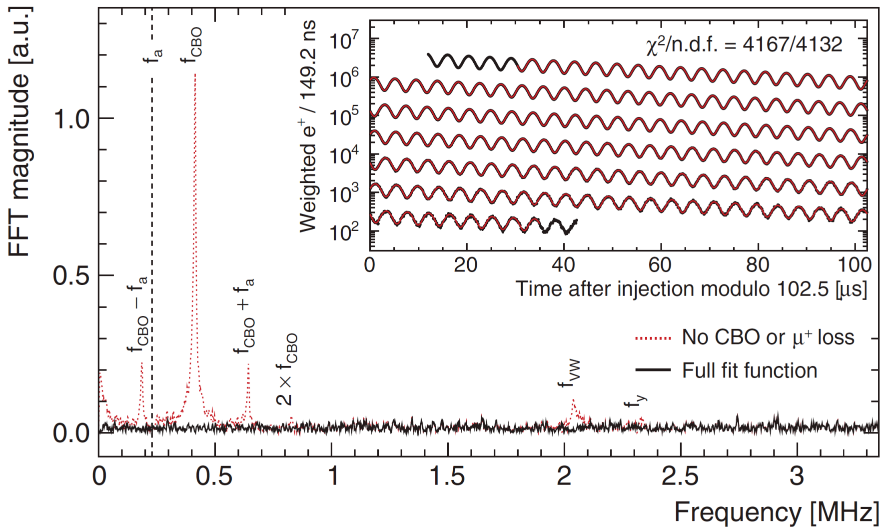

3 independent event reconstruction schemes
11 different and independent analyses
6 independent groups

Complex beam dynamics encoded in wiggle plot

Separate analyses for Runs 1a-1d

Extensive systematic checks passed:
→ "Software" unblinding to check consistency, hardware blinding still in place

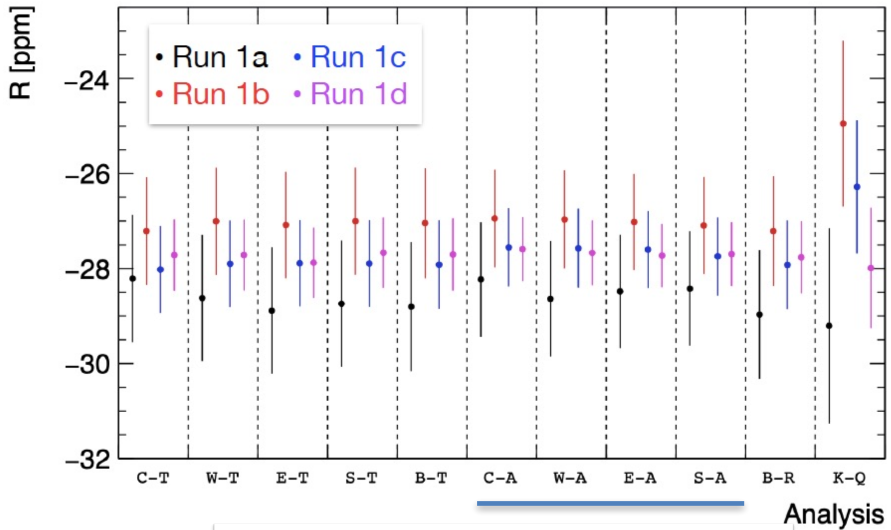

- **434 ppb** statistical uncertainty
- **56 ppb** systematic uncertainty

The long-known corrections: E-field and pitch correction

$$\vec{\omega}_{\mathrm{a}} = \vec{\omega}_{\mathrm{s}} - \vec{\omega}_{\mathrm{c}} = -\frac{e}{m}\left[a_\mu \vec{B} - a_\mu \left(\frac{\gamma}{\gamma+1}\right)\left(\vec{\beta}\cdot\vec{B}\right)\vec{\beta} - \left(a_\mu - \frac{1}{\gamma^2-1}\right)\frac{\vec{\beta}\times\vec{E}}{c}\right]$$

The long-known corrections: E-field and pitch correction

$$\vec{\omega}_{\mathrm{a}} = \vec{\omega}_{\mathrm{s}} - \vec{\omega}_{\mathrm{c}} = -\frac{e}{m}\left[a_\mu \vec{B} - a_\mu \left(\frac{\gamma}{\gamma+1}\right)\left(\vec{\beta}\cdot\vec{B}\right)\vec{\beta} - \left(a_\mu - \frac{1}{\gamma^2-1}\right)\frac{\vec{\beta}\times\vec{E}}{c}\right]$$

Pitch correction

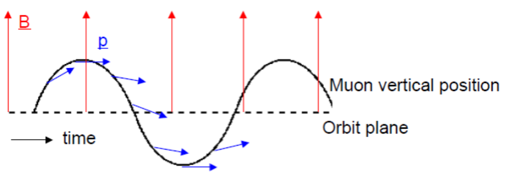

$$C_{\mathrm{p}} = \frac{n}{4R_0^2}\langle A^2\rangle$$

Trackers measure vertical oscillation amplitude

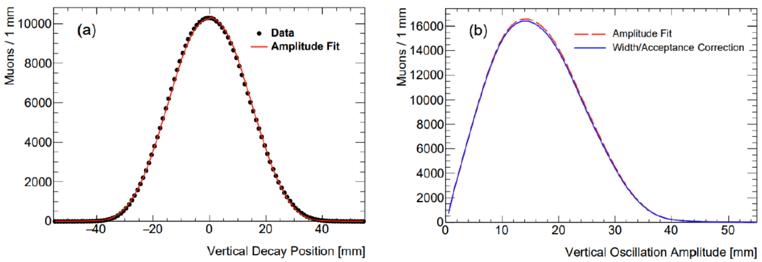

Correction: 180 ppb, Uncertainty: 13 ppb

The long-known corrections: E-field and pitch correction

$$\vec{\omega}_{\mathrm{a}} = \vec{\omega}_{\mathrm{s}} - \vec{\omega}_{\mathrm{c}} = -\frac{e}{m}\left[a_\mu \vec{B} - a_\mu \left(\frac{\gamma}{\gamma+1}\right)\left(\vec{\beta}\cdot\vec{B}\right)\vec{\beta} - \left(a_\mu - \frac{1}{\gamma^2-1}\right)\frac{\vec{\beta}\times\vec{E}}{c}\right]$$

Pitch correction

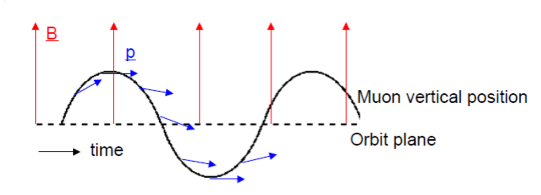

$$C_{\mathrm{p}} = \frac{n}{4R_0^2}\langle A^2\rangle$$

Trackers measure vertical oscillation amplitude

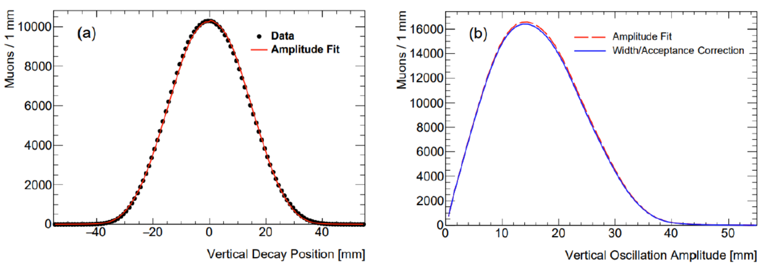

Correction: 180 ppb, Uncertainty: 13 ppb

Electric field correction

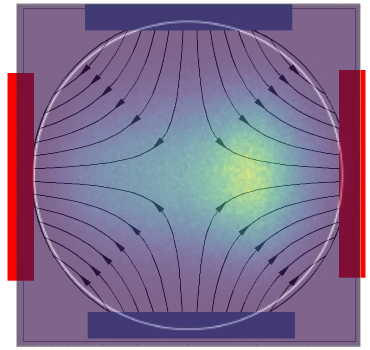

"Fast rotation analysis"

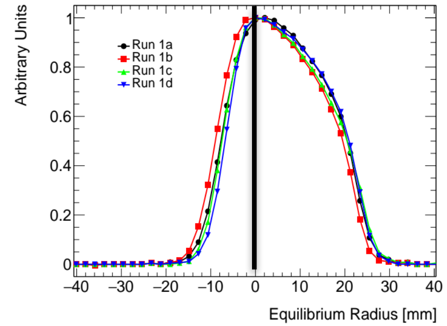

$$C_e = -2n(1-n)\beta^2\frac{\langle x_e^2\rangle}{R_0^2}$$

Correction: 489 ppb, Uncertainty: 53 ppb

Phase acceptance correction

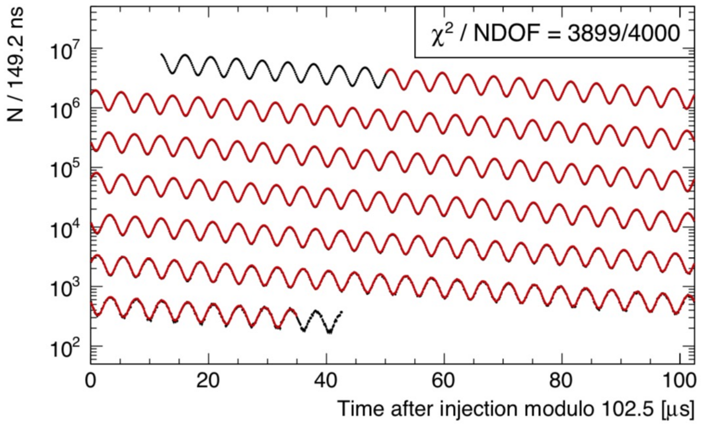

$$N(t) \approx N_0 e^{-\lambda t}\left[1 + A\cos\left(\omega_a t + \phi\right)\right]$$

Phase acceptance correction

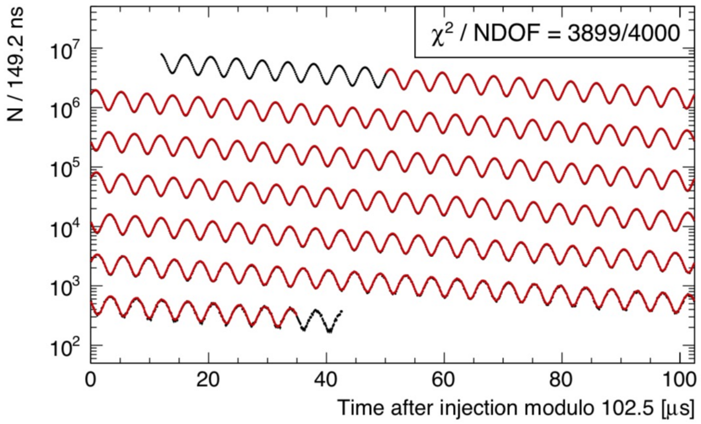

$$N(t) \approx N_0 e^{-\lambda t}\left[1 + A\cos\left(\omega_a t + \phi\right)\right]$$

If the phase of the muon ensemble is not stable, then:

$$\cos\left(\omega_a t + \phi_0 + \phi' t + \ldots\right) = \cos\left((\omega_a + \phi')t + \phi_0 + \ldots\right)$$

A possible frequency shift of ϕ'

Phase acceptance correction

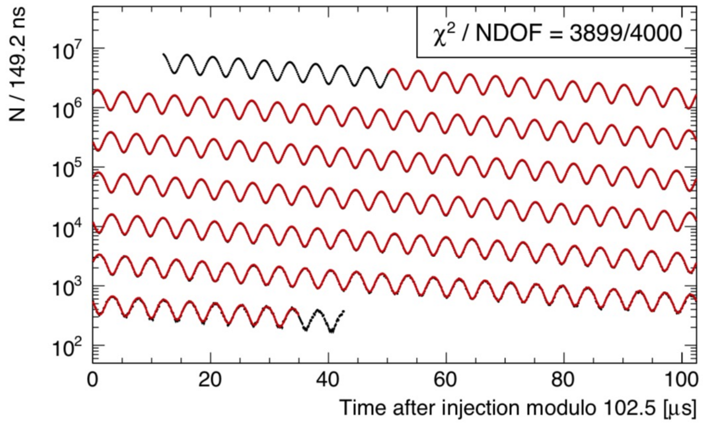

$$N(t) \approx N_0 e^{-\lambda t}\left[1 + \ldots \cos\left(\omega_a t + \phi\right)\right]$$

If the phase of the muon … not stable, then:

$$\cos\left(\omega_a t + \phi_0 + \ldots\right) = \cos\left((\omega_a + \phi')t + \phi_0 + \ldots\right)$$

early-to-late effect

… possible frequency shift of ϕ'

Phase acceptance correction

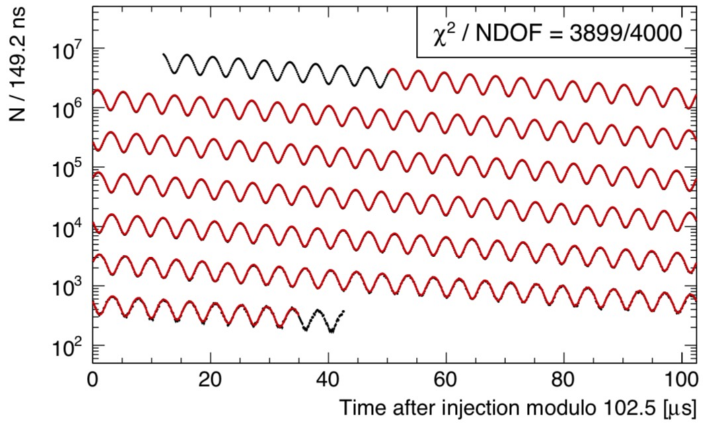

$$N(t) \approx N_0 e^{-\lambda t}\left[1 + A\cos\left(\omega_a t + \phi\right)\right]$$

If the phase of the muon … not stable, then:

$$\cos\left(\omega_a t + \phi_0 + \ldots\right) = \cos\left((\omega_a + \phi')t + \phi_0 + \ldots\right)$$

early-to-late effect

→ possible frequency shift of ϕ'

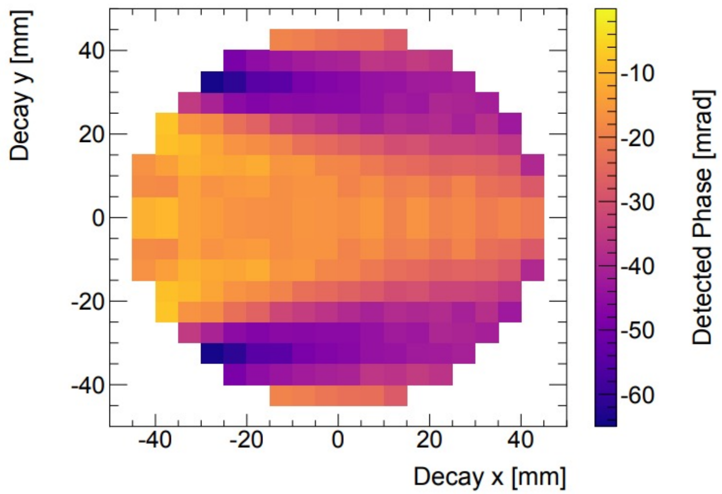

- The decay positrons carry a particular phase
- The phase depends on
  - Muon decay position
  - Decay positron energy
- Not a problem if muon distribution is stable in time, but…

Phase acceptance correction

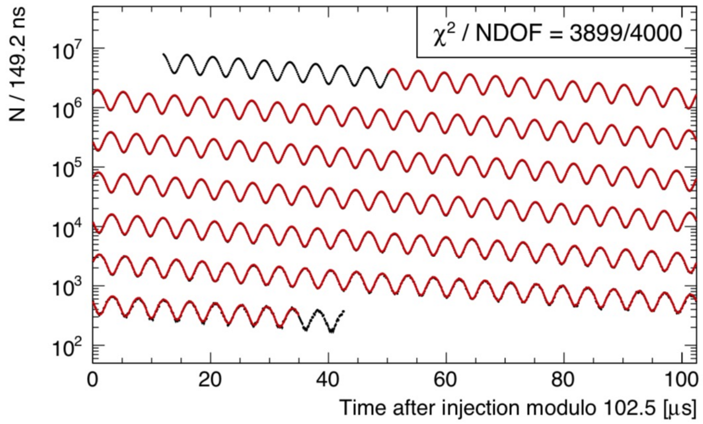

$$N(t) \approx N_0 e^{-\lambda t}\left[1 + A\cos\left(\omega_a t + \phi\right)\right]$$

early-to-late effect

If the phase of the muon … not stable, then:

$$\cos\left(\omega_a t + \phi_0 + \ldots\right) = \cos\left((\omega_a + \phi')t + \phi_0 + \ldots\right)$$

… possible frequency shift of ϕ'

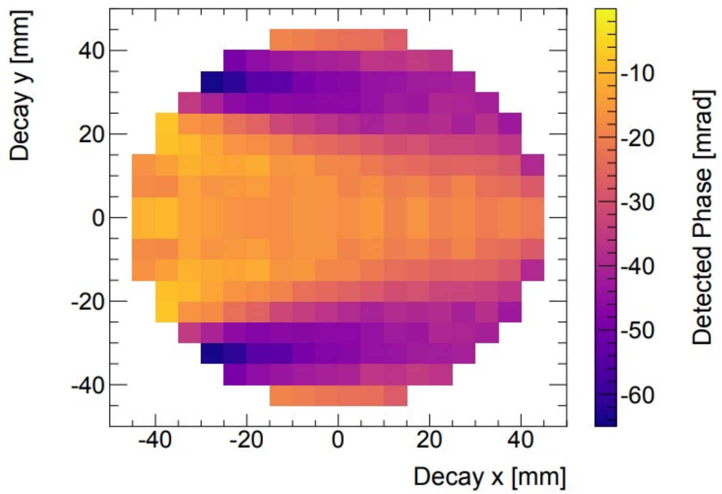

- The decay positrons carry a particular phase
- The phase depends on
  - Muon decay position
  - Decay positron energy

Extensive simulation campaign

- Not a problem if muon distribution is stable in time, but…

Phase acceptance correction: The voltage on the ESQs

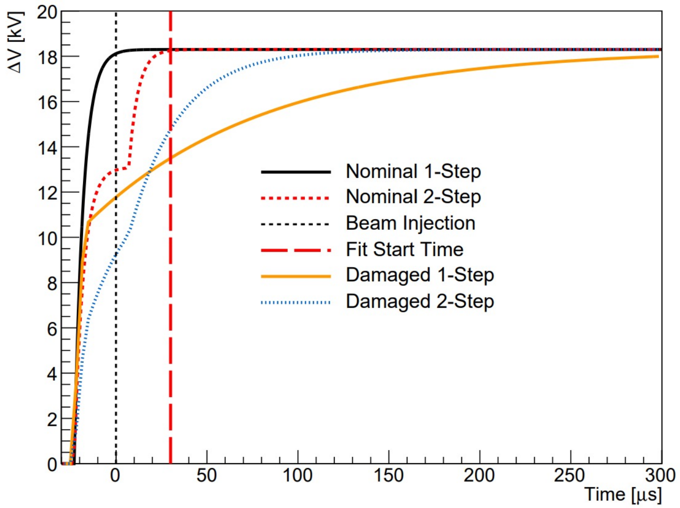

Systematic effect unique for Run 1 data (hardware fixed for run 2 and beyond):

- 2 high-voltage isolators for ESQ failed
- Time-dependent E-Field of on 2 ESQ plates
  → Change of vertical beam position and width

Phase acceptance correction: The voltage on the ESQs

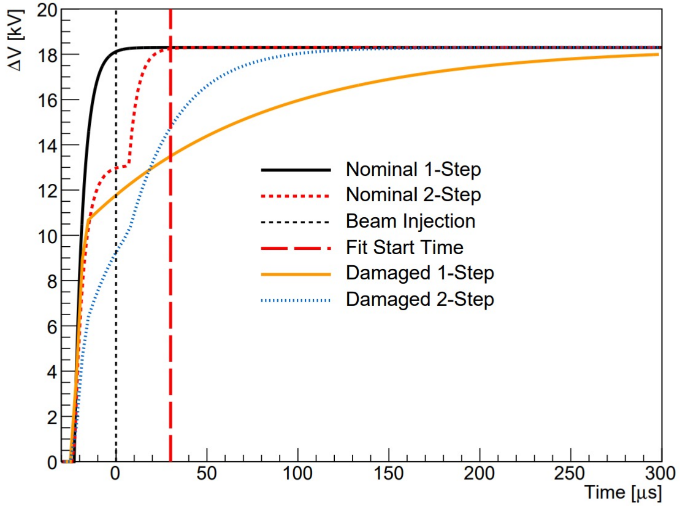

Systematic effect unique for Run 1 data (hardware fixed for run 2 and beyond):

- 2 high-voltage isolators for ESQ failed
- Time-dependent E-Field of on 2 ESQ plates
  → Change of vertical beam position and width

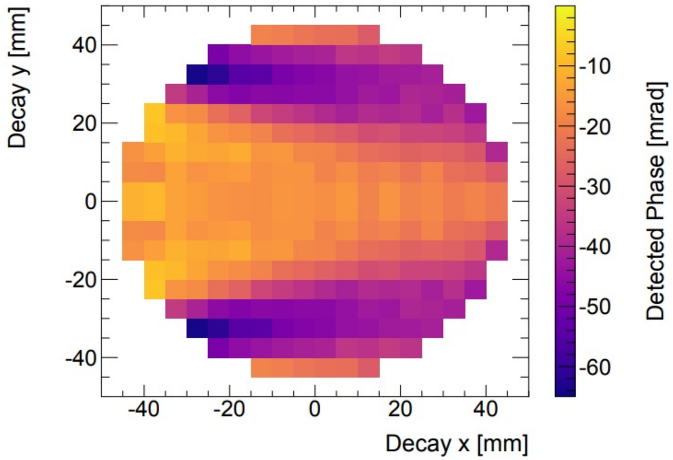

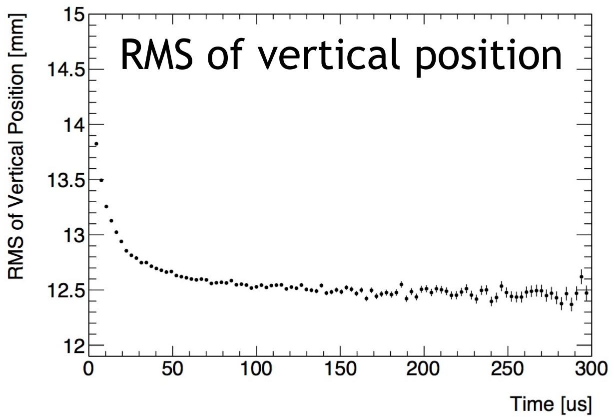

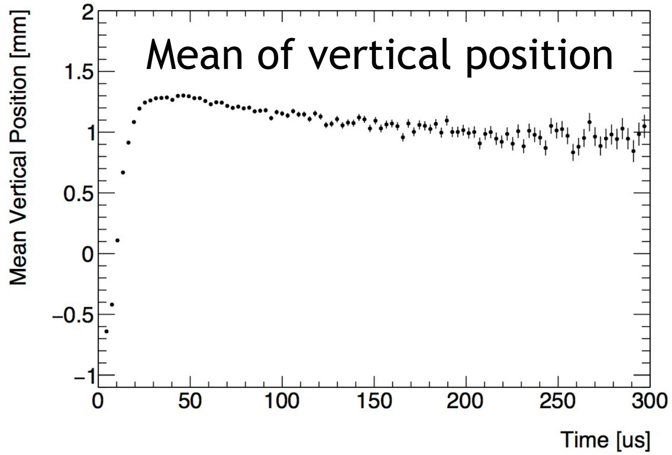

Phase acceptance correction: The voltage on the ESQs

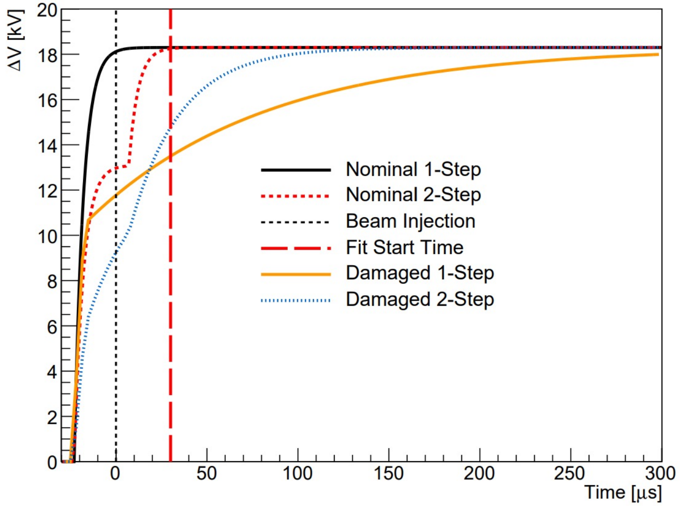

Systematic effect unique for Run 1 data (hardware fixed for run 2 and beyond):

- 2 high-voltage isolators for ESQ failed
- Time-dependent E-Field of on 2 ESQ plates
  → Change of vertical beam position and width

Correction: -158 ppb, Uncertainty: 75 ppb

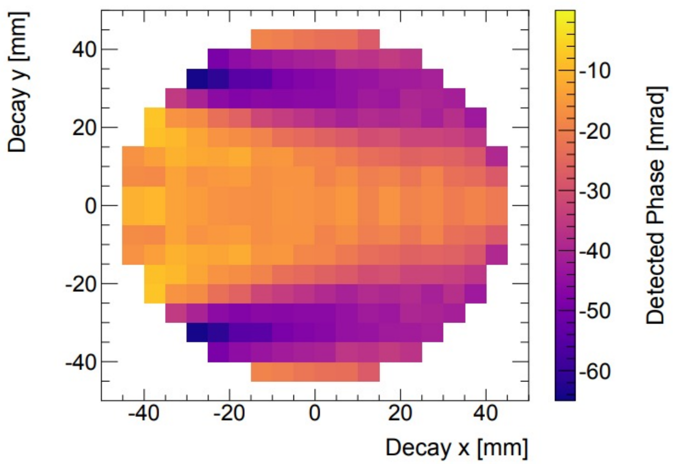

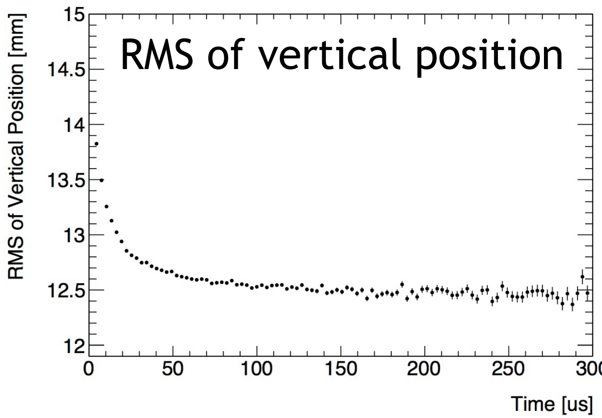

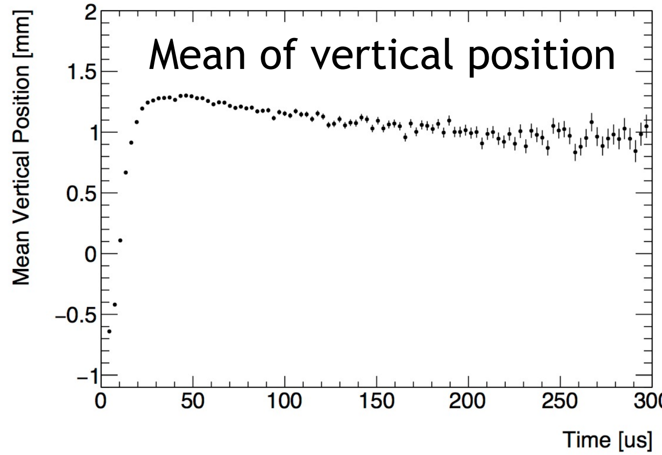

Lost muons correction

Another early-to-late effect: $\cos\left(\omega_{\mathrm{a}}t + \phi_0 + \phi' t + \ldots\right) = \cos\left((\omega_{\mathrm{a}} + \phi')t + \phi_0 + \ldots\right)$

Lost muons correction

Another early-to-late effect: $$\cos\left(\omega_a t + \phi_0 + \phi' t + \ldots\right) = \cos\left((\omega_a + \phi')t + \phi_0 + \ldots\right)$$

$$\frac{d\phi_0}{dt} = \frac{d\phi_0}{d\langle p\rangle}\frac{d\langle p\rangle}{dt}$$

Lost muons correction

Another early-to-late effect: $\cos\left(\omega_a t + \phi_0 + \phi' t + \ldots\right) = \cos\left((\omega_a + \phi')t + \phi_0 + \ldots\right)$

$$\frac{d\phi_0}{dt} = \frac{d\phi_0}{d\langle p\rangle}\frac{d\langle p\rangle}{dt}$$

Spin-momentum correlation
from dipole magnets in beamline

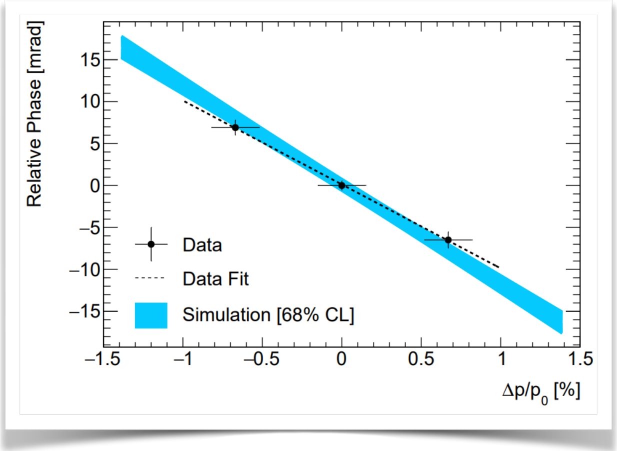

Lost muons correction

Another early-to-late effect: $\cos\left(\omega_a t + \phi_0 + \phi' t + \ldots\right) = \cos\left((\omega_a + \phi')t + \phi_0 + \ldots\right)$

$$\frac{d\phi_0}{dt} = \frac{d\phi_0}{d\langle p\rangle}\frac{d\langle p\rangle}{dt}$$

Spin-momentum correlation
from dipole magnets in beamline

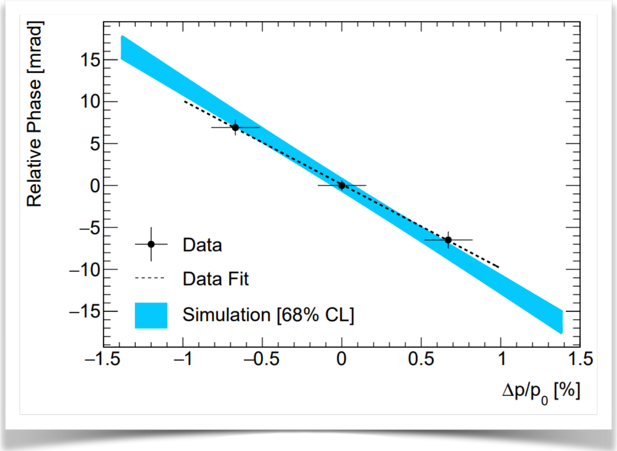

Momentum dependent losses
High-p muons lost faster!

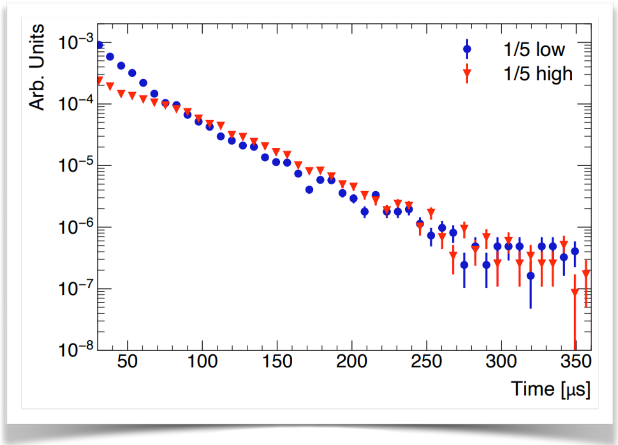

Lost muons correction

Another early-to-late effect: $\cos\left(\omega_a t + \phi_0 + \phi' t + \ldots\right) = \cos\left((\omega_a + \phi')t + \phi_0 + \ldots\right)$

$$\frac{d\phi_0}{dt} = \frac{d\phi_0}{d\langle p\rangle}\frac{d\langle p\rangle}{dt}$$

Time-dependent phase shift

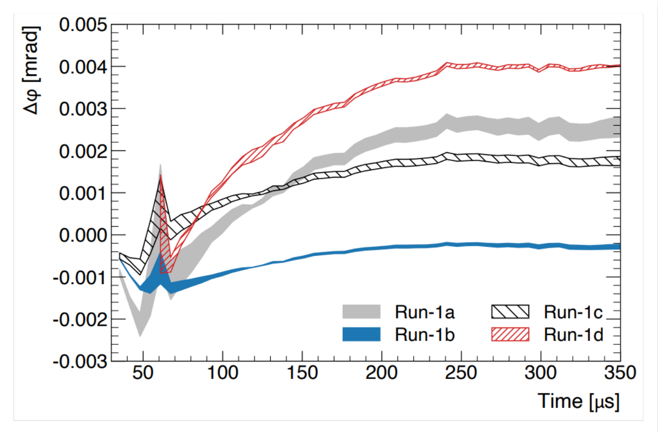

Spin-momentum correlation
from dipole magnets in beamline

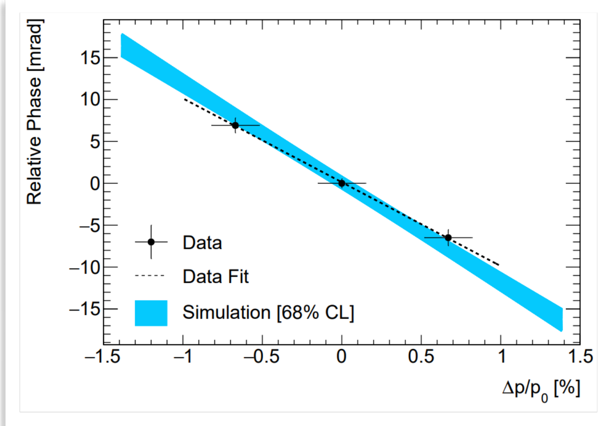

Momentum dependent losses
High-p muons lost faster!

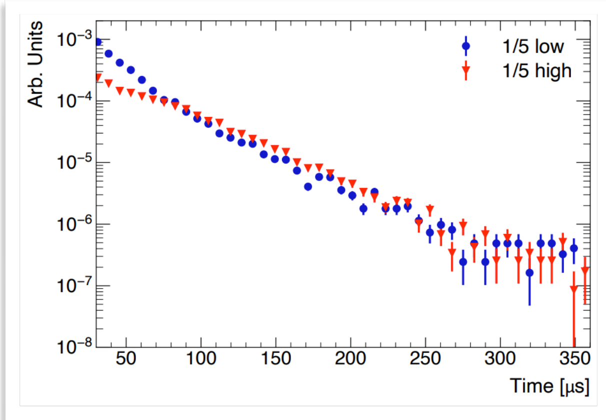

Lost muons correction

Another early-to-late effect: $\cos\left(\omega_a t + \phi_0 + \phi' t + \ldots\right) = \cos\left((\omega_a + \phi')t + \phi_0 + \ldots\right)$

$$\frac{d\phi_0}{dt} = \frac{d\phi_0}{d\langle p\rangle}\frac{d\langle p\rangle}{dt}$$

Time-dependent phase shift

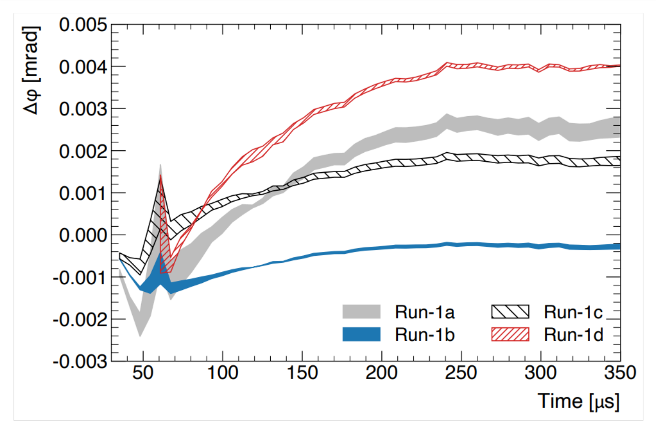

Spin-momentum correlation
from dipole magnets in beamline

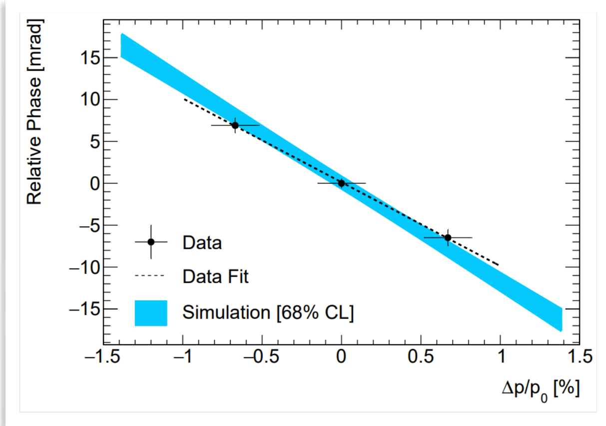

Momentum dependent losses
High-p muons lost faster!

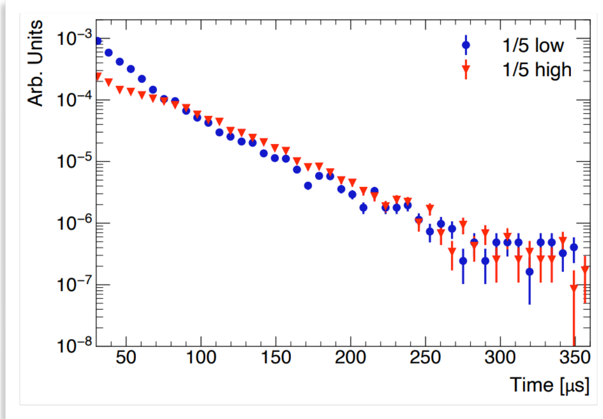

Correction: -11 ppb, Uncertainty: 5 ppb

Extracting a_μ: the magnetic field distribution and calibration

$$R' = \frac{\omega_a}{\omega'_p} = \frac{f_{\mathrm{clock}}\, \omega_a^{\mathrm{meas}} \left(1 + C_e + C_p + C_{ml} + C_{pa}\right)}{\boxed{f_{\mathrm{calib}}} \left\langle M\left(x, y, \phi\right) \boxed{\omega'_p\left(x, y, \phi\right)} \right\rangle \left(1 + B_k + B_q\right)}$$

The magnetic field calibration chain

"The trolley"

17 NMR probes, 3-day interval

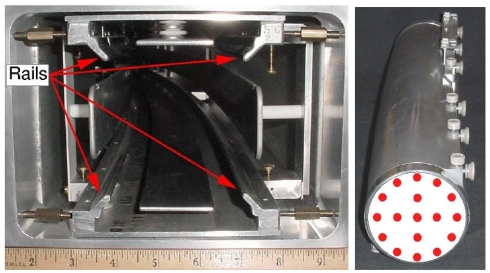

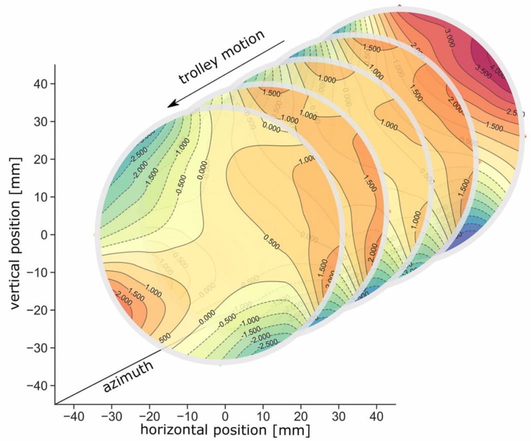

"The fixed probe array"

378 pulsed nuclear magnetic resonance probes measure 24/7 around μ beam

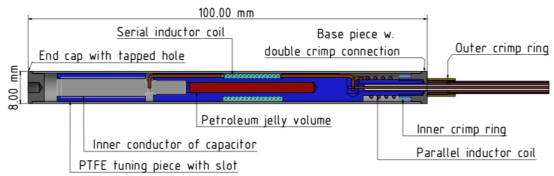

"The calibration"

"Plunging probe" to transfer absolute calibration to trolley probes

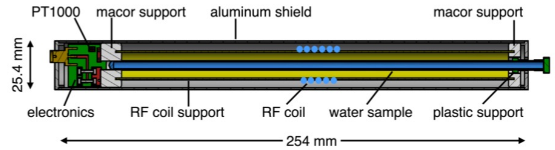

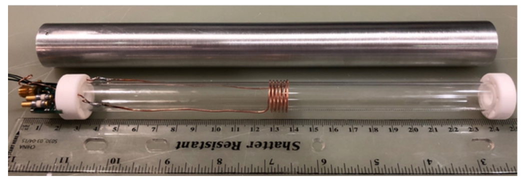

The precision magnetic field: passive shimming

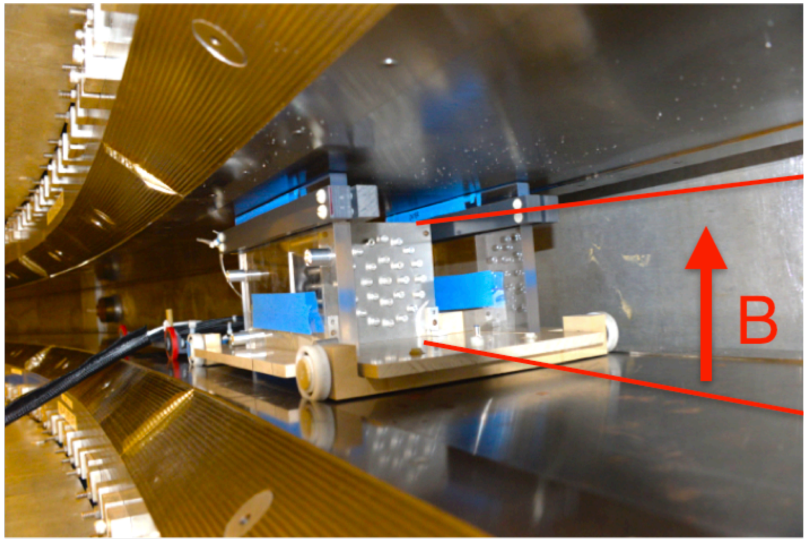

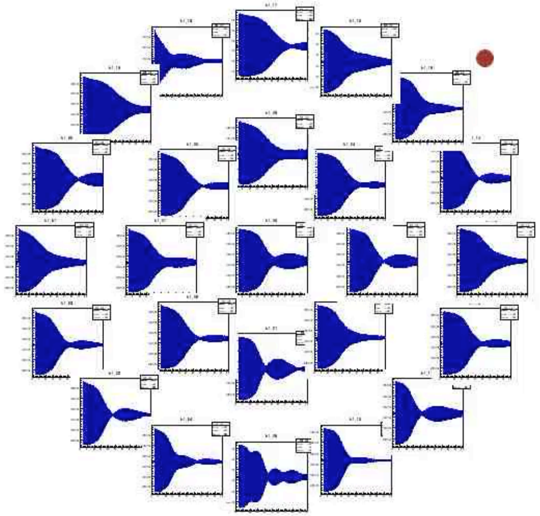

Adjust the position and orientation of pole pieces, wedged pieces (iron)
to minimize the field inhomogeneities

The precision magnetic field: passive shimming

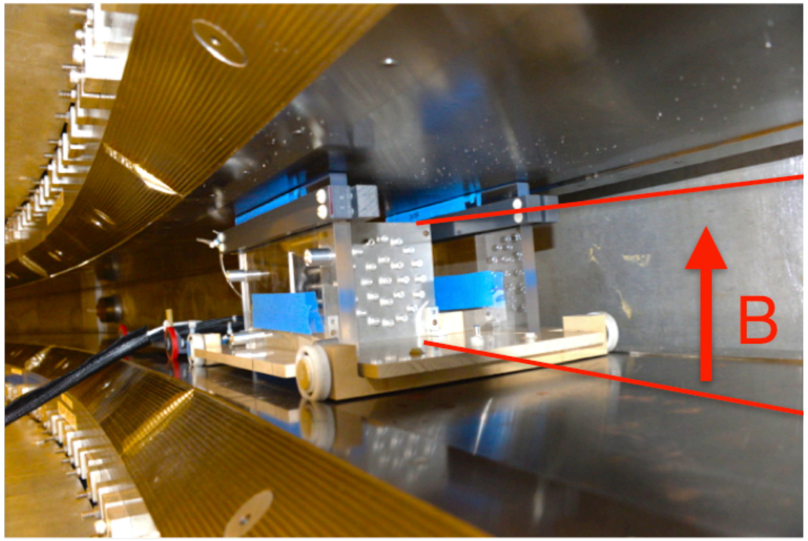

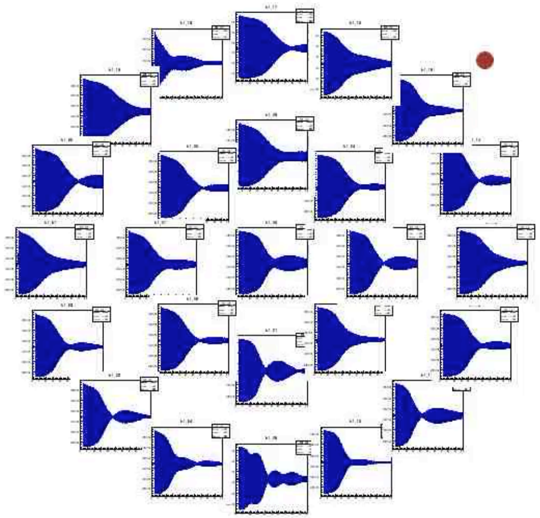

Adjust the position and orientation of pole pieces, wedged pieces (iron)
to minimize the field inhomogeneities

The precision magnetic field: passive shimming

Novel to E989: Provide about 10000 iron foil strips to shim out the residual magnetic field inhomogeneities

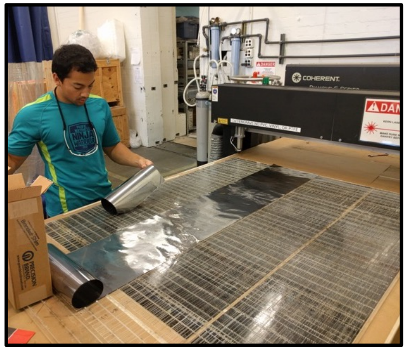

The precision magnetic field: passive shimming

Novel to E989: Provide about 10000 iron foil strips to shim out the residual magnetic field inhomogeneities

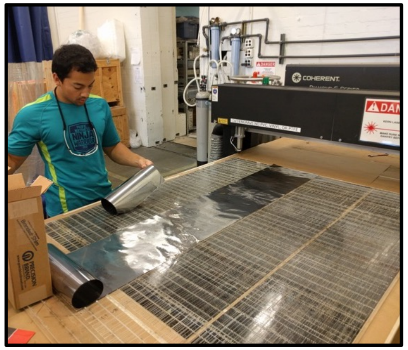

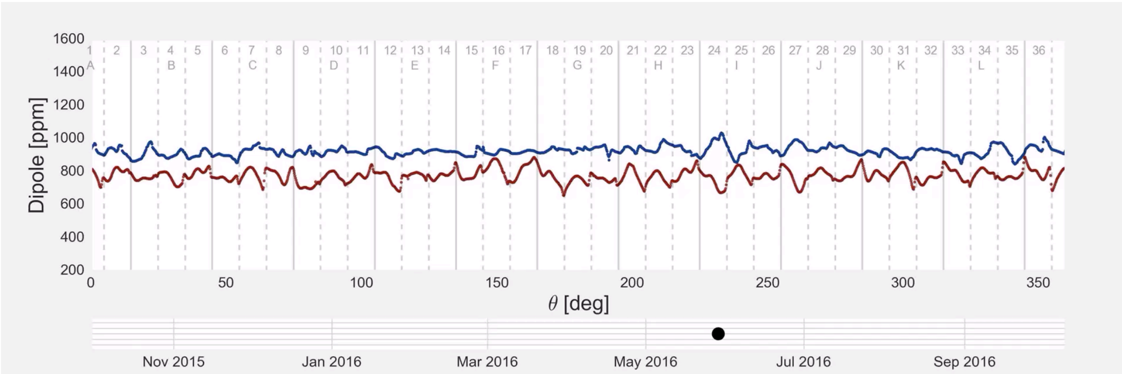

Factor 3 better homogeneity after passive shimming

The precision magnetic field: spatial mapping

"The trolley"

17 NMR probes, 3-day interval

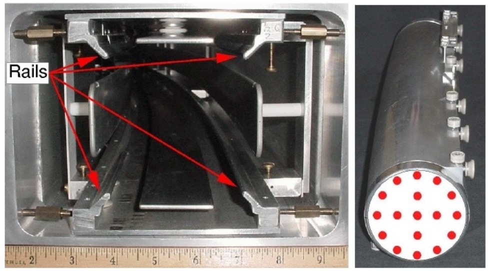

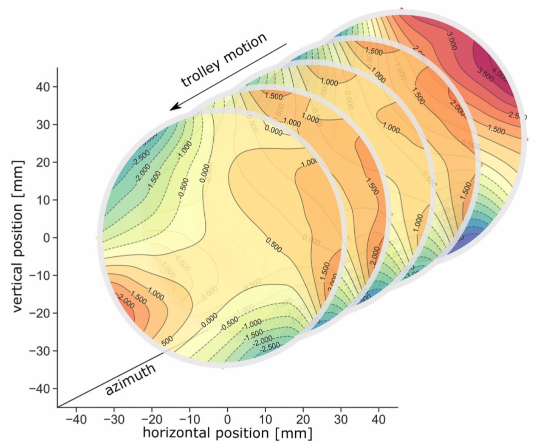

The precision magnetic field: spatial mapping

"The trolley"

17 NMR probes, 3-day interval

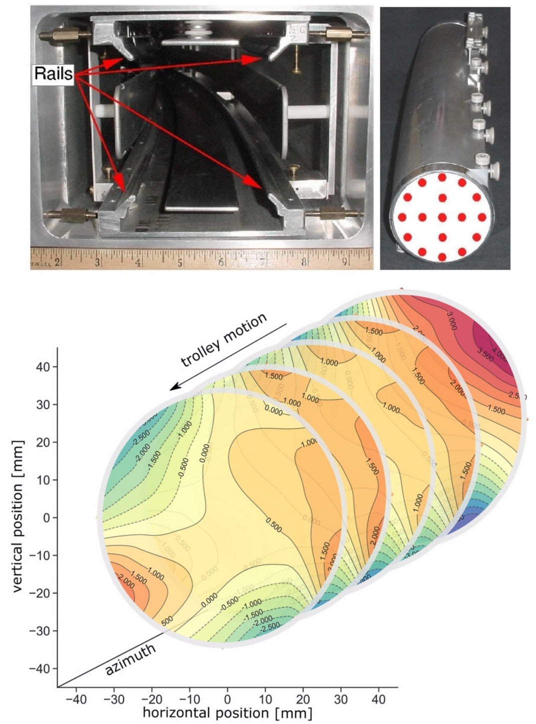

About 9000 azimuthal positions
to make a field decomposition into
2D spatial multipoles

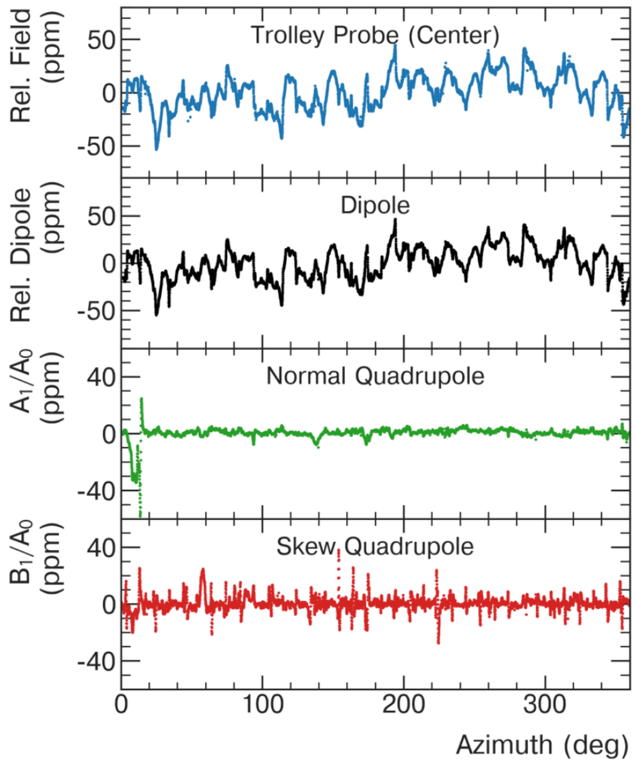

The precision magnetic field: spatial mapping

“The trolley”

17 NMR probes, 3-day interval

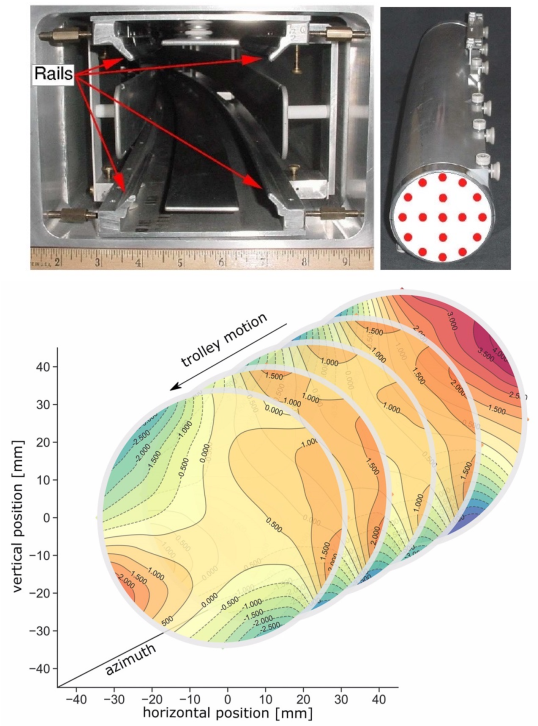

About 9000 azimuthal positions to make a field decomposition into 2D spatial multipoles

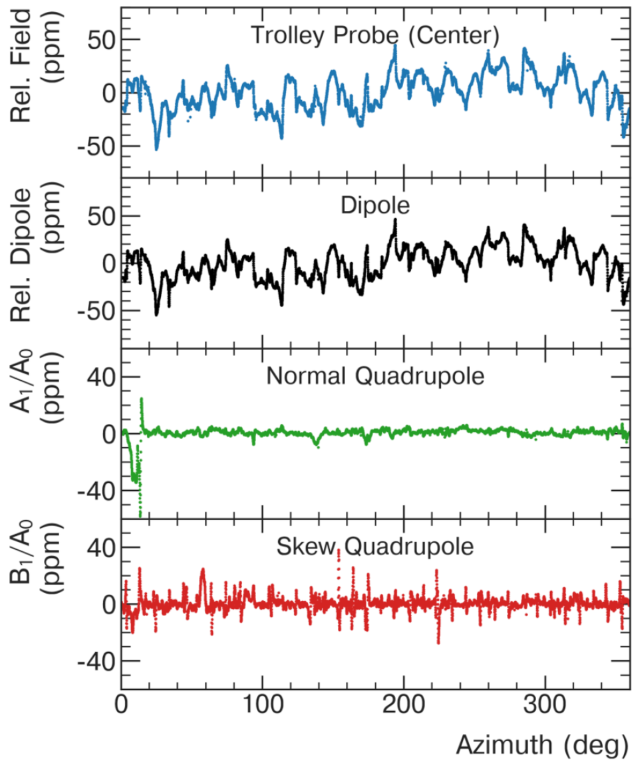

A typical azimuthally averaged magnetic field map

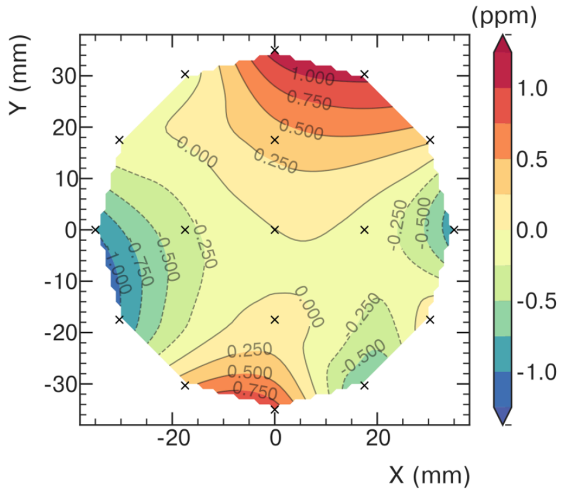

The precision magnetic field: tracking in time

"The fixed probe array"

378 pulsed nuclear magnetic resonance probes measure 24/7 around μ beam

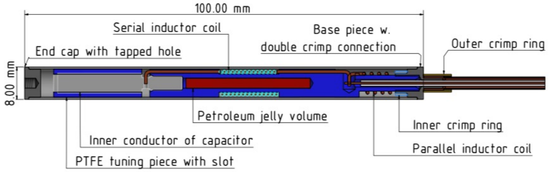

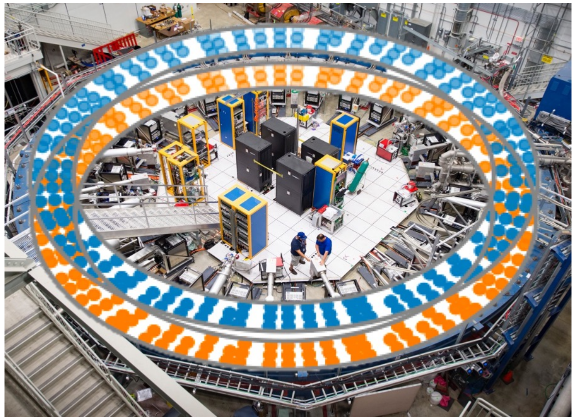

The precision magnetic field: tracking in time

“The fixed probe array”

378 pulsed nuclear magnetic resonance probes measure 24/7 around μ beam

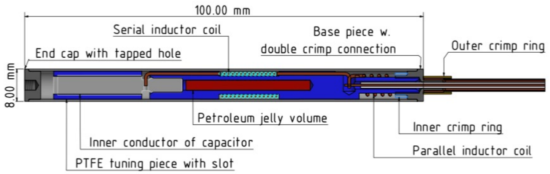

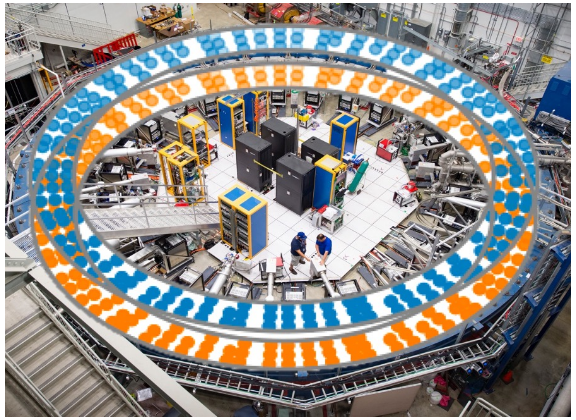

Established relation between multipoles measured by fixed probe stations and trolley

The precision magnetic field: tracking in time

"The fixed probe array"

378 pulsed nuclear magnetic resonance probes measure 24/7 around μ beam

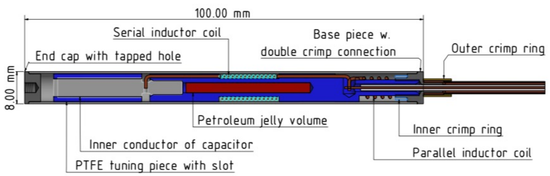

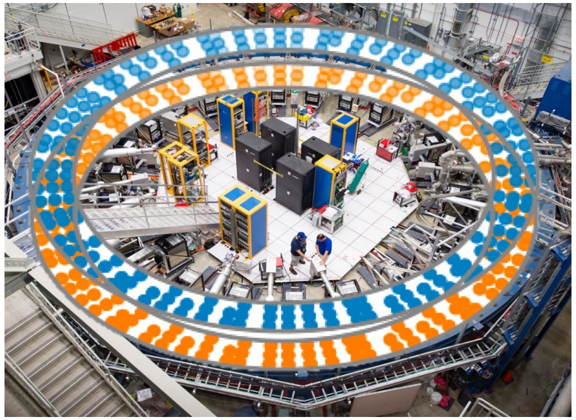

Established relation between multipoles measured by fixed probe stations and trolley

Tracking of the temporal variations of fixed probe stations

The precision magnetic field: tracking in time

"The fixed probe array"

378 pulsed nuclear magnetic resonance probes measure 24/7 around μ beam

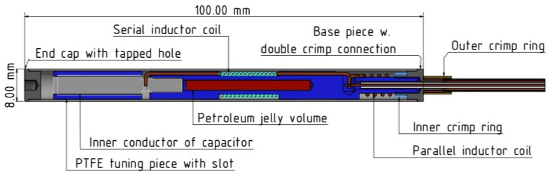

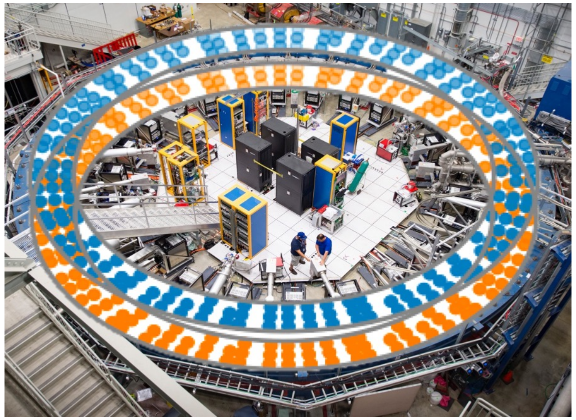

Established relation between multipoles measured by fixed probe stations and trolley

Tracking of the temporal variations of fixed probe stations

Application of correction for residual relative drifts

The precision magnetic field: tracking in time

"The fixed probe array"

378 pulsed nuclear magnetic resonance probes measure 24/7 around μ beam

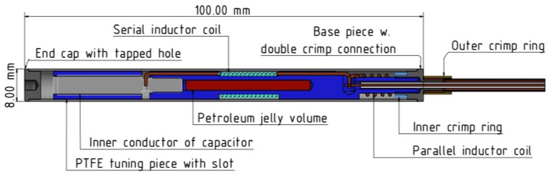

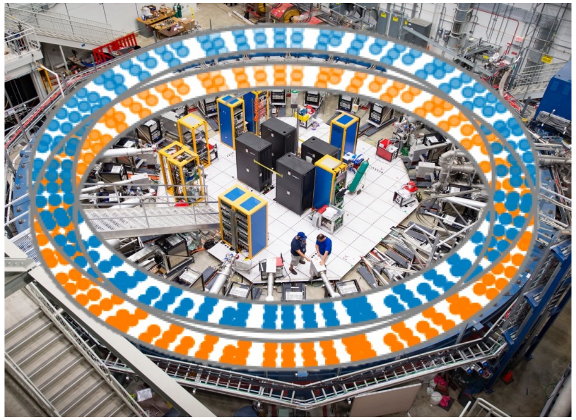

Established relation between multipoles measured by fixed probe stations and trolley

Tracking of the temporal variations of fixed probe stations

Application of correction for residual relative drifts

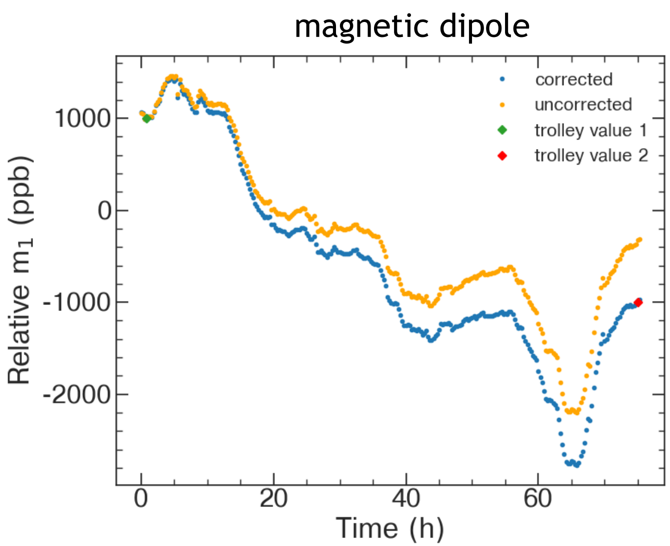

The precision magnetic field: tracking in time

"The fixed probe array"

378 pulsed nuclear magnetic resonance probes measure 24/7 around μ beam

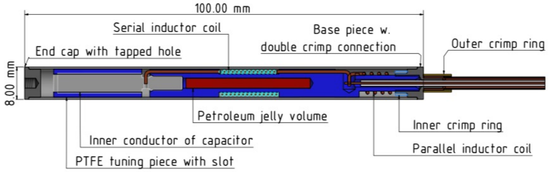

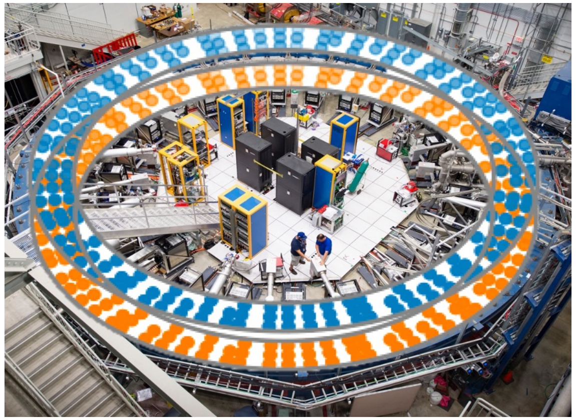

Established relation between multipoles measured by fixed probe stations and trolley

Tracking of the temporal variations of fixed probe stations

Application of correction for residual relative drifts

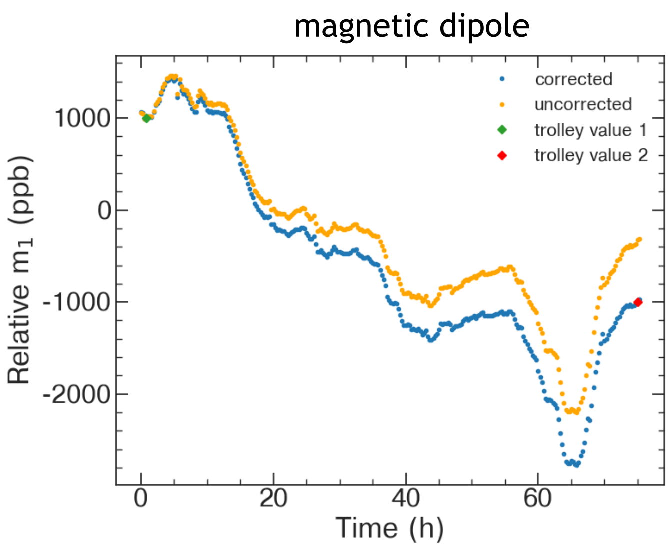

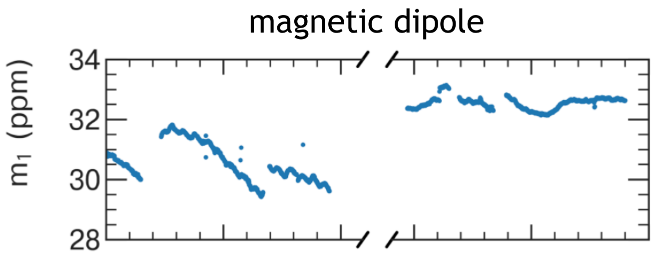

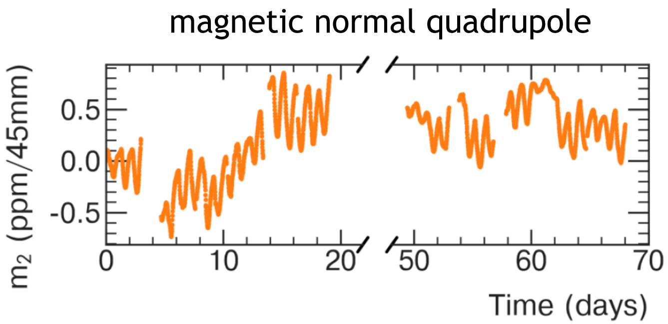

Extracting a_μ: the muon weighted average magnetic field

$$R' = \frac{\omega_a}{\omega'_p} = \frac{f_{\mathrm{clock}}\,\omega_a^{\mathrm{meas}}\left(1 + C_e + C_p + C_{ml} + C_{pa}\right)}{f_{\mathrm{calib}}\boxed{\left\langle M\left(x, y, \phi\right)\omega'_p\left(x, y, \phi\right)\right\rangle}\left(1 + B_k + B_q\right)}$$

JG|U

The muon weighted average magnetic field

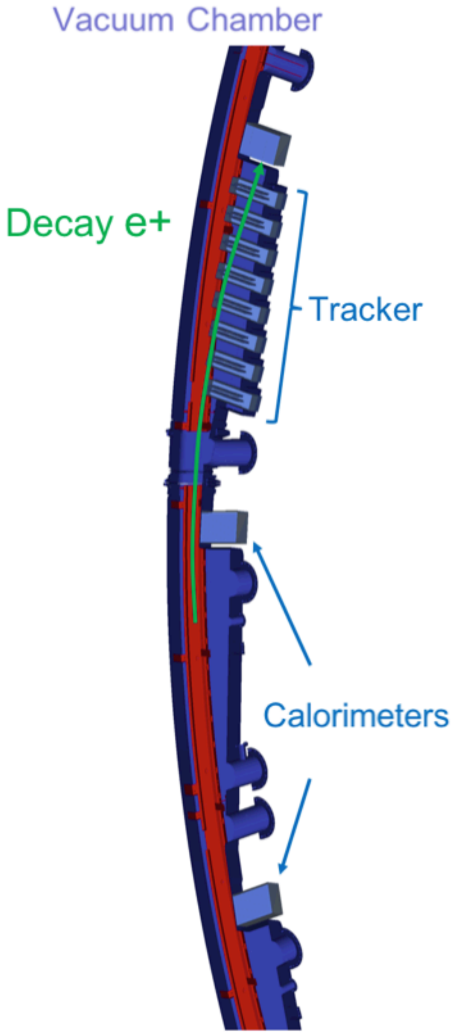

The muon weighted average magnetic field

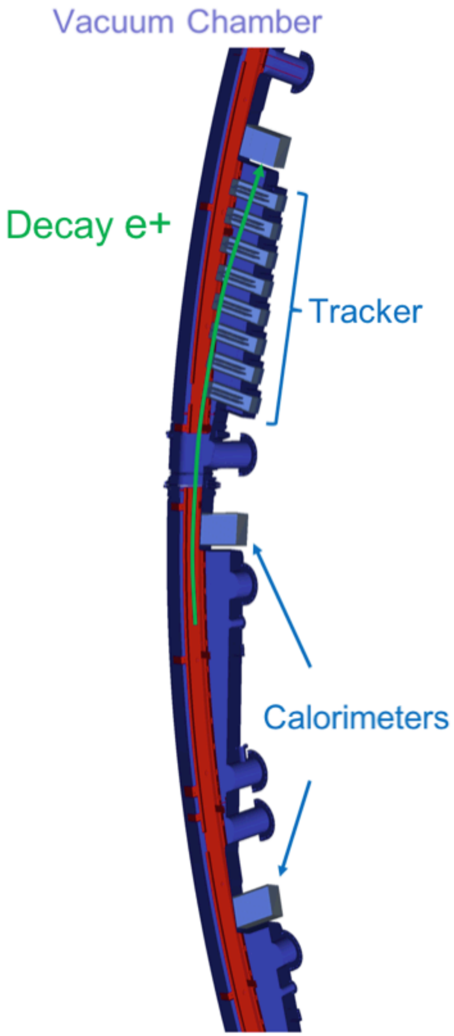

A muon's perspective of the tracker

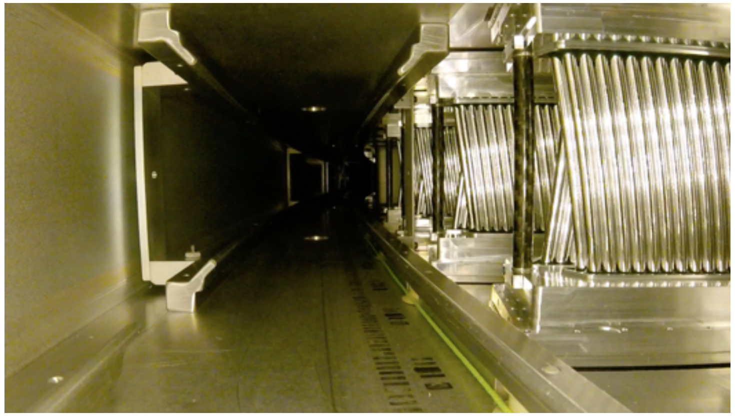

The muon weighted average magnetic field

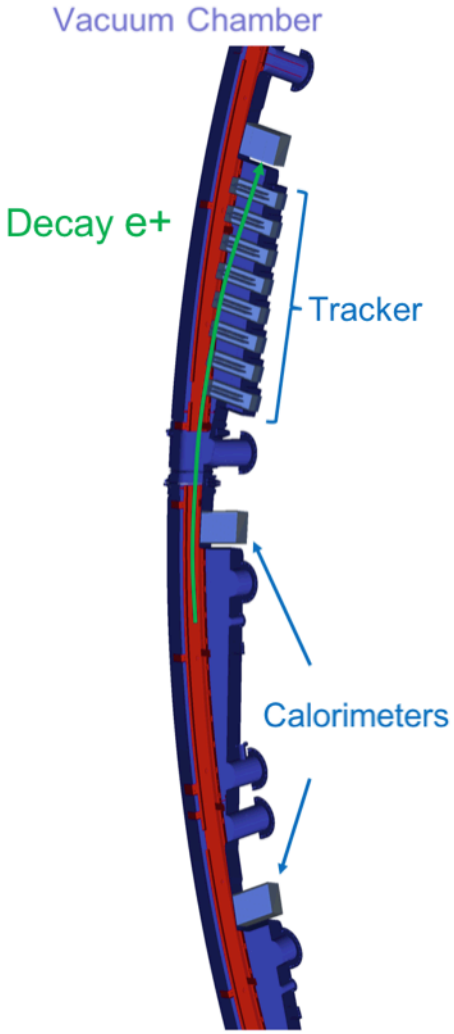

A muon's perspective of the tracker

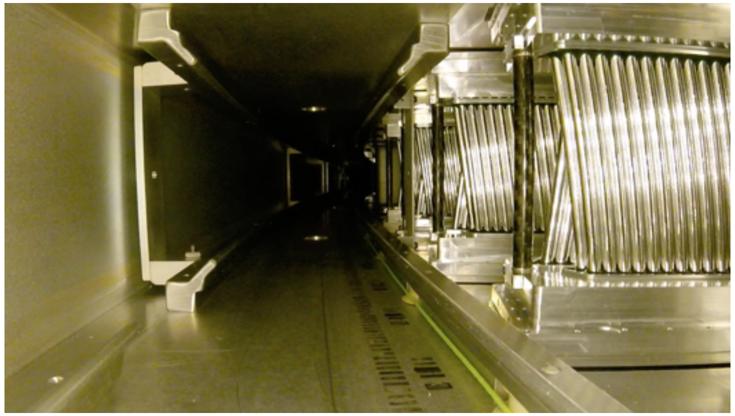

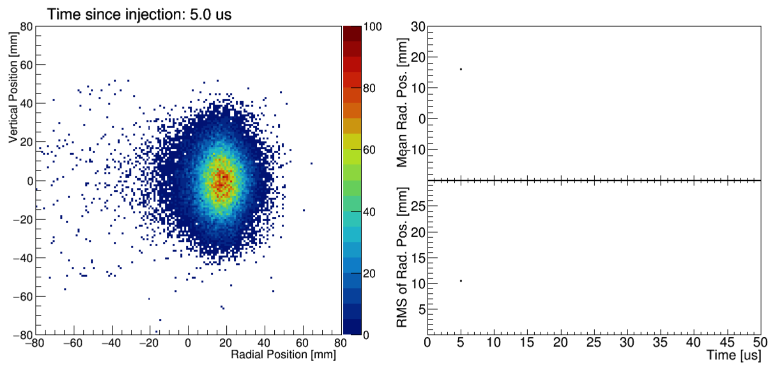

The muon weighted average magnetic field

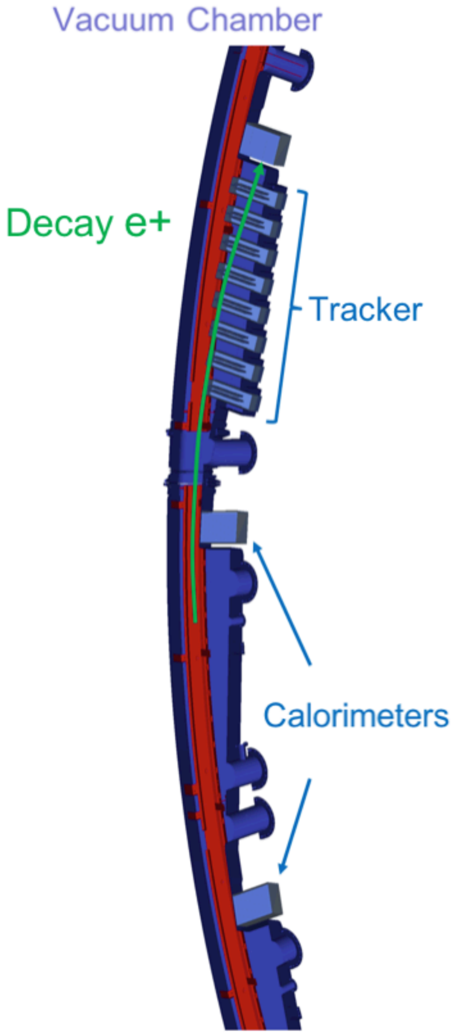

A muon's perspective of the tracker

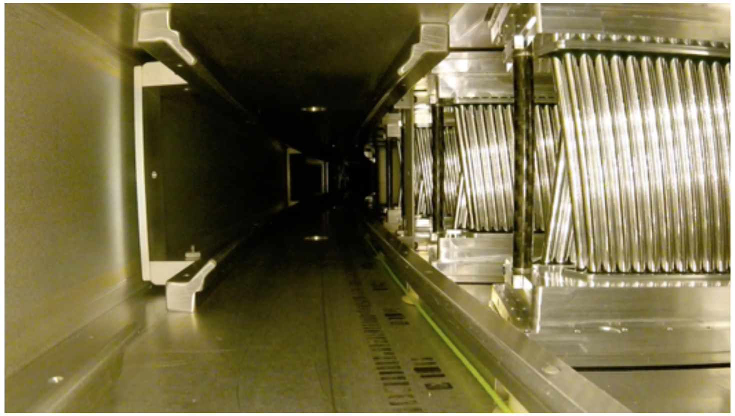

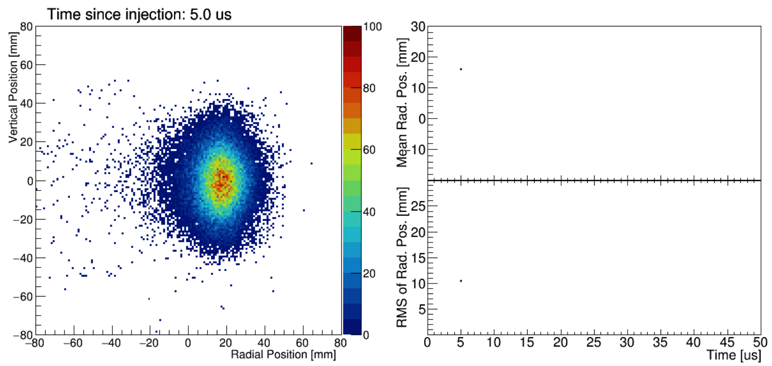

Beam tracker stations combined with beam dynamics simulations

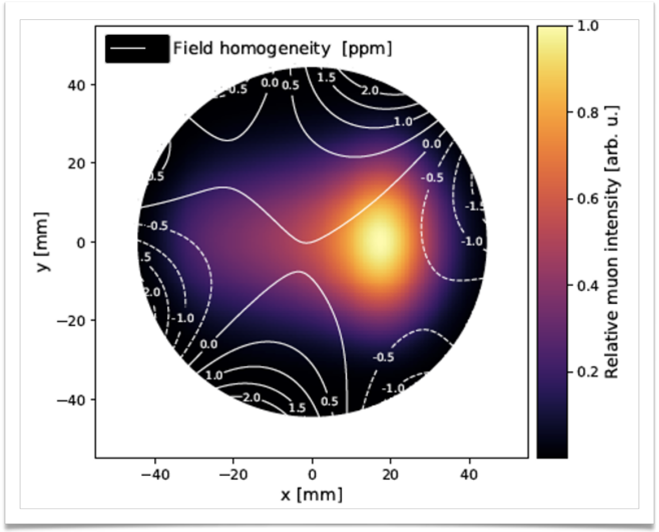

56 ppb uncertainty

Incl. probe calibrations, field map, tracker alignment, beam dynamics model

Extracting a_μ: transients from ESQ

$$R' = \frac{\omega_a}{\omega'_p} = \frac{f_{\mathrm{clock}}\, \omega_a^{\mathrm{meas}} \left(1 + C_e + C_p + C_{ml} + C_{pa}\right)}{f_{\mathrm{calib}} \left\langle M(x,y,\phi)\, \omega'_p(x,y,\phi) \right\rangle \left(1 + B_k + \boxed{B_q}\right)}$$

JG|U

Transients from electrostatic quadrupoles (ESQ)

ESQ only static on the time scale of an muon beam bunch injection:

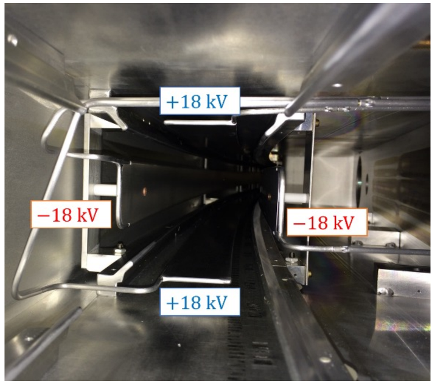

- Pulsing with high-voltage:
  - → mechanical vibrations of electric conductors
  - → perturbation of B field

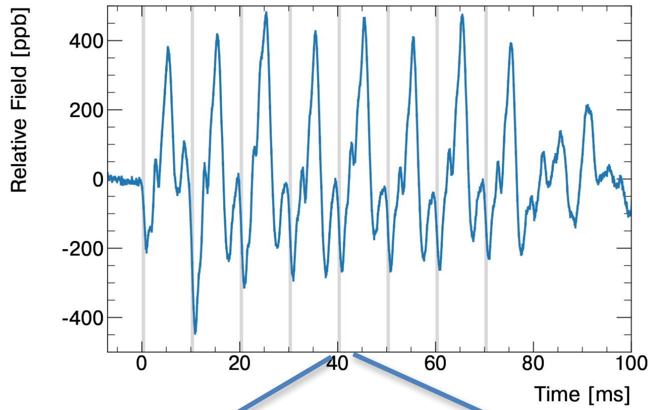

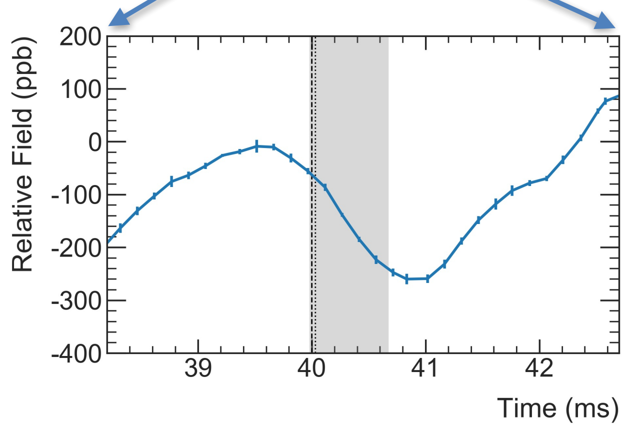

Transients from electrostatic quadrupoles (ESQ)

ESQ only static on the time scale of an muon beam bunch injection:

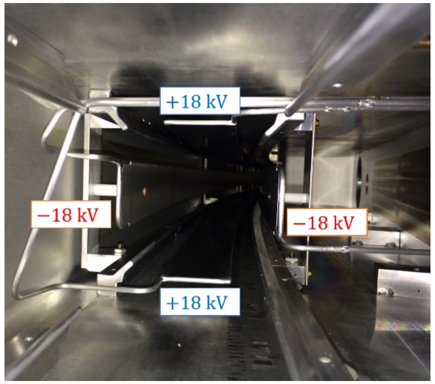

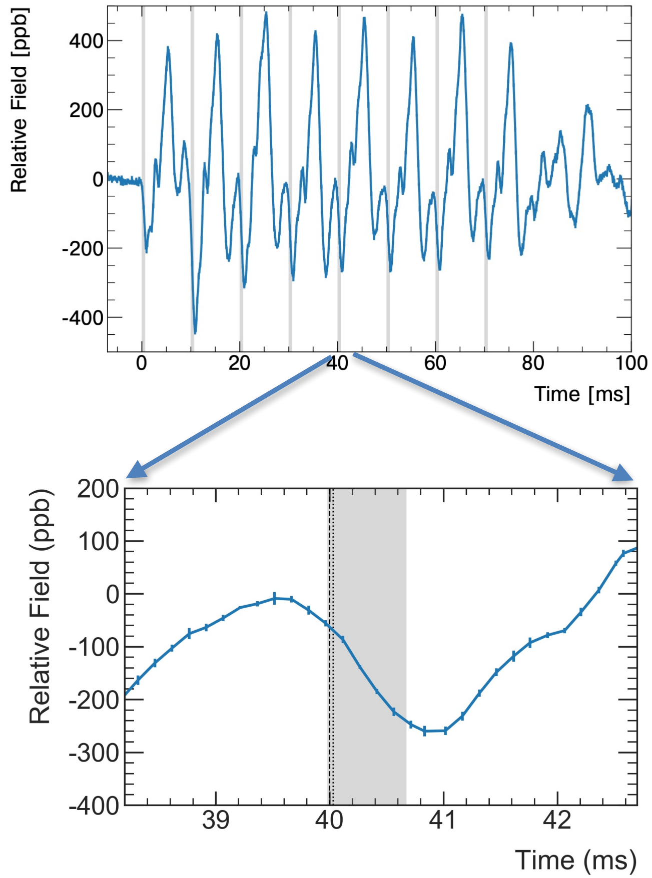

- Pulsing with high-voltage:
  - → mechanical vibrations of electric conductors
  - → perturbation of B field

- Measurement only after Run 2 → Conservative limit
- Included pNMR probe head in special casing (non conductive)
- Perform beam synchronized measurements

Transients from electrostatic quadrupoles (ESQ)

ESQ only static on the time scale of an muon beam bunch injection:

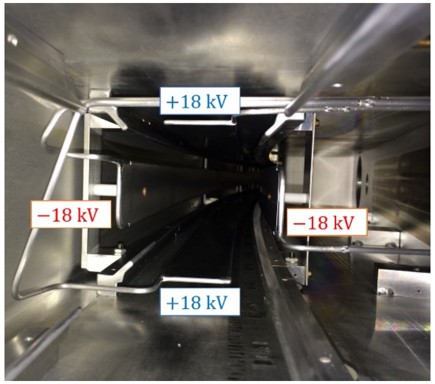

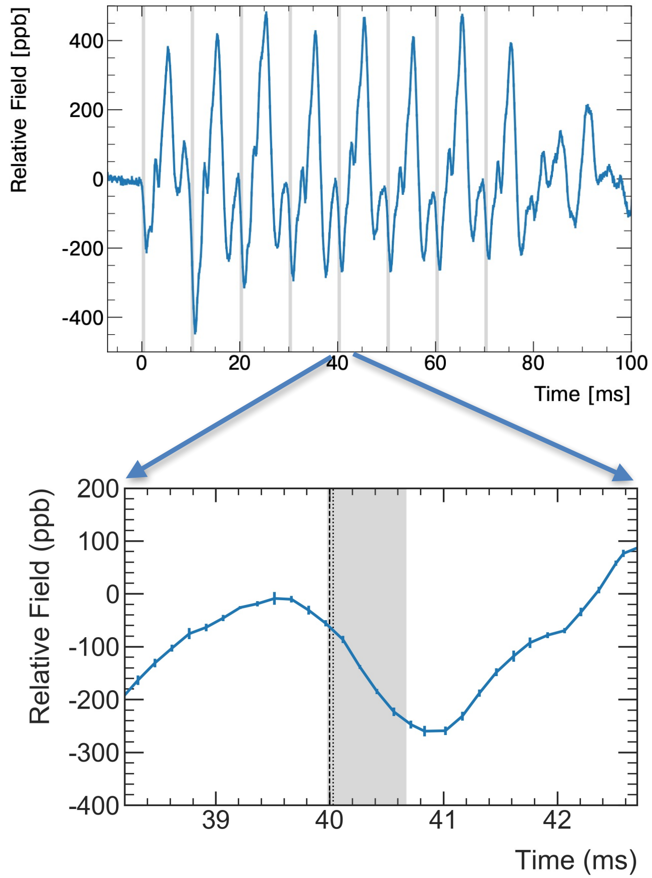

Correction: 17 ppb
Uncertainty: 92 ppb

- Pulsing with high-voltage:
  → mechanical vibrations of electric conductors
  → perturbation of B field

- Measurement only after Run 2 → Conservative limit
- Included pNMR probe head in special casing (non conductive)
- Perform beam synchronized measurements

Extracting a_μ: transients from kicker magnet

$$R' = \frac{\omega_a}{\omega'_p} = \frac{f_{\mathrm{clock}}\, \omega_a^{\mathrm{meas}} \left(1 + C_e + C_p + C_{ml} + C_{pa}\right)}{f_{\mathrm{calib}} \left\langle M\left(x, y, \phi\right) \omega'_p\left(x, y, \phi\right)\right\rangle \left(1 + \boxed{B_k} + B_q\right)}$$

Magnetic field transients from kicker magnet

Powerful kicker magnet induces eddy current in vacuum chamber walls:

Faraday magnetometer:

- fiber-based
- non-conducting
- non-magnetic
- 3D printed structure

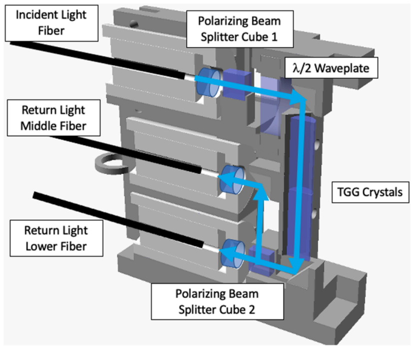

Magnetic field transients from kicker magnet

Powerful kicker magnet induces eddy current in vacuum chamber walls:

Faraday magnetometer:

- fiber-based
- non-conducting
- non-magnetic
- 3D printed structure

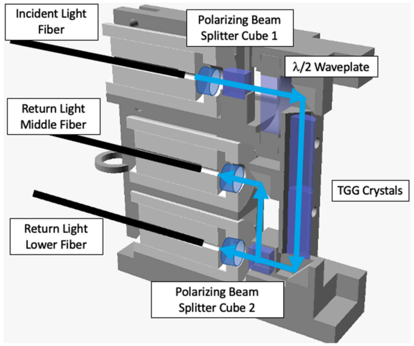

Kicker plates

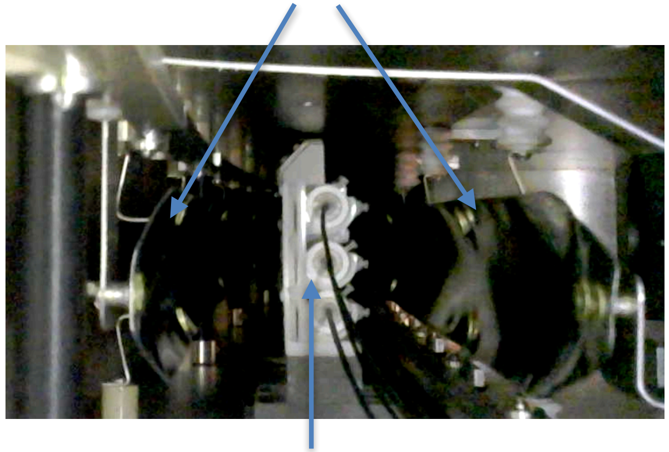

Faraday magnetometer

Signal modeled as a single exponential function: $\Delta B\,(t) = \Delta B\,(0)\,e^{-t/\tau_k}$

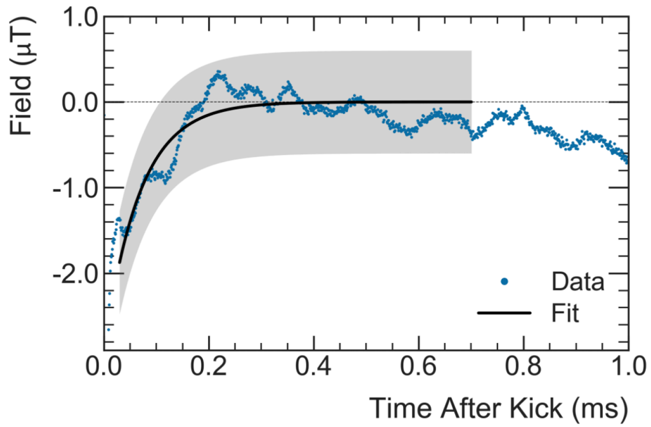

Magnetic field transients from kicker magnet

Powerful kicker magnet induces eddy current in vacuum chamber walls:

Faraday magnetometer:

- fiber-based
- non-conducting
- non-magnetic
- 3D printed structure

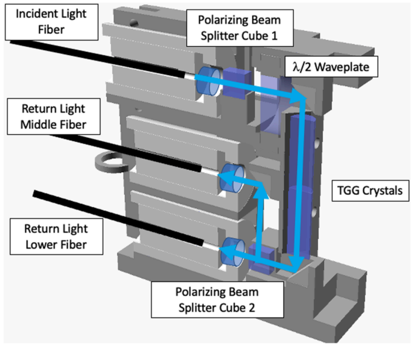

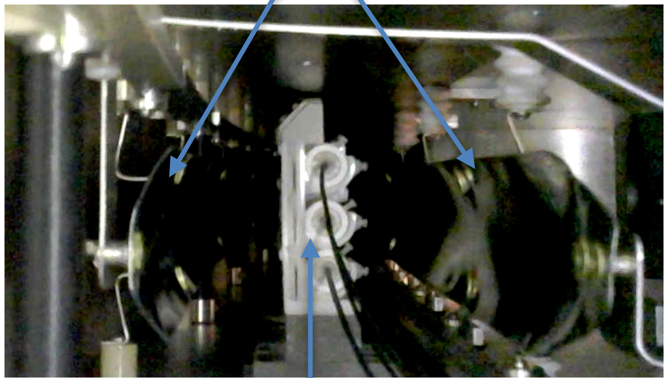

Signal modeled as a single exponential function: $\Delta B\,(t) = \Delta B\,(0)\, e^{-t/\tau_k}$

Effect weighted by:

- kicker coverage
- spatial muon distribution

Correction: -27 ppb
Uncertainty: 37 ppb

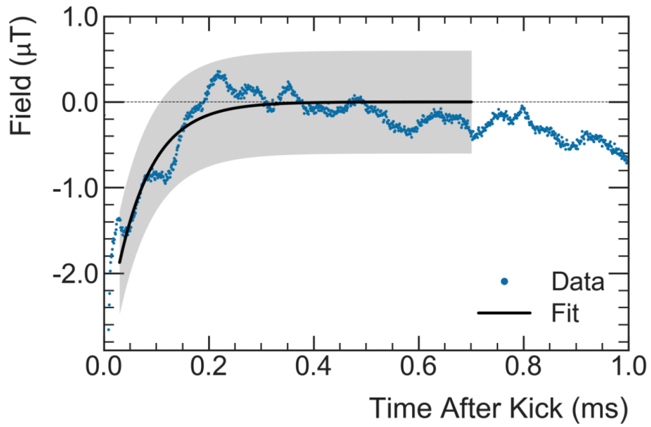

Extracting a_μ - our tools

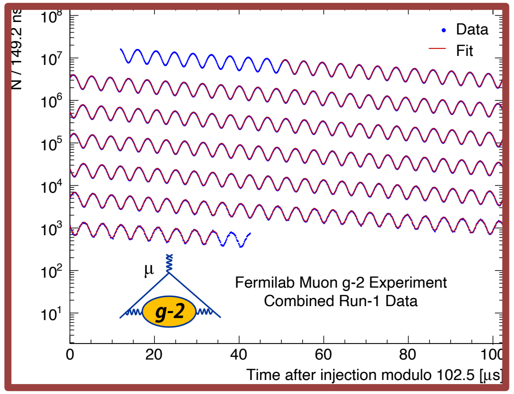

Anomalous spin precession frequency

Muon beam dynamics corrections

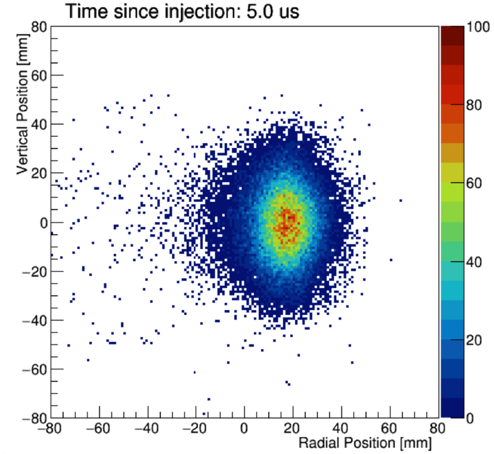

$$R' = \frac{\omega_a}{\tilde{\omega}'_p} = \frac{f_{\mathrm{clock}}\, \omega_a^{\mathrm{meas}} \left(1 + C_e + C_p + C_{ml} + C_{pa}\right)}{f_{\mathrm{calib}} \left\langle M(x, y, \phi)\, \omega'_p(x, y, \phi) \right\rangle \left(1 + B_k + B_q\right)}$$

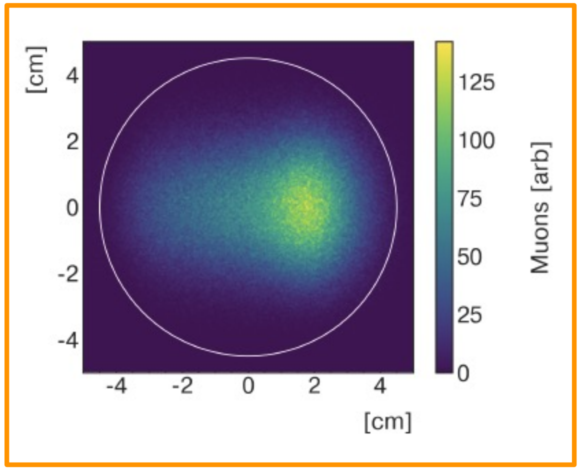

Spatial muon distribution

Spatial distribution of magnetic field

Transient magnetic fields

Calibration

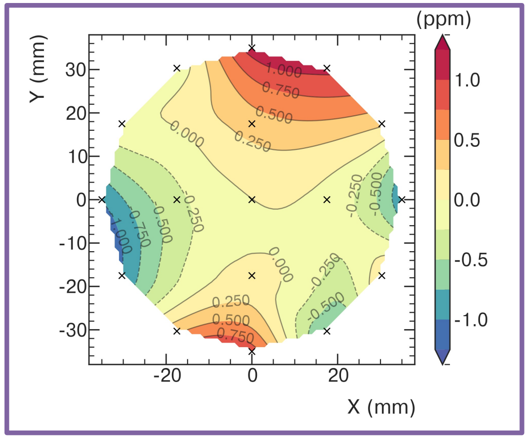

Extracting a_μ - our tools

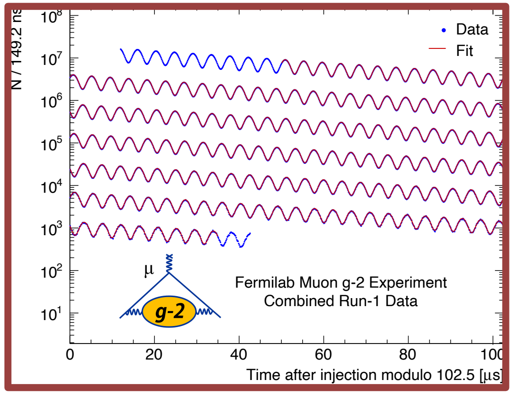

Anomalous spin precession frequency

Muon beam dynamics corrections

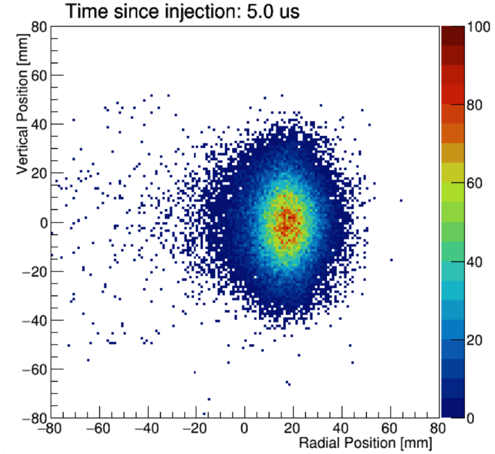

Clock blinding

$$R' = \frac{\omega_a}{\tilde{\omega}'_p} = \frac{f_{\mathrm{clock}}\,\omega_a^{\mathrm{meas}}\left(1 + C_e + C_p + C_{ml} + C_{pa}\right)}{f_{\mathrm{calib}}\left\langle M(x, y, \phi)\,\omega'_p(x, y, \phi)\right\rangle\left(1 + B_k + B_q\right)}$$

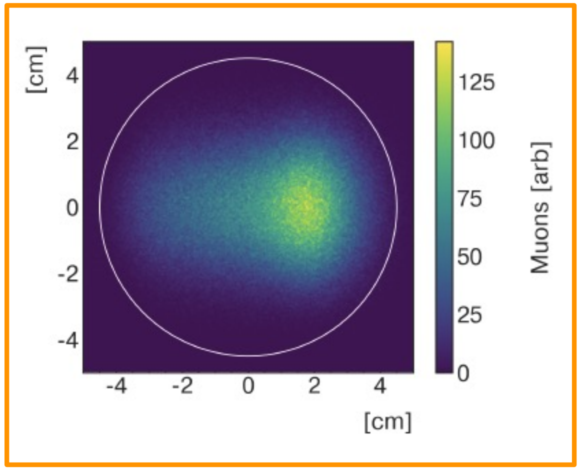

Spatial muon distribution

Spatial distribution of magnetic field

Transient magnetic fields

Calibration

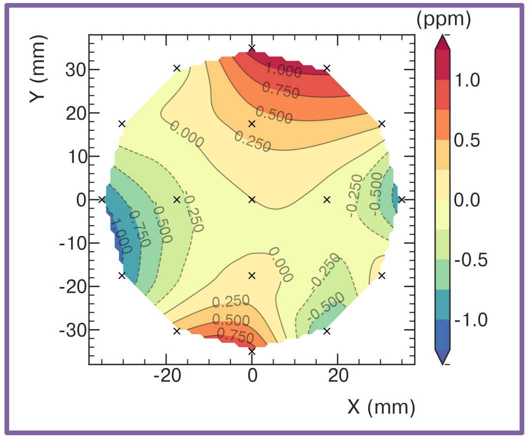

JG|U

The hardware blinding of the ω_a^{meas} data

- Hardware: Detuning of 40 MHz reference clock in the range of ± 25 ppm(!)

Greg Bock and Joe Lykken blinding the clock in 2018

Locked Clock Panel

- Software: unknown offset for ω_a analysis

After putting it all together, we are ready to unblind

February 25th, 2021

The 40 MHz clock was set really set to: 39 99X XXX MHz

Breaking the seals...

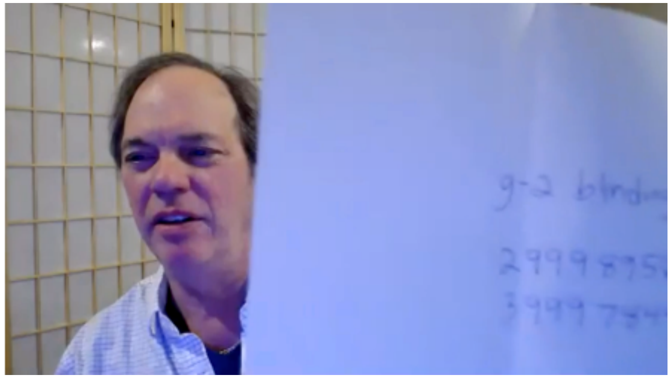

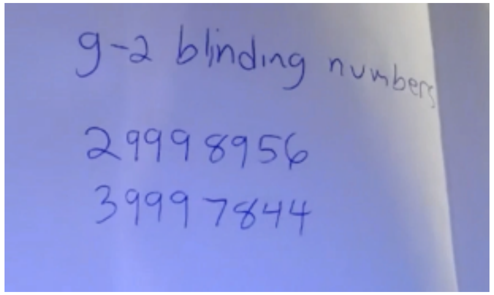

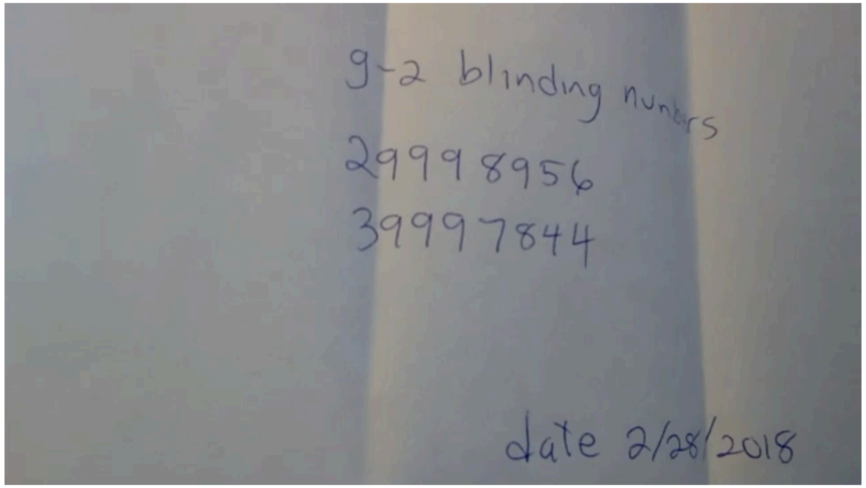

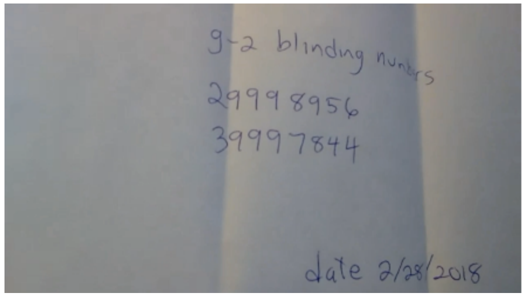

Breaking the seals...

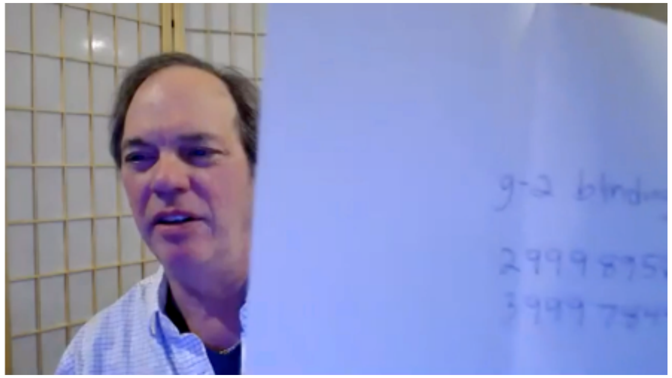

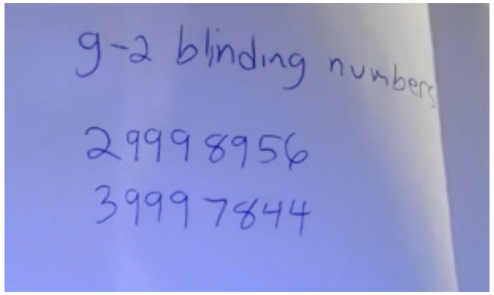

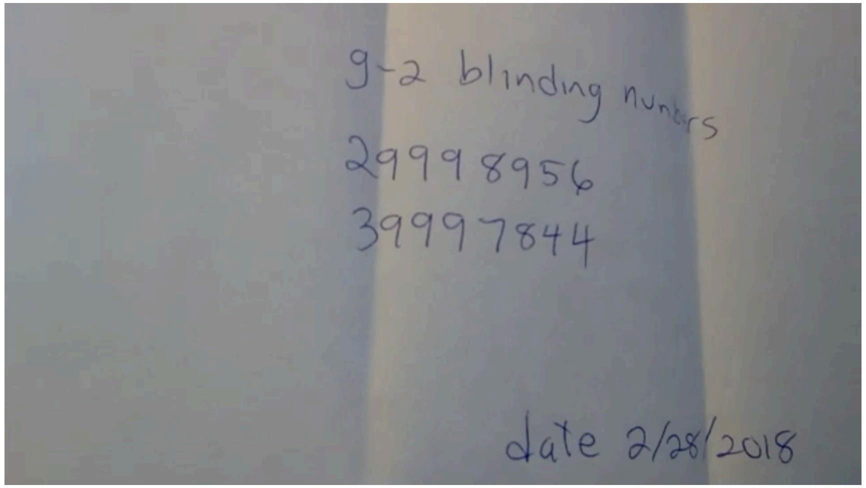

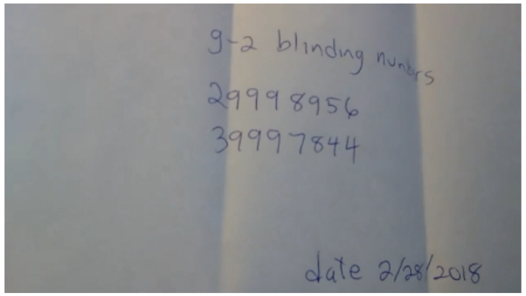

Result from combined Run 1 datasets

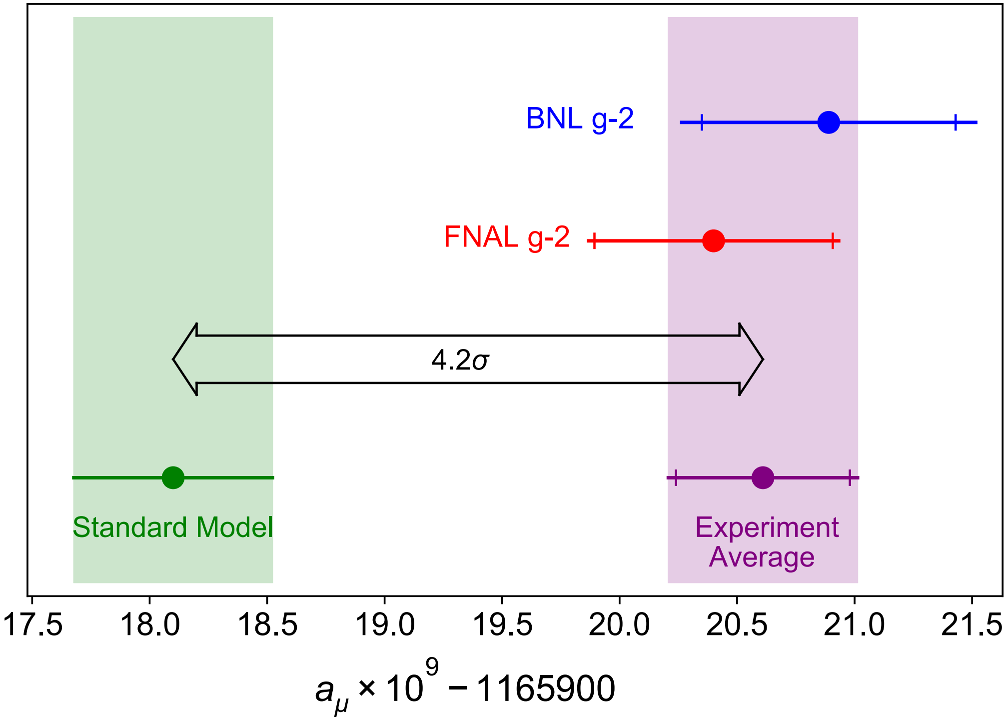

$a_\mu(\text{BNL}) = 0.00116592089(63) \rightarrow 540$ ppb

$a_\mu(\text{FNAL, R1}) = 0.00116592040(54) \rightarrow 463$ ppb

Both experiments uncertainty dominated by statistics:

$a_\mu(\text{Exp}) = 0.00116592061(41) \rightarrow 350$ ppb

$a_\mu(\text{SM}) = 0.00116591810(43) \rightarrow 350$ ppb

4.2 σ discrepancy between experiment and community approved SM prediction

Outlook to the future

Vastly improved temperature stability of the magnet an in MC1 overall

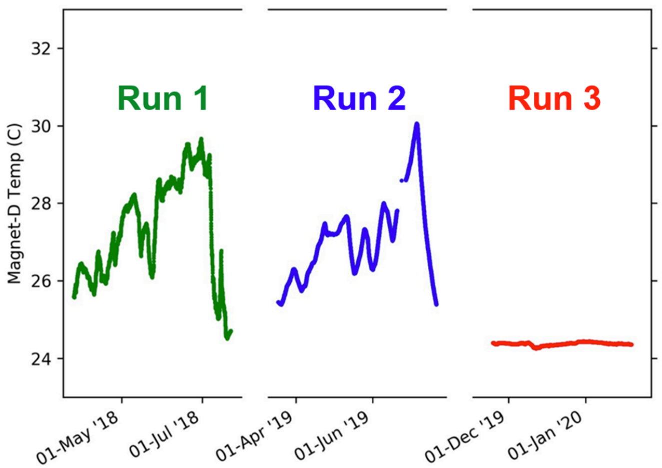

Run 4 is currently ongoing

Run 5 set to start in fall

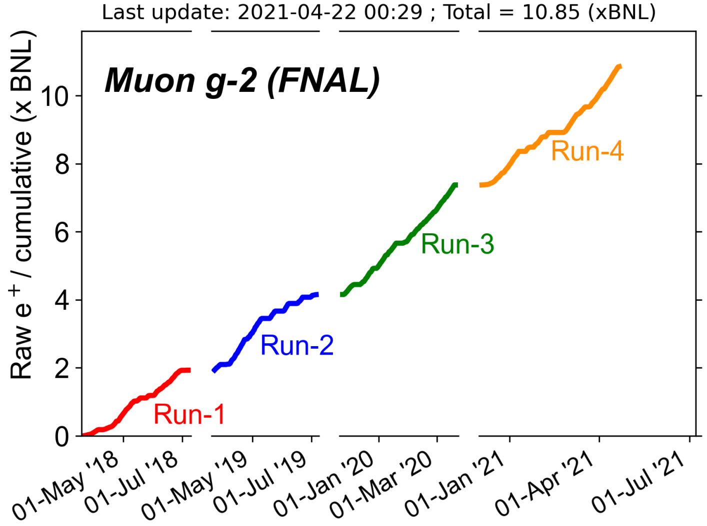

Full strength of kicker in Run 3

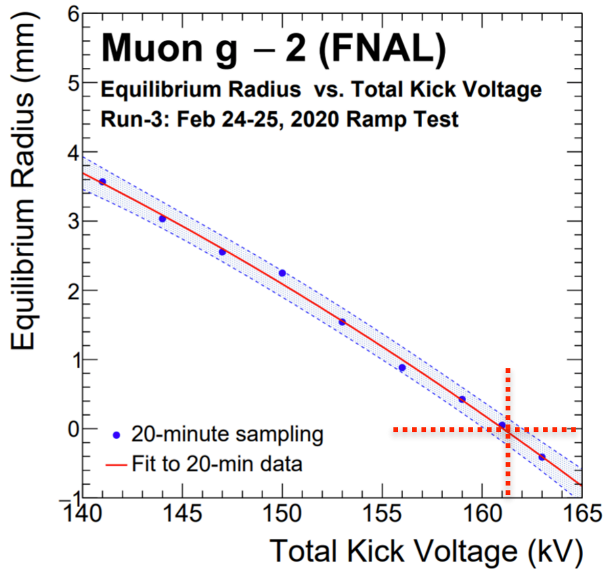

Summary and Conclusions

- We have determined a_μ with unprecedented 460 ppb precision!

- The Run 1 results represent:
  - 6% of ultimate data sample
  - 15% smaller uncertainty than BNL
  - 3.3 σ tension with SM

- After 20 years, we confirm the BNL results
- Combined result shows a 4.2 σ tension with SM prediction